Kingdom of Saudi Arabia

Ministry of Education

Umm Al-Qura University

Faculty of Applied Sciences

Department of Chemistry

ELECTROCATALYTIC OXIDATION OF SOME ORGANIC MOLECULES AT MODIFIED ELECTRODES

A Thesis Presented to
Chemistry Department, Faculty of Applied Sciences,
Umm Al-Qura University

For

Partial Fulfillment of The Ph.D Degree of Science, Chemistry

(Physical Chemistry)

By:

MAHA EID ALHAZEMI

M. Sc. In Chemistry

College of Science, Emporia State University

Under Supervision of :

PROF. DR. MOHAMAD ISMAIL AWAD

Professor of Physical Chemistry

Department of Chemistry, Faculty of Applied Sciences
Umm Al-Qura University

1441 H -2020 M


بسم الله الرحمن الرحيم


رَبِّ زِدْنِي عِلْمًا

PUBLSHED PAPER

Int. J. Electrochem. Sci., 15 **(2020)** xx – yy

International Journal of
ELECTROCHEMICAL
SCIENCE
www.electrochemsci.org

Impact of Glucose as an Additive on the Deposition of Nickel: Application for Electrocatalytic Oxidation of Glucose

Maha E. Al-Hazemi[1], and Mohamed I. Awad[1,2,]*

[1] Chem. Department, Faculty of Applied Sciences, Umm Al-Qura University, Makkah, Saudi Arabia.
[2] Chem. Department, Faculty of Science, Cairo University, Cairo, Egypt.
[*]E-mail: mawad70@yahoo.com

Received: 1 xxx 2020 / *Accepted:* 1 xxx 2020 / *Published:* 1 xxx 2020

A nickel oxide (NiO_x) nanoparticles modified glassy carbon (GC) electrode, designated as GC_{ox}/NiO_x(Glu), were fabricated from a nickel bath (0.02 M $NiSO_4$ + 0.03 M $NiCl_2$ + 0.03M H_3BO_3) containing a suitable additive, typically glucose. The GC was electrochemically pretreated prior to the deposition of nickel. The thus modified electrode was applied for the electrooxidation of glucose in alkaline medium. For the sake of comparison, a similar modification was conducted but in the absence of glucose as an additive, and the modified electrode is designated as GC_{ox}/NiO_x. The effect of loading of NiO_x was optimized. Cyclic voltammetry (CV), and chronoamperometry were used for the voltammetric characterization. Several surface techniques were used for probing the morphology and composition of the deposited modifier, including field emission scanning electron microscopy (FE-SEM), EDX and X-ray diffraction. The highest electrocatalytic activity towards glucose oxidation was obtained at GC_{ox}/NiO_x(Glu) using five potential cycles in the range from 0.0 to -1.0 V vs. Ag/AgCl(Kcl sat.). Possible reason(s) behind the enhancement of glucose electrocatalytic oxidation was (were) explored.

Keywords: Modified electrodes, Nickel oxide nanoparticles, Glucose, Electrocatalysis

1. INTRODUCTION

Environmentally friendly materials have become very important at the moment, so research has turned to fuel with these specifications, leading researchers to use glucose to fuel cell work. Based on the type of the catalyst if glucose fuel cells, it can be classified into three categories; first one, enzymatic glucose fuel cell, which utilizes enzymes as catalysts. As such they are of limited long-term stability. Second, microbial glucose fuel cell in which immobilized bacteria capable of oxidizing glucose are used as the catalysts. Bacterial and enzymatic fuel cells contain defects and complications so they can be replaced by non-enzymatic fuel cells counter or part for oxidation of glucose on the

noble electrode. However, enzymes are unstable at high temperatures and aggressive environments. Many researches have been done to obtain non-enzymatic glucose sensors. Third, direct glucose fuel cell (DGFC): they are fuel cell that use inorganic catalysts [1-4]. The latter one is characterized by the advantage that they are the most robust, and biocompatible. Commercializing glucose fuel cells face several problems; of these problems the cost of the electrocatalyst and its susceptibility to poisoning are the dilemma. Glucose oxidation to CO_2 involves the exchange of and 24 electrons and yields very high energy (-2.87×10^6 J/mol) [5-8]. Theoretically, an open-circuit of 1.24 V voltage can be obtained from DGFC [7,8].

Over the past decade, many studies have been conducted on the electrochemical oxidation of sugars resulting in the conclusion that single sugars such as glucose is oxidized at catalysts based on platinum and gold electrodes [9-11]. However, these electrodes showed their long term inefficiency due to several reasons: of these lack of selectivity and low sensitivity. A lot of research has been done on transition metal oxides to solve these problems either by replacing the costly platinum electrocatalyst or the co-deposition of a secondary catalyst [2,3]. Of these modifiers, nickel is the first choice as it is naturally active for glucose oxidation. Nickel and nickel oxide (NiO_x) electrodes have many technological applications which led to research in the past years. Of these applications: use in densities [12,13] alkaline batteries [14] biological sensors [15, 16] and energy conversion devices [17,18] .The electrooxidation rate of glucose in alkaline environments is facile than in neutral or acidic media [9,10, 19-22]. On the other hand, the use of nanoscale materials has led to the development of huge sensors, particularly glucose sensors [2]. The following electrodes Au, Pt ,Fe ,Ni ,Cu have been extensively studied for the oxidation of glucose in the alkaline medium [23-27].

In this research, the electrochemical fabrication of the electrode is based on the electrochemical activation of GC electrode, and then the decoration of the oxidized GC by nickel nanoparticles (nano-NiO_x) from solution containing nickel ions and glucose onto the thus oxidized glassy carbon electrode. Then, the deposited nickel is oxidized electrochemically in alkaline medium for the formation of NiO_x. The experimental parameters are optimized to sustain the highest electrocatalytic activity towards glucose oxidation.

2. EXPERIMENTAL

2.1. Chemicals

Chemicals, of analytical grade, used in this work were purchased from Sigma Aldrich and they were used as received. Solutions were prepared using deionized water.

2.2. Electrochemical measurements

An EG&G potentiostat (model 273A) operated with E-chem 270 software were used for the Electrochemical measurements. A conventional cell with a three-electrode configuration was used in this work. An Ag/AgCl/KCl (sat.) as a counter electrode and a platinum spiral wire as reference electrodes were utilized. The electrochemical measurements were performed at room temperature (25 °C). Stated potentials in this work were presented with respect to the reference electrode. The working

electrode was glassy carbon (GC, d = 3.0 mm). It was cleaned by mechanical polishing with aqueous slurries of successively finer alumina powder then washed thoroughly with deionized water.

2.3. Fabrication of nickel oxide (NiO_x) nanoparticles

Nickel oxide nanoparticles modified GC were prepared as follows; first, the underlying GC electrode was activated in 0.5 M of H_2SO_4 by suitable number of potential cycles in the range (- 0.2 to 2.0 V), designated as GC_{ox}. Second, GC_{ox} is subjected to several potential cycles, in the range of 0.0 to -1.0 V vs. Ag/AgCl/KCl (sat.), in a solution containing 0.02 M $NiSO_4$, 0.03 M $NiCl_2$ and 0.03 M H_3BO_3, either in the presence or absence of 5 mM glucose as additive. Then, the addressing of the electrocatalytic activity of the modified electrode toward glucose oxidation was conducted at different scan rates, different concentrations, different loading of nano-NiO_x. To prove reproducibility of the results the CVs were repeated several times.

2.4. surface characterization

A field emission scanning electron microscope, FE-SEM, (QUANTA FEG 250) was used to image the nano-NiO_x. X-ray diffraction, XRD (PANalytical, X'Pert PRO) operated with Cu target (λ = 1.54 Å) were used to probe the crystallographic structure of deposited nano-NiO_x at bare GC, GC_{ox}, GC_{ox}/NiO_x nanoparticles, and GC_{ox}/NiO_x(Glu) nanoparticles.

3. RESULTS AND DISCUSSION

3.1. Morphological characterizations

SEM images of nano-NiO_x, prepared by a cyclic voltammetric technique described in the experimental section, is presented in Fig. 1. Also, the atomic ratios of C/O/Ni from EDX test were examined. In image (a) a a smooth surface is shown and in EDX (plot B), as expected, the weight of carbon element (97.07%) is large compared with oxygen. In case of GC_{Ox} (image C), the electrode surface becomes rougher, and as revealed from EDX (plot D) the percent of oxygen increased to 10 %. The increase in the percent of oxygen is attributed to the electrooxidation of GC which results in the formation of several containing oxygen functional groups. In image E, obtained at GC_{ox}/NiO_x electrode; i.e., at nickel oxide deposited onto oxidized GCE, a deposition of NiO_x is observed, as revealed from the EDX (plot E) in which new peaks for nickel at 0.9 KeV, 7.4 KeV are observed [28]. At GC_{ox}/NiO_x(Glu) electrode which is fabricated similarly to GC_{ox}/NiO_x but in the presence of glucose in the deposition bath, EDX (plot H) presents a larger ratio of Ni at GC_{ox}/NiO_x-as revealed from the increase of intensities of peaks corresponds to nickel at 0.9, 7.6 ,and 8.2 KeV [29].

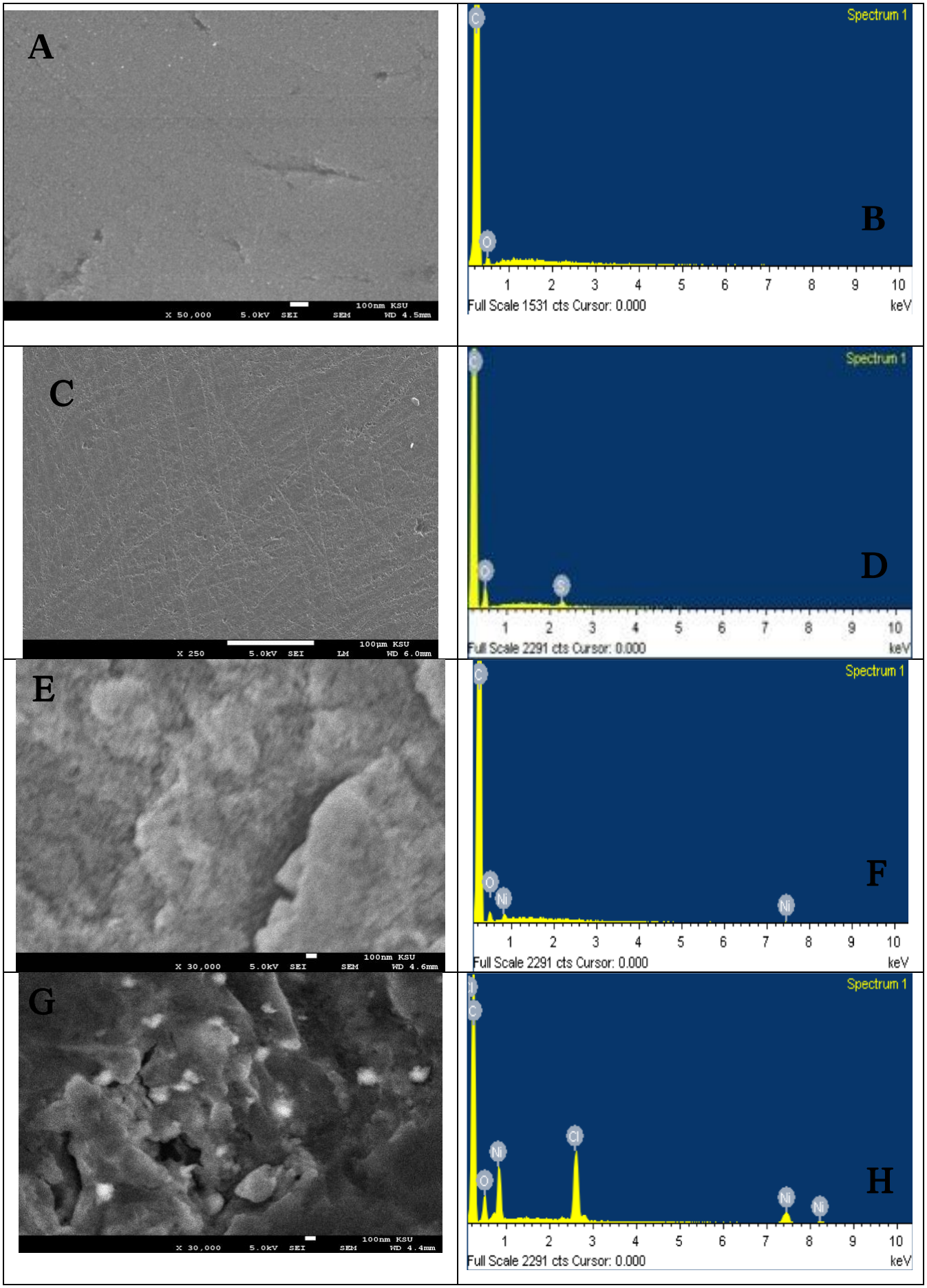
A
X 50,000 5.0kV SEI SEM WD 4.5mm
100nm KSU
B
Spectrum 1
C O
1 2 3 4 5 6 7 8 9 10
Full Scale 1531 cts Cursor: 0.000
keV
C
X 250 5.0kV SEI LM WD 6.0mm
100µm KSU
D
Spectrum 1
C O S
1 2 3 4 5 6 7 8 9 10
Full Scale 2291 cts Cursor: 0.000
keV
E
X 30,000 5.0kV SEI SEM WD 4.6mm
100nm KSU
F
Spectrum 1
C O Ni Ni
1 2 3 4 5 6 7 8 9 10
Full Scale 2291 cts Cursor: 0.000
keV
G
X 30,000 5.0kV SEI SEM WD 4.4mm
100nm KSU
H
Spectrum 1
C Ni O Cl Ni Ni
1 2 3 4 5 6 7 8 9 10
Full Scale 2291 cts Cursor: 0.000
keV

Figure 1. SEM (A,C,E,G) and EDX (B,D,F,H) of (A,B) GC, (C,D) GC_{ox} , (E,F) GC_{ox}/NiO_x, and (G,H) GC_{ox}/NiO_x(Glu).

Fig. 2 depicts XRD patterns obtained at the modified electrodes electrodes. The sharp peak at 19 ₀ corresponds to the (002) diffraction of the glassy carbon underlying substrate. At GC_{ox}/NiO_x (curve b) and GC_{ox}/NiO_x(Glu) (curve c) electrodes, the XRD pattern of NiO showed several diffraction peaks at 2θ = 37.20°, 43.20°, 44.4°, 75.20° which are indexed as (101), (012), (111), (113) and (220) crystal planes of the NiOx, respectively. Those peaks are assigned to the face-centered cubic (FCC) crystalline structure of NiO_x based on the standard spectrum (JCPDS, No. 04-0835) [30].

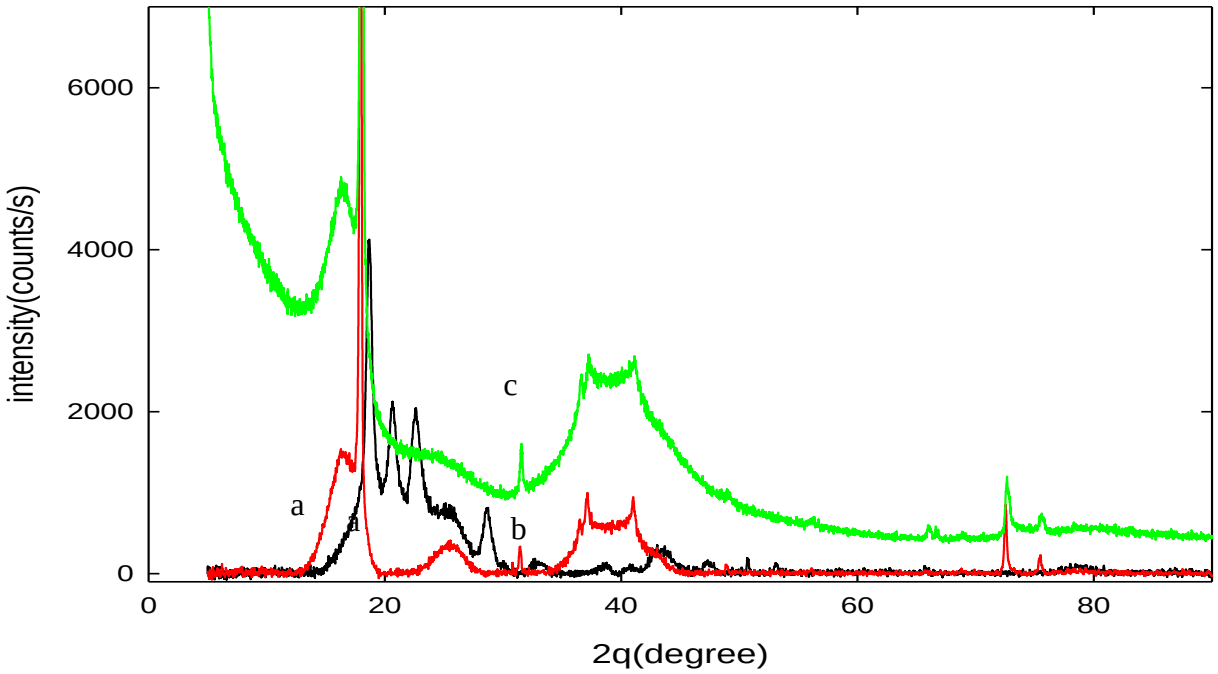

Figure 2. XRD of (a) GC, (b) GC_{ox}/NiO_x, and (C) GC_{ox}/NiO_x(Glu).

3.2. *Electrochemical characterizations*

The electrochemical oxidation of glucose has been an interesting topic for the last decade, especially at nickel modified electrodes, which presents a unique electrocatalytic properties. Nickel deposition is critically affected by the ingredient of the deposition bath [31]. Here, the effect of adding glucose, as an additive, in the deposition bath of nickel is examined. Fig. 3 shows CVs responses obtained at the modified electrodes in 0.5 M NaOH. Similar potential cycles were used for decoration Ni onto the different studied electrodes. As clearly shown, in Fig. 3 (curve a), obtained at GC electrode, the CV is featureless. Curve b, obtained at GC/NiO_x(Glu) electrode in which nickel oxide was deposited, in the presence of glucose in the deposition bath, on GC electrode, a well-defined couple of redox peaks corresponds to the nickel oxidation to oxide and the subsequent reduction in the reverse scan is obtained. Curves C and d shows CV responses obtained at GC_{ox}/NiO_x and

$GC_{ox}/NiO_x(Glu)$ electrodes, respectively. The peak current for nickel/nickel oxide redox couple increases at both electrodes compared with that on the $GC/NiO_x(Glu)$ (b). Probably, the functional groups of the underlying substrate participate in this enhancement. Comparing curves c and d indicates that including glucose in the deposition bath (curve d) promotes the nickel-nickel oxide redox couple.

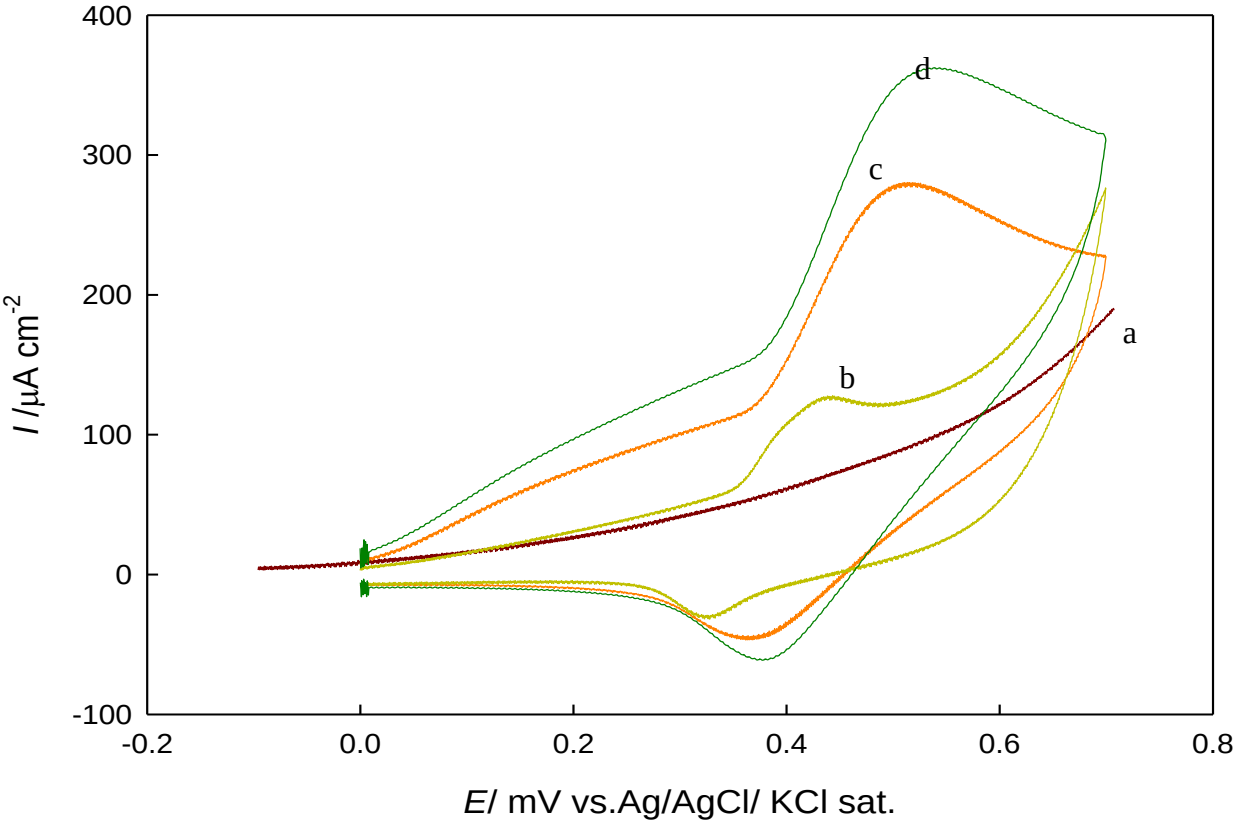

Figure 3. CV obtained at (a) GC, (b) $GC/NiO_x(Glu)$, (C) GC_{ox}/NiO_x (d) $GC_{ox}/NiO_x(Glu)$ electrodes in 0.5 M NaOH at SR = 100 mV/S.

Fig. 4 is similar to 3 but in the presence of glucose. Inspection of this figure reveals several interesting points;

i. GC is inactive towards glucose oxidation.

ii. At $GC/NiO_x(Glu)$ (curve b), a well-defined oxidation response with a fast increase in the current of the glucose oxidation is obtained.

iii. At GC_{ox}/NiO_x (curve c) and $GC_{ox}/NiO_x(Glu)$ (curve d), the oxidation of glucose is significantly enhanced, with the one at the latter is larger indicating the significant effect of the underlying substrate (GC_{ox}) as well as the including of glucose in the deposition bath. The prominent role of the underlying substrate (GC_{ox}) surface is proved by comparing curves b and d in which nickel was deposited from a bath containing glucose and the only difference is the case of the underlying substrate, whether it is electrochemically oxidized or not. It has been reported that electrochemical

oxidation of GC in H_2SO_4 at large anodic potentials increases of the percentage surface composition of functional groups bearing –OH group. Those generated–OH groups on the GC surface (i.e., OH_{ads}) enhances the electrocatalytic oxidation of glucose [32,33] and other small organic molecules such as methanol via enhancing their adsorption [34].

iv. The role of glucose in the deposition bath is confirmed by comparing curves c and d in which the modification of the underlying substrates is the same. Curve d was obtained for $GC_{ox}/NiOx(Glu)$ electrode, this electrode was fabricated in a similar way to GC_{ox}/NiO_x (curve c) with only one difference. In the former one, i.e., $GC_{ox}/NiOx(Glu)$ glucose was added to the deposition bath. Interestingly, in this case the response for glucose oxidation is the largest among studied electrodes. It seems that a synergistic effect from the different conditions results in such increase along with the morphology presented in SEM images shown above. In previous study they assumed [35] a combination of direct electrooxidation of glucose on the surface of oxide layer and mediated oxidation by NiOOH.

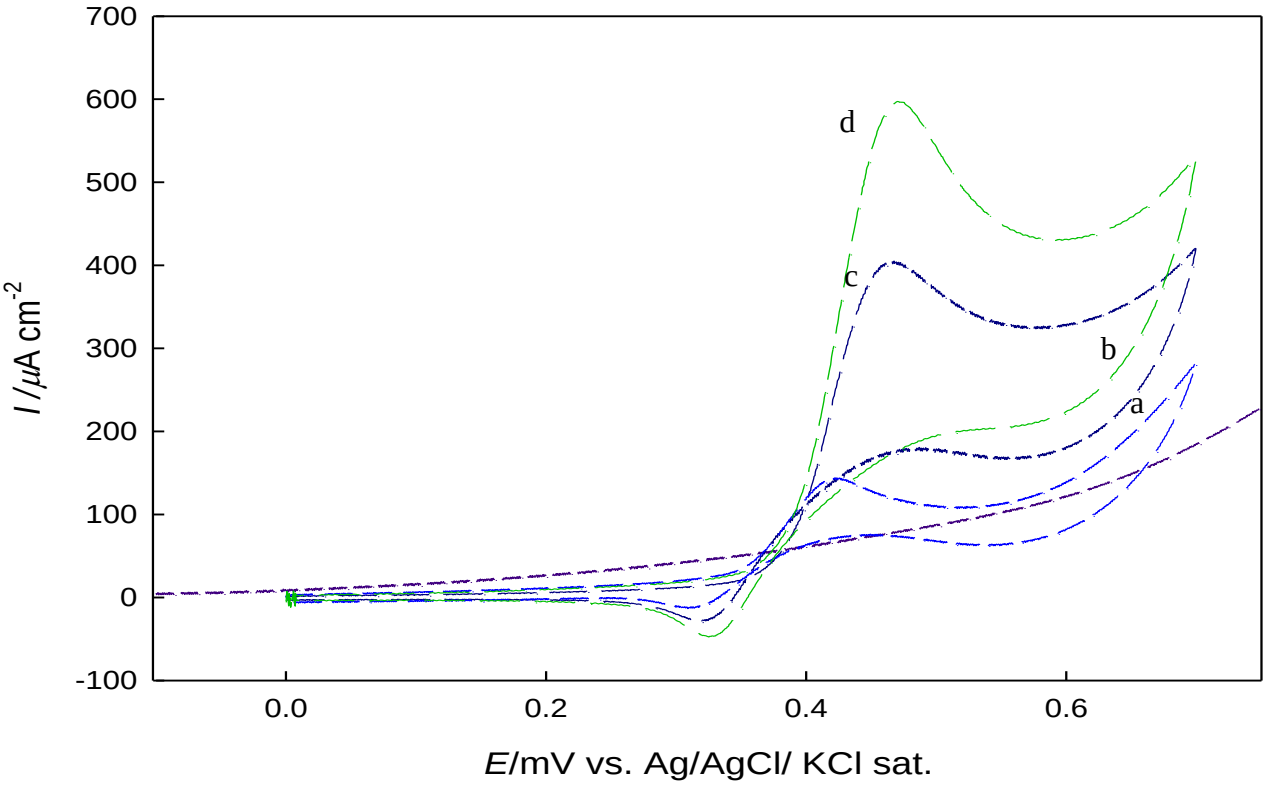

Figure 4. CV obtained at (a) GC, (b) $GC/NiO_x(Glu)$, (C) GC_{ox}/NiO_x (d) $GC_{ox}/NiO_x(Glu)$ electrodes in 0.5 M NaOH containing 2.5 mM glucose at SR = 100 mV/S.

First Ni (II) is converted to Ni(III), then in a following chemical step glucose is according to the following reactions:

$$Ni(III) + glucose \rightarrow intermediate + Ni(II) \quad (1)$$

$$Ni(III) + intermediate \rightarrow products + Ni(II) \quad (2)$$

where Ni^{3+} sites are regenerated by direct electrooxidation to Ni^{2+} [36,37]:

$$Ni(III)–glucose \rightarrow Ni(III)–intermediate \quad (3)$$

Ni(III)–intermediate → Ni(III)–products (4)

Mechanism based on Eqs. (1) and (2) is called Fleischmann mechanism [37, 38]. Gluconolactone [39, 40] as well as methanoates and oxalates [41] have been reported as the oxidation products of glucose electrooxidation.

3.3. Effect of loading of nickel nanoparticles

Fig. 5 shows that the redox couple which correspond to nickel/nickel oxide oxidation-reduction is enhanced as the loading level increases up to loading level of 5 cycles for deposition of Ni, in the potential range of 0.0 to -1.0 V vs. Ag/AgCl(Kcl sat.). After this loading the peak current decreases significantly. It may be concluded that a loading NiO_x nanoparticles of five cycles is the optimum loading under the present experimental conditions and will be used hereafter for further investigation.

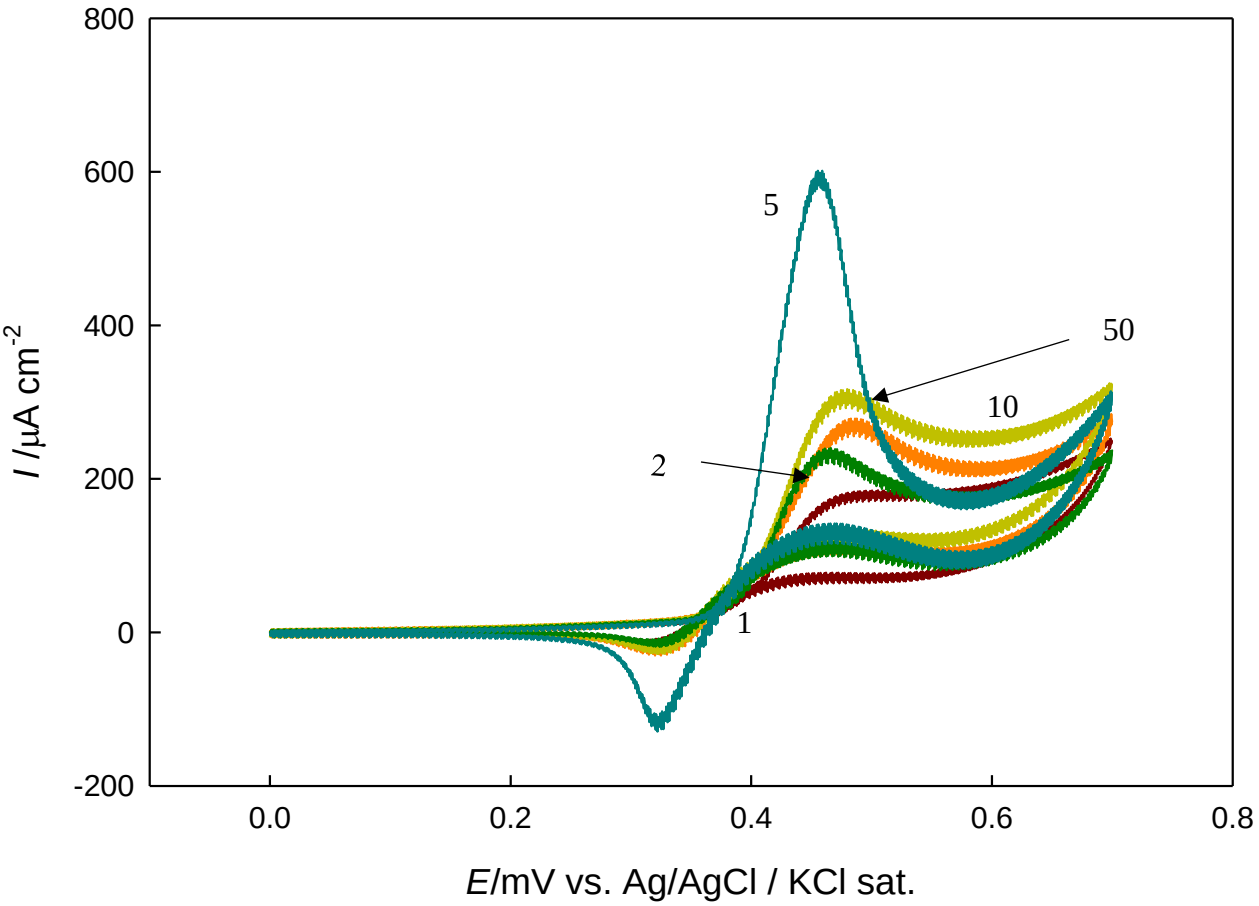

Figure 5. CV obtained at GC_{ox}/NiO_x(Glu) in 0.5 M NaOH containing 2.5 mM glucose, NiO_x was prepared by different potential cycles in the range of 0.0 to -1.0 V vs Ag/AgCl (KCl sat.) Potential cycles are 1, 2, 5, 20 and 50 cycles at SR = 100 mV/S.

It was evident that CVs for glucose oxidation GC_{ox}/NiO_x(Glu) electrode in solution of 0.5M NaOH gave a higher current than CVs for glucose oxidation on GC_{ox}/NiO_x electrode that approved

adding glucose in the deposition bath made the electrode more active toward the oxidation of the glucose.

In order to get further insight about the mecahnsism of glucose oxidation, Tafel plots for the two modified electrodes were recorded in 0.5 M NaOH containing 2.5 mM glucose at a scan rate 5 mV/s and shown in Fig. 6. Tafel slopes of ca. 38 mV/dec was obtained at GC_{ox}/NiO_x(Glu), while at GC_{ox}/NiO_x the Tafel slope equals 60 mV/decade. The former one points to a possibly an electron-transfer step is controlling the oxidation process. At GC_{ox}/NiO_x electrode, it is likely that a chemical step is the controlling for the glucose oxidation. This means that at GC_{ox}/NiO_x electrode, the removal of an adsorbed species (represented by Eq. 5) is the rate determining step. At GC_{ox}/NiO_x(Glu) electrode at which the Tafel slope is 40 mV/decade, the electron transfer represented by Eq. 6 is the rate determining step [42]. The plots confirmed the enhancment of the glucose oxidation on GC_{ox}/NiO_x(Glu) comparatively.

$$NiOOH + [Glucose]_{ads} \rightarrow Ni(OH)_2 + \text{radical intermediate} \quad (5)$$

$$\text{Radical intermediate} + 2NiOOH \rightarrow 2Ni(OH)_2 + \text{gluconolactone} + 2e^- \quad (6)$$

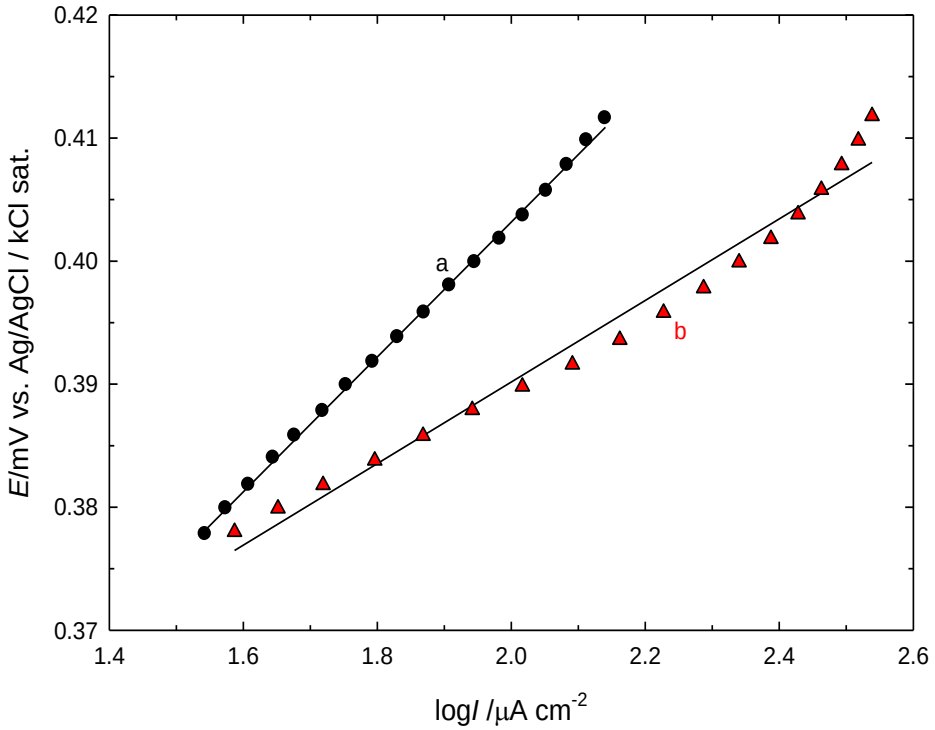

Figure 6. Tafel plots obtained at (a) GC_{ox}/NiO_x and, (b) GC_{ox}/NiO_x(Glu) in 0.5 M NaOH containing 2.5 mM glucose at SR = 5 mV/S.

3.4. Long-term stability of the prepared electrocatalysts

The stability of the NiO_x (the active oxide) modified GC electrode prepared in the absence and presence of glucose was examined using current–time curves for glucose oxidation and shown in Fig. 7. The data is obtained at constant potential of 0.4 V for (a) GC_{ox}/NiO_x, (b) GC_{ox}/NiO_x (Glu)

electrodes in 0.5 M NaOH containing 2.5 mM glucose. The initial large current obtained at the the two electrodes is attributed to the charging of the double layer. This spiked current is followed by a slight decrease which is indicative of a loss in the catalytic activity. GC_{ox}/NiO_x (Glu) electrode exhibits the highest initial currents and steady state currents compared with that obtained at GC_{ox}/NiO_x electrode in which Ni was deposited in the absence of glucose as additive. The order obtained using chronoamperometric measurements sustain that observed above using cyclic voltammetry shown above. This confirmed the higher activity of the GC_{ox}/NiO_x (Glu) electrode, compared with GC_{ox}/NiO_x electrode towards glucose oxidation, and the prominent role of glucose in the deposition bath.

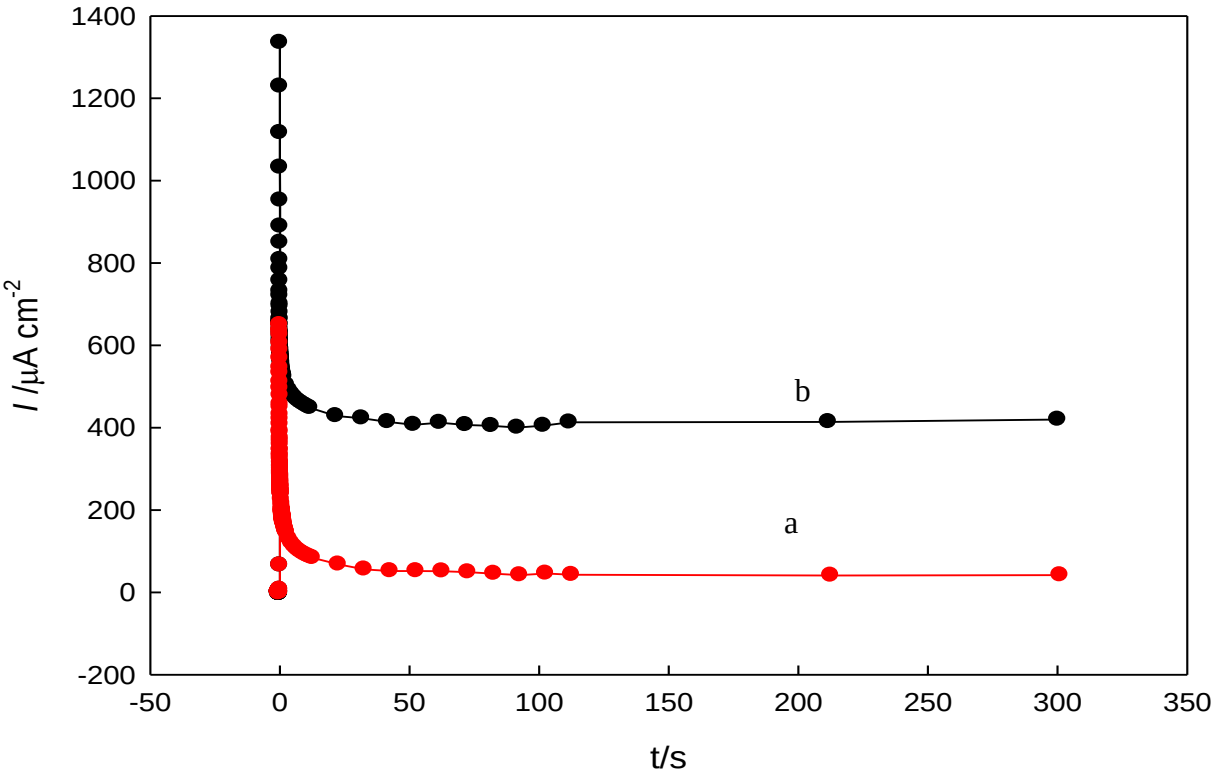

Figure 7. chronoampergram obtained at constant potential of 0.4 V for (a) GC_{ox}/NiO_x, (b) GC_{ox}/NiO_x (Glu) electrodes in 0.5 M NaOH containing 2.5 mM glucose.

Fig. 8 shows the dependence of the function ($Ip/v^{1/2}$) with v obtained at the GC_{ox}/NiO_x (Glu) electrode. At scan rate higher than 40 mV s^{-1}, $Ip/v^{1/2}$ almost keeps constant with the scan rate. This behavior characterizes catalytic reactions [42], i.e., EC mechanism (Eqs 1 and 2). The glucose oxidation is mediated by Ni/nickel oxide redox couple. It is clear that the inclusion of glucose in the deposition bath significantly modify deposited nickel oxide in such a manner that glucose oxidation is enhanced.

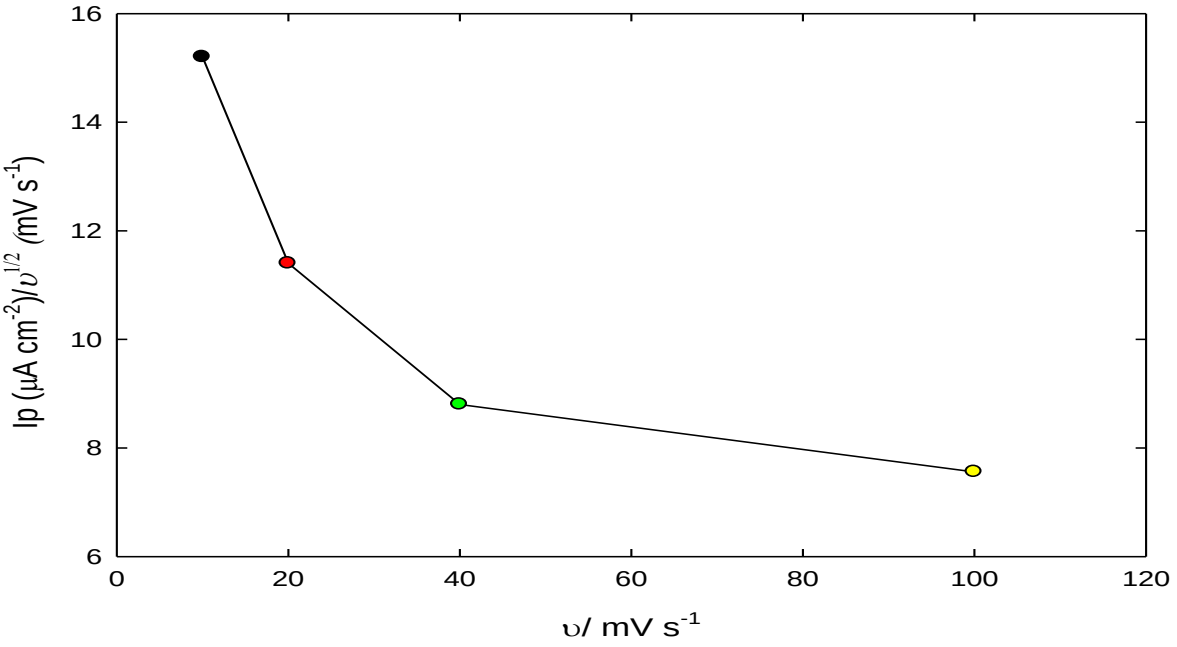

Figure 8. Variation of $Ip/v^{1/2}$ with v for glucose electrooxidation obtained at GC_{ox}/NiO_x(Glu) electrode in 0.5 M NaOH containing 2.5 mM glucose.

4. CONCLUSIONS

GC_{ox}/NiO_x (Glu) electrode was fabricated by electrodeposition of nickel from Watts bath both in the absence and presence of glucose, as an additive, and then examined for glucose electrooxidation. The modified electrode significantly enhanced the glucose electrooxidation as compared with $GCox/NiO_x$ electrode which was prepared similarly to GC_{ox}/NiO_x (Glu) electrode but in the absence of glucose. The relation between $Ip/v^{1/2}$ and v denoted an EC mechanism for glucose oxidation and the nominal equalities of Tafel slopes obtained at the two modified electrodes pointed to a similar mechanism at both electrodes.

References

1- W. Zheng, Y. Li, C. Tsang, L. Hu, M. Liu, B. Huang, L. Y. S. Lee, K-Y. Wong, *ChemElectroChem*, 4 (2017) 2788-2792.

2- H. Guo, H. Yin, X. Yan, S. Shi, Q. Yu, Z. Cao, J. Li, *Sci. Rep.*, 6 (2016) 39162.

3- M. Pasta, F.L. Mantia, Y. Cui, *Electrochim. Acta,* 55 (2010) 5561–5568.

4- A.S. Danial, M. Saleh, S. Salih, M. Awad, *J. Power Sources*, 293 (2015) 101–108.

5- V. Soukharev, N. Mano, A. Heller, *J. Am. Chem. Soc., 126* (2004) 8368-8369.

6- P. Kavanagh, S. Boland, P. Jenkins, D. Leech, *Fuel Cells*, 9 (2009) 79-84.

7- S. K. Chaudhuri, D. R. Lovley, *Nat. Biotechnol.*, 21 (2003) 1229.

8- F. Stetten, S. Kerzenmacher, A. Lorenz, V. Chokkalingam, N. Miyakawa, R. Zengerle, *19th IEEE International Conference*, (2006), p. 934.

9- G. Moggia, T. Kenis, N. Daems, T. Breugelmans, *ChemElectroChem* ,7 (2020) 86-95.

10- J. McGinley, F. N. McHale, P. Hughes, C. N. Reid, A.P.McHale, *Biotechnol. Lett.*,26 (2004) 1771.

11- C.P. Wilde, M. Zhang, *J. Chem. Soc., Faraday Trans.*, 89 (1993) 385-389.

12- F. Xiao, F. Zhao, D. Mei, Z. Mo, B. Zeng, *Biosens. Bioelectron.*, 24 (2009) 3481-3486.

13- W. Xing, F. Li, Z. F. Yan, G. Q. Lu, *J. Power Sources*, 134 (2004) 324-330.

14- M. S. Wu, H.H. Hsieh, *Electrochim. Acta*, 53 (2008) 3427-3435.

15- G.A. Snook, N.W. Duffy, A.G. Pandolfo, *J. Electrochem. Soc.*, 155 (2008) A262-A267.

16- Y. Hu, J. Jin, P. Wu, H. Zhang, C. Cai, *Electrochim. Acta*, 56 (2010) 491-500.

17- S. Hui, J. Zhang, X. Chen, H. Xu, D. Ma, Y. Liu, B. Tao, *Sens. Actuators, B,* 155 (2011) 592-597.

18- J.T. C. Barragan, S. K. Jr, E.T.S.G. da Silva, L.T. Kubota**,** *Anal. Chem.,*90 (2018) 3357-3365.

19- M. A. Rahim, R. A. Hameed, M.W. Khalil, *J. Power Sources*, 134 (2004) 160-169.

20- K.Đ. Popović, A.V. Tripković, R.R. Adžić, *J. Electroanal. Chem.*,339 (1992) 227-245.

21- C.P. Wilde, M. Zhang, *J. Chem. Soc.,* 89.2 (1993) 385-389.

22- H.W. Lei, B. Wu, C.S. Cha, H. Kita, *J. Electroanal. Chem*., 382 (1995) 103-110.

23- D. Chai, X. Zhang , S. Chan, G. Li, *J. Taiwan Inst. Chem. Eng.*,95 (2019) 139-146.

24- S. B. Aoun, I. Taniguchi, *Chem. Lett*., 37 (2008) 936-937.

25- L.E. Yei, B. Beden, C. Lamy, *J. Electroanal. Chem. Interfacial Electrochem*., 246 (1988) 349-362.

26- N.N. Nikolaeva, O.A. Khazova, Y.B. Vasil'ev, *Elektrokhimiya*, 19 (1983) 1476-1481.

27- N. Neha, B.S.R. Kouamé, T. Rafaïdeen, S. Baranton, C. Coutanceau, *Electrocatalysis*, 11 (2020) 1-14 .

28- S.M. El-Refaei, M.M. Saleh, M. I. Awad, *J. Solid State Electrochem.*, 18 (2014) 5-12.

29- Y. Ren, L. Gao, *J. Am. Ceram. Soc.*, 93 (2010) 3560.

30- T. Im, J. Lee, Y. Song, J. K. Lee, Y. Sh. Song, T. Yim, KR2010083623-A (2010).

31- Y.B. Vassilyev, O.A. Khazova, N.N. Nikolaeva, *J. Electroanal. Chem. Interfacial Electrochem.*, 196 (1985) 105-125.

32- M. Hsiao, R. Adzic, E. Yeager, *Electrochim. Acta,* 37 (1992) 357–363.

33- S. Stevanović, V. Panić, D. Tripković, V.M. Jovanović, *Electrochem. Commun*., 11 (2009) 18-21.

34- S. M. El-Refaei, M.I. Awad, B. E. El-Anadouli, M.M. Saleh, *Electrochim. Acta*, 92 (2013) 460-467.

35- I. Danaee,M. Jafarian, F. Forouzandeh, F. Gobal, M.G. Mahjani*, Int. J. Hydrogen Energy*, 33 (2008) 4367-4376.

36- I. Danaee, M. Jafarian, A. Mirzapoor, F. Gobal, M.G. Mahjani, *Electrochim. Acta,* 55 (2010) 2093-2100.

37- M. Fleischmann, K. Korinek, D. Pletcher, *J. Electroanal. Chem. Interfacial Electrochem.*, 31 (1971) 39-49.

38- C. Zhao, C. Shao, M. Li, K. Jiao, *Talanta*, 71 (2007) 1769-1773.

39- I. Becerik, F. Kadirgan, *Electrochim. Acta,* 37 (1992) 2651-2657.

40- S.I. Mho, D.C. Johnson, *J. Electroanal. Chem*., 500 (2001) 524-532.

41- S.M. El-Refaei, M.M. Saleh, M.I. Awad, *J. Power Sources*, 223 (2013) 125-128.

42- M. Fleischmann, K. Korinek, D. Pletcher, *J. Chem. Soc., Perkin Trans. 2*, 2 (1972) 1396.

ABSTRACT

ABSTRACT

Glucose electrooxidation are considered a promising future energy source for portable electronic devices. However, a suitable cheap anode with fast oxidation kinetics is still in need. Nanomaterials modified electrodes can provide the avenue for developing glucose fuel cells. A brief introduction followed by reviewing literature relevant to the present work is summarized. Results and discussion section includes the suggestion of promising electrocatalysts for glucose electro-oxidation in alkaline medium.

In the first part of the results section, the electrochemical behavior of glucose at gold electrode was studied. Nickel oxide (NiOx) nanoparticles electrodeposited onto gold electrode both in the presence and absence of glucose in the deposition bath was assembled. Next, the enhancement of the electrochemical behavior of glucose at the thus modified electrode was investigated. The modified electrodes were morphologically characterized using scanning electron microscopy and their composition were probed using energy dispersive x-ray.

In the second part, the electrochemical behavior of glucose on a catalyst fabricated of nickel oxide (NiOx) nanoparticles electrodeposited consecutively onto a preelectrochemically activated glassy carbon electrode has been investigated. Also, the effect of adding glucose to the deposition bath was

examined. Modified electrodes, i.e., GCox/NiOx (deposited in the absence of glucose) and GCox/NiOx(Glu) (deposited in the presence of glucose) electrodes were electrochemically characterized using cyclic voltammetry and chronoamperometry, and morphologically using SEM, EDX and XRD. It has been found that the electrocatalytic activity critically depends on the presence of the additive (glucose) at deposition bath. The GCox/NiOx(Glu) electrode presented a larger electrocatalytic activity towards glucose oxidation compared to GCox/NiOx electrode. Also, poisoning of the thus modified electrode by halides was studied.

In the third part, the glassy carbon electrode was modified by graphene (Gr) and then (NiOx) nanoparticles were deposited in similar scenario to the second part. The GCox/Gr/NiOx(Glu) electrode was applied in enhancing the electrochemical oxidation of glucose. Cyclic voltammetry (CV), and chronoamperometry were used for the voltammetric characterization. Several surface techniques were used for probing the morphology and composition of the deposited modifier, including field emission scanning electron microscopy (FE-SEM), Dispersive X-Ray Analysis (EDX). In all cases the effect of loading of nickel was studied. Mechanism was explored via studying the effect of several parameters on the electrochemical behavior.

Keywords: Catalysts, Nickle oxide nanoparticles, Cyclic voltammetry, Glucose electrooxidation, Chronoamperometry, Glassy carbon electrode, Gold electrode.

ACKNOWLEDGMENT

ACKNOWLEDGMENT

This thesis becomes a reality with the kind support and help of many individuals. I would like to extend my sincere thanks to all of them.

Foremost, I want to offer this endeavor to our Allah Almighty for the wisdom he bestowed upon me, the strength, peace of my mind and good health in order to finish this thesis.

Then, I want to express my deep gratitude and thanks to my supervisor Prof. Mohammad Awad, for encouragement and valuable efforts throughout this dissertation. I am highly thankful to my professor for the valuable knowledge that he gave me throughout this thesis.

I would like to express my gratitude towards my family for the encouragement which helped me in completion of this thesis. My beloved and supportive husband, Nasser who is always by my side when times I needed his most and helped me a lot in making this study, and my lovable children, Latyne and Lareen who served as my inspiration to pursue this under taking. Thank you all for sticking with me through all the times, for the joy and optimism you spread around and for never failing to lift my spirits.

It is of immense pleasure to thanks my friends specially **Dr.Zahrah** and **Walaa** for their continuous assistance and support throughout this thesis.

I am highly thankful to my department for providing different facilities support to complete my studies.

Maha EiD Alhazemi

DEDICATION

DEDICATION

First of all, my source of understanding, knowledge, wisdom, and inspiration is Allah. He is the strong pillar and Creator of the world. He remained the source of my strength throughout this course of study.

I want to dedicate my thesis work to all of my family members: my parents, husband and my daughters.

I also want to dedicate this thesis to my beloved sisters and brother who encouraged me to pursues higher education in my field of study.

I would like to dedicated my thesis to my country and my friends.

Finally, this thesis is dedicated to all humanity, the world, chemists, chemistry teachers and students.

MAHA

CONTENTS

TABLE OF CONTENTS

LIST OF TABLES

LIST OF FIGURES

LIST OF SYMBOLS

R	Redaction
O	Oxidation
E_θ	Standard electrode potential
a_i	Unit activity
v_i	Stoichiometric numbers
γ_i	Activity coefficient of species i
k_d	Mass transfer coefficient
k_0	Standard rate constant
η	Over potentially
α_a	Charge transfer coefficients (ANODIC)
α_c	Charge transfer coefficients (CATHODIC)
I_0	Exchange current
E_{eq}	Equilibrium potential
I	Current
E_1	Initial potential
E_2	Potential
A	Area
Q	Charge
Qdl	Double layer charge
i-E	Current-potential
v	Scan rate
Eeq	Equation
Ep	Peak potential
ip	Peak current
CV	Cyclic voltammetry
E°	Formal potential,
ipa	Anodic peak current
Epa	Oxidation peak at a given potential
ipc	Cathodic currents
Epc	Reduction peak at a given potential
k_o	Rate constant
n	Number of electrons change
S	Entropy
G	Gibb's free energy
D_o	Diffusion coefficient
C_{ox}	Concentration of oxidization
C_{red}	Concentration of redaction
F	Faraday
R	Gas constant
T	Temperature
V	Voltage
E	Potential
C	Concentrations
t	Time
s	Seconds

ABBREVIATIONS

Glu	Glucose
NiOx	Nickle oxide
Au	Gold
Gr	Graphene
GO	Graphene oxide
M	Matel
IHOAM	incipient hydrous oxide adatom mediator
MWCNTs	multi-walled carbon nanotubes
SWCNTs	single-walled carbon nanotubes
CNTs	carbon nanotubes
HPLC	high-performance liquid chromatography
EPGC	electrochemically pretreated glassy carbon
3D	three-dimensional
NPs	nanoparticles
Ag/AgCl	Silver/Silver Chloride Reference Electrode
CV	Cyclic Voltammetry
LSV	linear sweep voltammetry
CA	Chronoamperometry
FE-SEM	field emission scanning electron microscopy
XRD	X-ray powder diffraction
EDAX or EDX	Energy Dispersive X-ray spectroscopy
TEM	high resolution transmission electron microgr XP
RSD	relative standard deviation
XPS	X-ray photoelectron spectroscopy
EIS	Electrochemical impedance spectroscopy
AFM	atomic force microscopy
CTAB	cetyl trimethylammonium bromide
LOD	low limit of detection
GC/GCE/GCD	Glassy Carbon electrode
GCox	Oxidized Glassy Carbon electrode
NiONFs	NiO nanofibers
NA	Nafion

AIM OF THE WORK

AIM OF THE WORK

The present work is devoted for the development of a novel anode for the non-enzymatic glucose oxidation, i.e., Nickle oxide(NiOx) nanoparticles modified onto a suitable underlying modified electrode. It is expected that the properties of the deposited nanoparticles via controlling its morphology and crystallographic orientation to catalyse the glucose oxidation. Direct glucose fuel cells offer the potential for longevity as compared with other types of fuel cells. The catalyst is fabricated electrochemically, and is characterized by SEM, EDX and cyclic voltammetry.

- In definite points, the present work aimed at:

1- Electrocatalytic oxidation of glucose at nickel oxide modified gold electrode.

2- Impact of glucose as an additive on the deposition of nickel on the electrooxidation behavior of glucose in alkaline medium.

3- Improve the quality of electrocatalytic oxidation of glucose by using graphene as an underlying substrate for the deposition of nickel nanoparticles.

SUMMARY

IN

ENGLISH

SUMMARY

Traditional non-renewable energy suffers the accelerating consumption and the world is in an ever-urgent need for innovative solutions for a green power source. Glucose based fuel cells are a promising solution. However, the electrooxidation of glucose is a sluggish one and obtained only at a considerable overpotential at precious metals. In addition, the electrode suffers poisoning from the oxidation products. Thus, replacing the precious metal with a cheap one and/or decreasing the cost using deposition of nanoparticles with exceptional catalytic properties might be a good solution.

Catalytic properties of metal and metal oxides nanoparticles depend extensively on the morphology and the crystallographic orientation of such catalyst, in addition to the underlying substrate which could enlarges the useful use of the deposited nanoparticles and enhances the adsorption properties of glucose. In this work the fabrication of a metal nanoparticles and/or metal oxides nanoparticles on a suitable underlying substrate aiming at a superior electrocatalytic oxidation of glucose at those modified electrodes are introduced. A suitable underlying substrate, like glassy carbon electrodes, with its extraordinary high conductivity, specific surface area and chemical inertness could serve as an optimum underlying substrate for metal and metal oxides nanoparticles, especially if it is specifically functionalized with some groups that

could control the interphase properties enlarging the useful use of the deposited tailored nanoparticles.

The present thesis includes four chapters ; brief outlines of these chapters are given below;

***Chapter I*:** is the "Introduction and literature survey " part. It outlines Scope of electrochemistry of the work presented in this thesis. In addition, some applications of electrochemistry paying attention to glucose electrooxidation. Also, the literature survey of the electrocatalytic oxidation of glucose, enzymatically and non-enzymatically, on various electrocatalyst either mono, binary or ternary catalysts along with the underlying substrates commonly used is outlined.

***Chapter II*:** Experimental details including fabrication and characterization of modified electrodes, working procedures and apparatus used are given.

***Chapter III*:** Results and discussion section, it includes three parts III1, III2and III3. It presents the results regarding;

1- Fabrication of nickel oxide (NiO_x) nanoparticles catalyst modified gold (Au) electrode for the electro-oxidation of glucose in alkaline medium. The modified electrodes were morphologically and electrochemically characterized. It has been found that the electrocatalytic activity critically depends on the additive (glucose) in deposition bath.

2- A nickel oxide (NiO_x) nanoparticles modified glassy carbon (GC) electrode, designated as GC_{ox}/NiO_x (Glu), were fabricated from a nickel bath (0.02 M $NiSO_4$ + 0.03 M $NiCl_2$ + 0.03M H_3BO_3) containing a suitable additive, typically glucose, and then applied for the electrocatalytic oxidation of glucose.

3- The glassy carbon (GC) electrode casted by graphene (Gr) and then modified with (NiOx) nanoparticles is also applied for glucose oxidation.

CHAPTER
I

INTRODUCTION

AND

LITERATURE SURVEY

CHAPTER I

INTRODUCTION AND LITERATURE SURVEY

1. Introduction

In this chapter, a brief overview of electrochemistry fundamentals relevant to results presented in the present work will be overviewed. The main character of the thesis (glucose oxidation) is described by introducing some of its biological fundamental, chemistry, and utilization. Glucose electrooxidation will then be discussed starting from its history, classification and definitions emphasizing the most important applications involving this topic.

1.1. Scope of electrochemistry [1]

Electrochemistry is the branch of chemistry that deals with the chemical changes produced by electricity and the reverse. These changes occur in solutions in a homogeneous or heterogeneous manner on the electrode surface. The transshipment reaction causes two or more opposing events in opposite directions to ensure electroneutrality. In the case of homogeneous oxidation and reduction reactions, they often occur on electrodes immersed in the cell solution and separated into space. The

charges are transported between electrodes either ionically in solution or externally by electric wire. The products can be separated in the two electrode reactions if the cell configuration permits. For batteries energy, the sum of the free energy changes at both electrodes need to be negative. External electrical energy can be provided if the total free energy is positive, leading to the binding of electrode reactions and the conversion of chemicals.

1.2. The nature of electrode reactions [1]

1.2.1. Electrode reactions.

Heterogeneous electrode reactions occur in an area where the charge distribution differs from those phases between the electrode and the solution. The structure of the interlayer affects the electrode process. In the following section, the kinetics and thermodynamics of electrode processes are summarized.

1.2.2. Thermodynamics and kinetics of electrode reaction

For half-reactions at equilibrium, the potential, *E,* can be related to the standard electrode potential through the *Nernst equation:*

$$E = E^{\theta} - \frac{RT}{nF}\sum Vi \ \ln a_i \qquad (1.1)$$

where a_i are the activity of species and v_i, are the stoichiometric numbers, positive for products (reduced species) and negative for reagents (oxidized species). The tendency for the reduction to occur, relative to the NHE reference, is thus given by;

$$AG^{\theta} = -n\,FE^{\theta} \qquad (1.2)$$

In term of activity ($a_i = \gamma_i c_i$ with γ_i, the activity coefficient of species I and c is the concentration of this species) The Nernst equation (1.1) is rewritten as

$$E = E^{\theta} - \frac{RT}{nF}\sum Vi\ \ln c_i \qquad (1.3)$$

in which E^{θ} is the formal potential.

Nernst equation can be applied if the oxidized and reduced species are in equilibrium at the electrode surface. The electrode reaction is then known as a *reversible* reaction. Thus, Nernst equation, and therefore reversibility is considered in the term of the time allowed for the electrode reaction to reach equilibrium.

The concentrations of species at the interface depend on the mass transport of these species from bulk solution, often described by the mass transfer coefficient k_d. *A* reversible reaction corresponds to the case where

the kinetics of the electrode reaction is much faster than the transport. The kinetics is expressed by a standard rate constant, k_0, which is the rate constant when $E = E^{\theta}$. So, the criterion for a reversible reaction is $k_o \gg k_d$.

By contrast, an *irreversible* reaction is one where the electrode reaction cannot be reversed. A high kinetic barrier has to be overcome, which is achieved by application of an extra potential (extra energy) called the *overpotentially,* η , and in this case $k_o \ll k_d$.

Quasi-reversible reactions exhibit behavior intermediate between reversible and irreversible reactions, the overpotential having a relatively small value, so that with this overpotential reactions can be reversed.

The potential-dependent expression for the rate constant of an electrode reaction is, for a reduction,

$$k_c = k_0 exp\left[-\alpha_c nF(E - E^{\theta})/RT\right] \qquad (1.4)$$

and for an oxidation

$$k_a = k_0 exp\left[\alpha_a nF(E - E^{\theta})/RT\right] \qquad (1.5)$$

In these equations α_c and α_a are the cathodic and anodic *charge transfer coefficients* and are a measure of the symmetry of the activation barrier, being close to 0.5 for a metallic electrode and a

simple electron transfer process. As mentioned above, the standard rate constant is the rate constant at $E = E^{\theta}$.

An alternative way used to express the rates of electrode reactions is through the *exchange current,* I_0. This is the magnitude of the anodic or cathodic partial current at the equilibrium potential, E_{eq}.

1.3. Applications of electrochemistry

There are a wide range of applications including: voltammetric, electroanalysis and potentiometric, electroplating, fuel cells, industrial electrolysis, electrochemical machining, as well as a lot of related applications, for example, suppression of corrosion; bioelectrochemistry and biosensors.

1.3.1. Electrocatalysis:

The *electrochemical* reaction is carried out in three basic steps as shown in Figure 1.1(I) the transfer of the reactive material in the electrolyte interface, (II) the transfer of the electron between the reactant and the electrode, and the adsorbent (III) which results in the formation of products. The main reason for the use of a catalyst in an electrochemical reaction is to either reduce the activation energy to a step limiting the rate or to look for an alternative reaction pathway [2] as

shown in Figure 1.2. *Electrocatalysis* includes either homogeneous or heterogeneous processes as in conventional chemical catalysis.

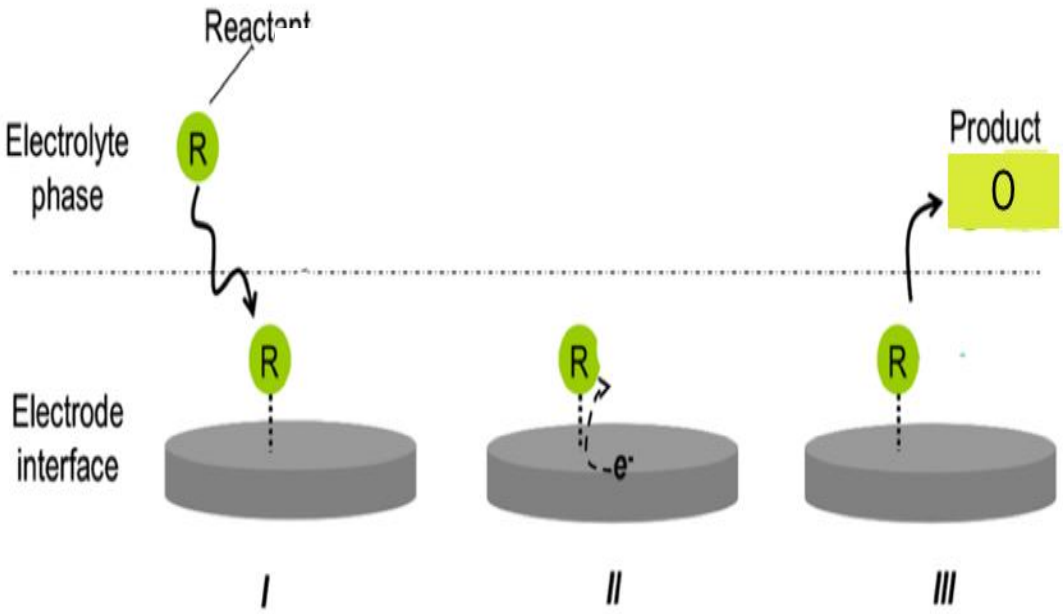

Figure 1.1. Main steps (I – III) of an electrochemical reaction with electron transfer from the electrode to an adsorbed species on its surface (a reduction reaction).

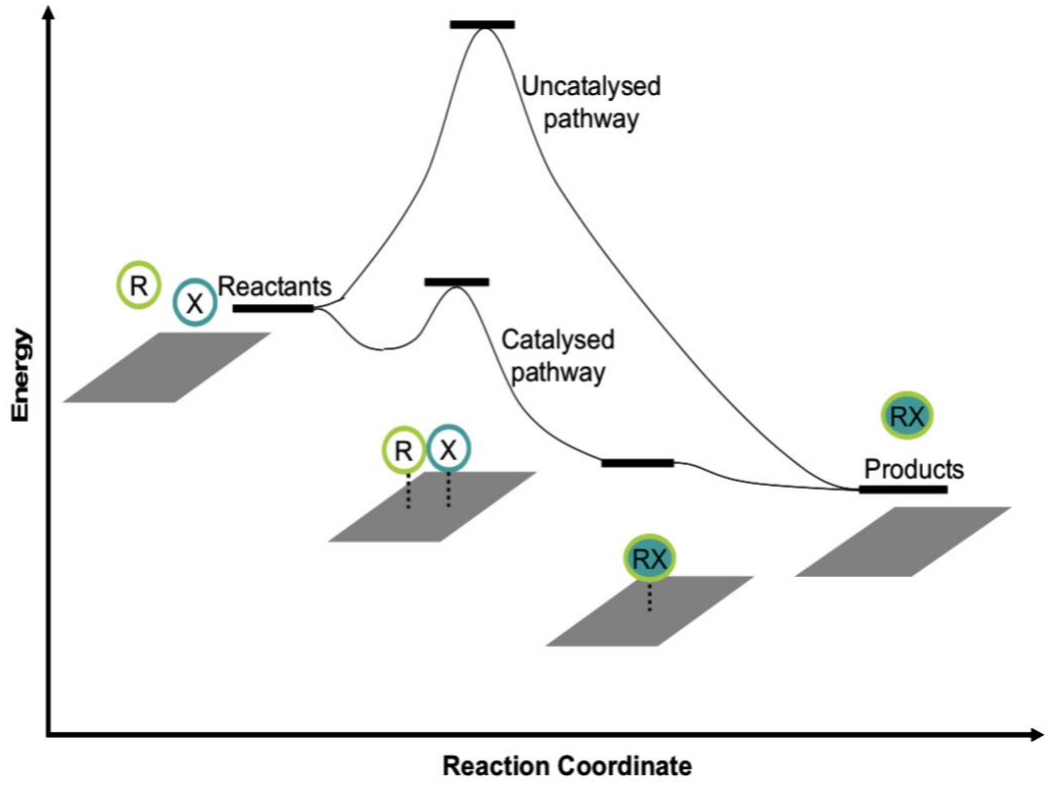

Figure 1.2. Schematic representation of catalysed and uncatalysed reaction pathways [3].

As represented in Fig. 1.2, the reaction activation barrier decreases and the reaction rate rises because the reaction rate is mainly controlled by the highest activation along the reaction coordinates. The reaction mechanism is called Langmuir-Hinshelwood when there is a reaction of adsorbed species on the catalyst surface. The mechanism is known as Eley-Rideal [4] if one of the reactants is obtained directly from the liquid or gas phase.

There are many applications of electrocatalysis as shown in Figure 1.3 for heterogeneous catalysts and the basis for development and research. The use of electrical catalysts has many advantages, including more efficient conversion of chemistry to electrical energy (in a fuel cell), more efficient use of energy (in an electrolysis cell), a more selective way of reacting (i.e., greater productivity than the desired product), and low cost of materials.

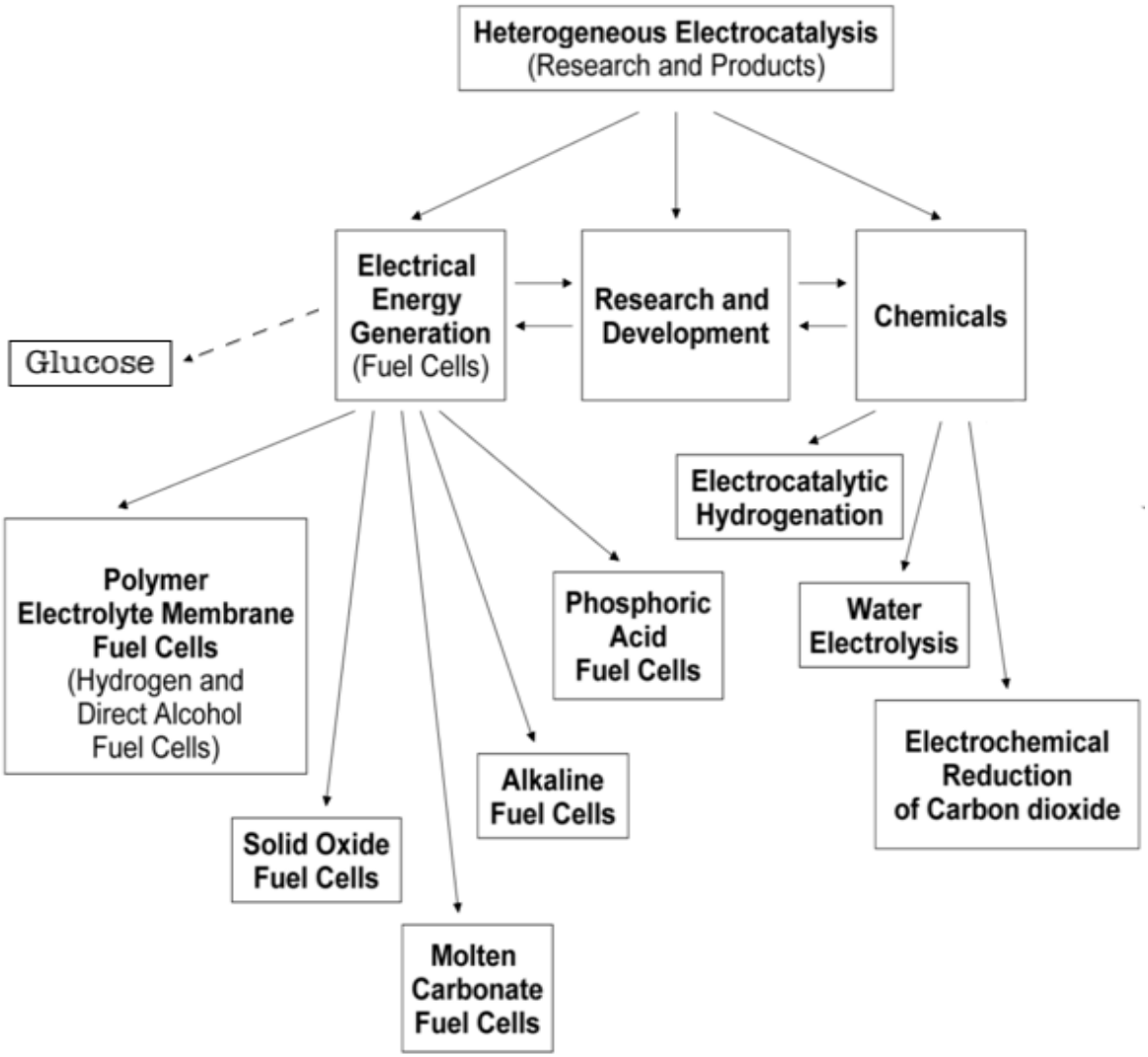

Figure 1.3. Various applications, research and development areas of heterogeneous electrocatalysis [5].

1.3.2. Potential step and sweep techniques [2]

1.3.2.1. Chronoamperometry

Chronoamperomety is where the current from an electrochemical procedure is estimated carefully as a function of time [6,7]. The potential of the working electrode is stepped to a certain potential and the resulting current from faradaic processes occurring at the electrode (caused by the potential step) is monitored as a function of time. A single (Figure 1.4) or double potential step to the working electrode of the electrochemical system is applied.

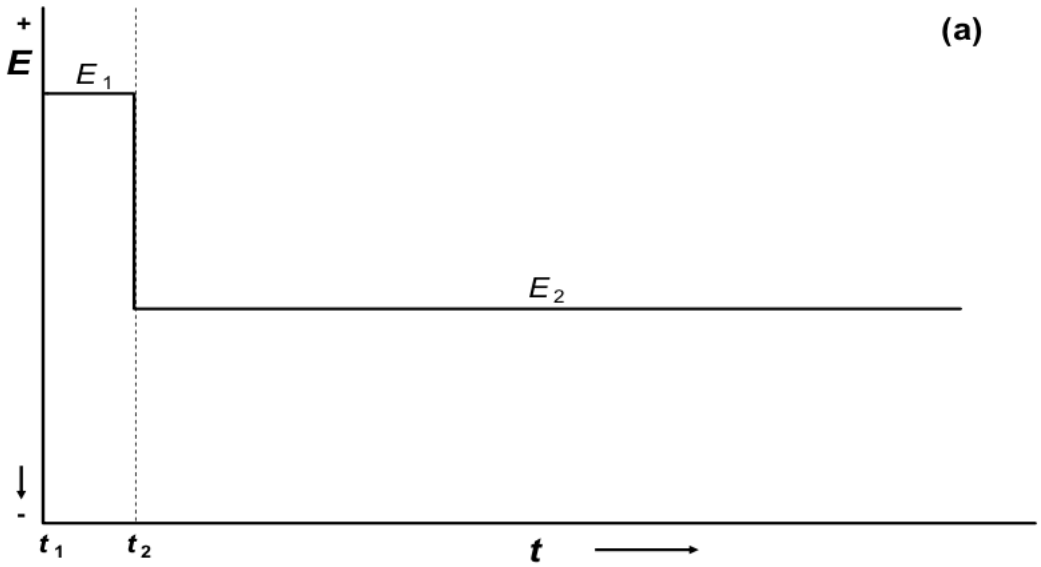

Figure 1.4. (a) Potential stepping waveform in a typical experiment in which a species of interest is electro inactive at E_1, but is reduced at a diffusion-controlled rate at E_2 [2].

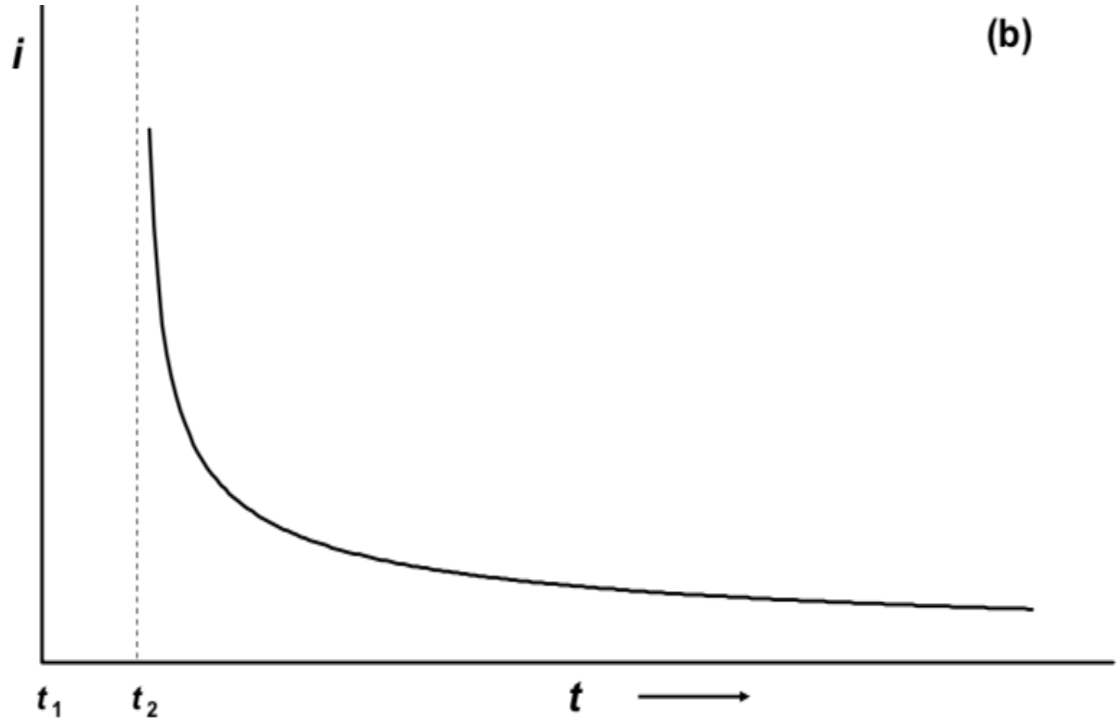

Figure 1.4. (b) Chronoamperometric response as a result of the waveform perturbation described in (a) [2].

1.3.2.2. Voltammetry

Voltammetry (*volt-amperometry*) contains a unique gathering of chronoamperometric electrochemical techniques in which data about an electrochemically-active species is gotten from the measurement of current through a working electrode as a function of time, while the applied potential to the electrode is controlled as a linear function of time [8]. The utilization of the three electrodes (working, counter, and reference), alongside the potentiostat instrument, allows accurate

application from the electrochemical cell of a perturbation potential waveform and the measurement of the resultant signal. Usually, a voltammogram is acquired during the potential sweep by measuring the current at the working electrode. The primary event is the oxidation or reduction of a chemical species at a working electrode and the *i-E* response measured can be considered as an 'electrochemical spectrum' in particular, information is obtained as if oxidation and reduction occurs [6, 9,10].

The technique can provide thermodynamic information as well as kinetic parameters related to electron transfer reactions at an electrode-solution interface. In addition, voltammetry can provide information related to the kinetics and mechanisms of chemical reactions subsequent to an electron transfer step. Some of the main advantages of sweep voltammetry are based on the fact that a wide potential range can be scanned rapidly for reducible and oxidizable species. These experiments can also be performed with variable time scales by applying different potential scan rates [6, 9,10].

Cyclic voltammetry (CV)

Cyclic voltammetry is a method for investigating the electrochemical behavior of a system. It was first reported in 1938 and

described theoretically by Randies [11]. Cyclic voltammetry is the most widely used technique for acquiring qualitative information about electrochemical reactions. The power of cyclic voltammetry results from its ability to rapidly provide considerable information on the thermodynamics of redox processes, on the kinetics of heterogeneous electron-transfer reactions, and on coupled chemical reactions or adsorption processes. Cyclic voltammetry is often the first experimental approach performed in an electroanalytical study, since it offers rapid location of redox potentials of the electroactive species and convenient evaluation of the effect of media upon the redox process [12-14].

Basic principles of Cyclic Voltammetry

A cyclic voltammogram is obtained by applying a linear potential sweep (that is, a potential that increases or decreases linearly with time) to the working electrode. As the potential is swept back and forth past the formal potential, E°, of an analyte, a current flow through the electrode that either oxidizes or reduces the analyte. The magnitude of this current is proportional to the concentration of the analyte in solution, which allows cyclic voltammetry to be used in an analytical determination of concentration.

The equipment required to perform cyclic voltammetry consists of a conventional three-electrode potentiostat connected to three electrodes (working, reference and auxiliary) immersed in a test solution. The potentiostat applies and maintains the potential between the working and reference electrode while at the same time measuring the current at the working electrode.

Voltammetry is a collection of electroanalytical techniques in which the current is measured as a function of applied potential of certain waveform (Fig. 1.5). The excitation signal for CV is a linear potential scan with triangular waveform as shown in Fig. 1.5. This triangular potential excitation signal sweeps the potential of an electrode between two values, sometimes called the switching potential. It is widely used by chemists for non-analytical purposes including fundamental studies on redox processes, adsorption processes on surfaces, electron transfer mechanisms and electrode kinetics. Oxidation potentials, diffusion coefficients and electron transfer rates are readily obtained using electroanalytical methods.

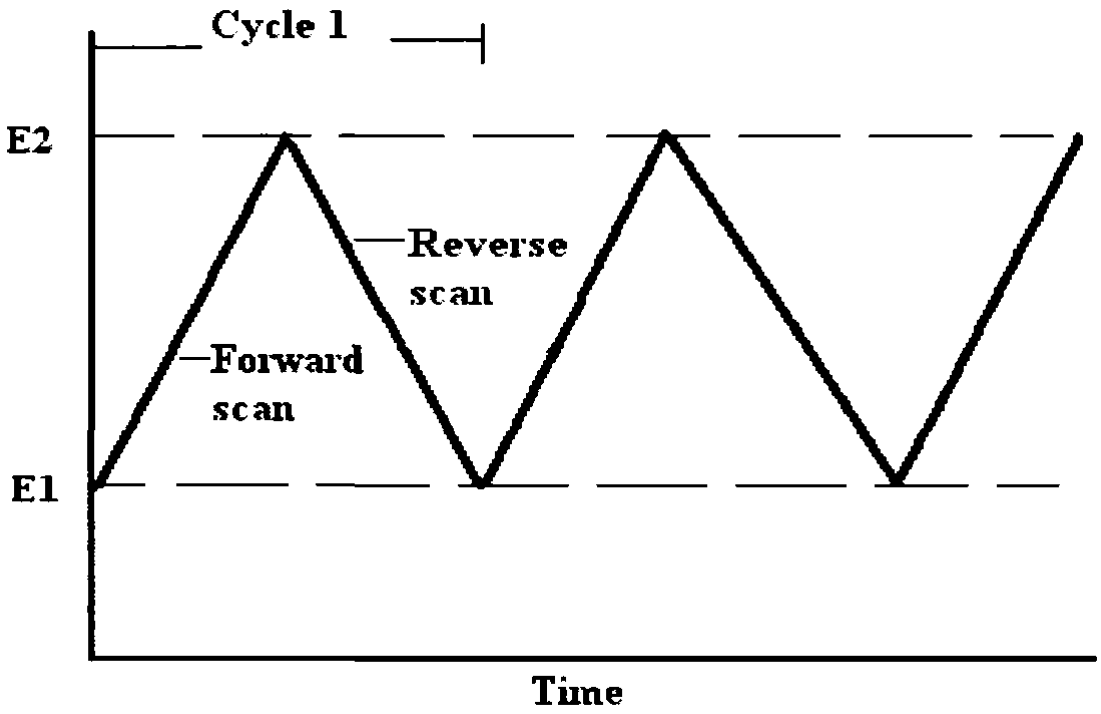

Figure 1.5. Variation of the applied as a function of time in a cyclic voltammetry experiment [11].

In CV the electrode potential between potential limits E1 and E2 at a known sweep rate (also called scan rate) is scanned. On reaching limit E2 the sweep is reversed to E1 to obtain a cyclic scan. The CV scan is a plot of current verses potential and indicates the potential at which redox process occur, and the result is referred to as a cyclic voltammogram. A peak in the measured current is seen at a potential that is characteristic of any electrode reaction taking place. The peak width and height for a particular process may depend on the sweep rate, electrolyte concentration and the electrode material [15,16].

The CV is usually initiated at a potential where species are not electroactive. The important parameters of a cyclic voltammogram are the magnitudes of anodic peak current (i_{pa}), the cathodic peak current (i_{pc}), the anodic peak potential (E_{pa}) and cathodic peak potential (E_{pc}). The basic shape of the current versus potential response for a cyclic voltammetry experiment is shown below (Fig. 1.6).

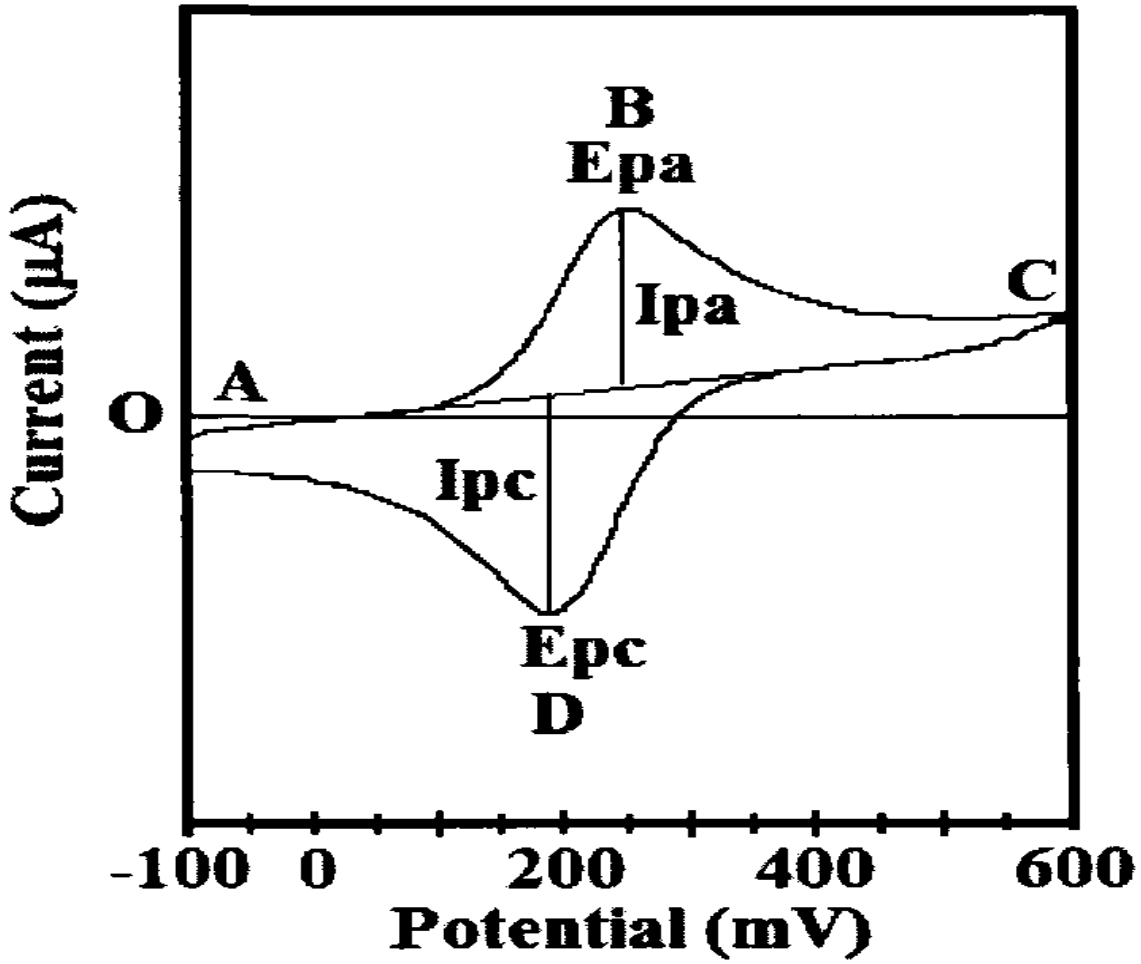

Figure 1.6. A typical cyclic voltammogram of current potential [11].

At the start of the experiment, the bulk solution contains only the reduced form of the redox couple (R) so that at potentials lower than the redox potential, i.e. the initial potential, there is no net conversion of R into O, the oxidized form (point A). As the redox potential is approached, there is a net anodic current which increases exponentially with potential. As R is converted into O, concentration gradients are set up for both R and O, and diffusion occurs down these concentration gradients. At the anodic peak (point B), the redox potential is sufficiently positive that any R that reaches the electrode surface is instantaneously oxidised to O. Therefore, the current now depends upon the rate of mass transfer to the electrode surface. Upon reversal of the scan (point C), the current continues to decay and a peak shaped response (point D). If a redox system remains in equilibrium throughout the potential scan, the electrochemical reaction is said to be reversible. In other words, equilibrium requires that the surface concentrations of O and R are maintained at the values required by the Nernst Equation.

The transfer of electrons to or from the substrate is an activated process. The electron transfer process can be

i. Reversible process
ii. Irreversible process and
iii. Quasi-reversible process

Reversible Electron Transfer Process

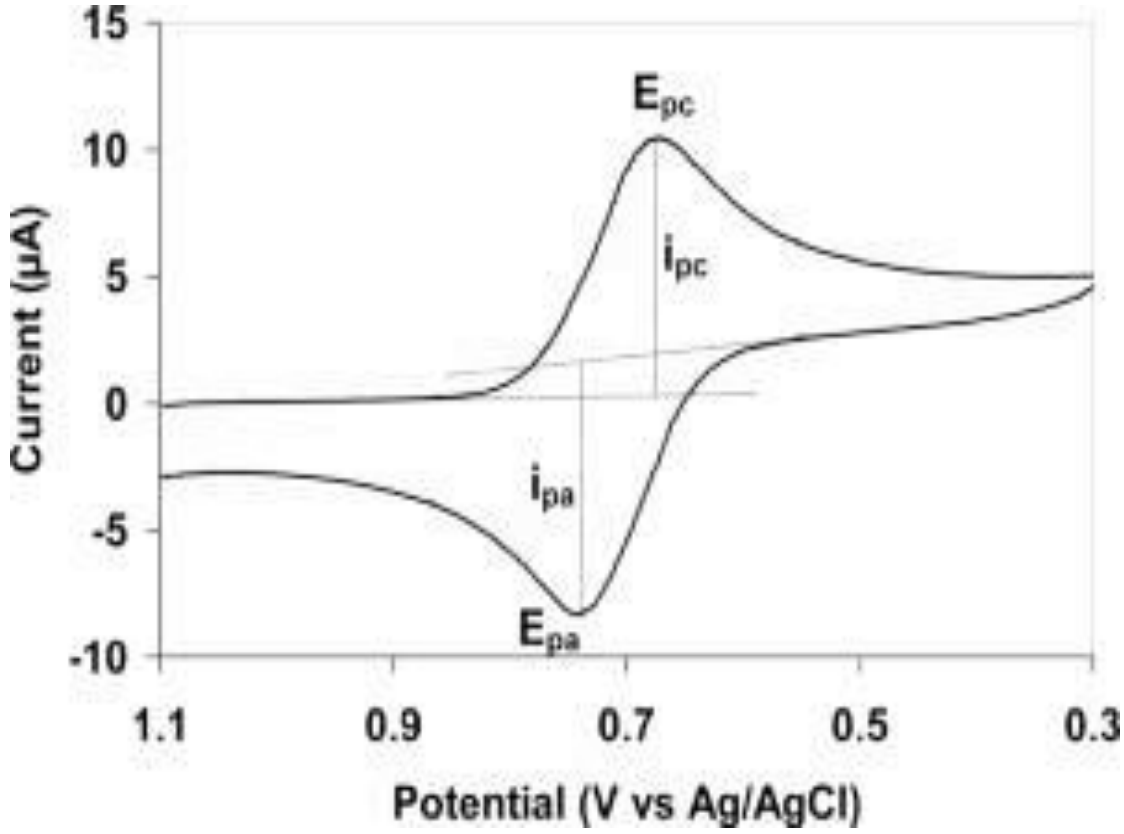

Figure 1.7. Typical voltammogram for a reversible process.

For a reversible process, oxidation and reduction peak is observed as shown in Fig. 1.7 in which E_{pa} and E_{pc} are potentials of anodic and cathodic peaks, respectively, and i_{pa} and i_{pc} are the corresponding currents. Reversibility can be defined as chemical or electrochemical. In an electrochemically reversible process the electron transfer is not rate limiting. For a chemically reversible process, both forms of redox couple (O for oxidized form and R for reduced form) are stable in the time scale

of measurement. The rate of electron transfer is fast compared to the rate of mass transport and does not control the overall rate. In this process the rate of the reaction is fast enough to maintain equal concentration of the oxidized and reduced species at the surface of electrode. The concentration C_{ox} and C_{red} of oxidized and reduced forms of the redox couple respectively follow the Nernst equation

$$E = E^{\circ} + \frac{RT}{nF}\, Ln\, \frac{C_{ox}}{C_{red}} \qquad (1.6)$$

where, n= number of electrons transferred, F= Faraday constant, R= gas constant and T= temperature. If the system is diffusion controlled then the Fick's law of diffusion holds for both oxidation and reduction. Under these conditions, peak current is given by Randies Sevcik equation;

$$i_p = (2.69 \times 10^5) n^{3/2}\, A\, D_o^{1/2}\, C_o\, \nu^{1/2} \qquad (1.7)$$

where n is the stoichiometric number of electrons involved in the electrode reaction, A is the area of electrode in cm^2. D_o is the diffusion coefficient of the species O in $cm^2 s^{-1}$, C_o is the concentration of the species O in mol/cm^3 and υ is the scan rate in Vs^{-1}.

Irreversible Electron Transfer Process

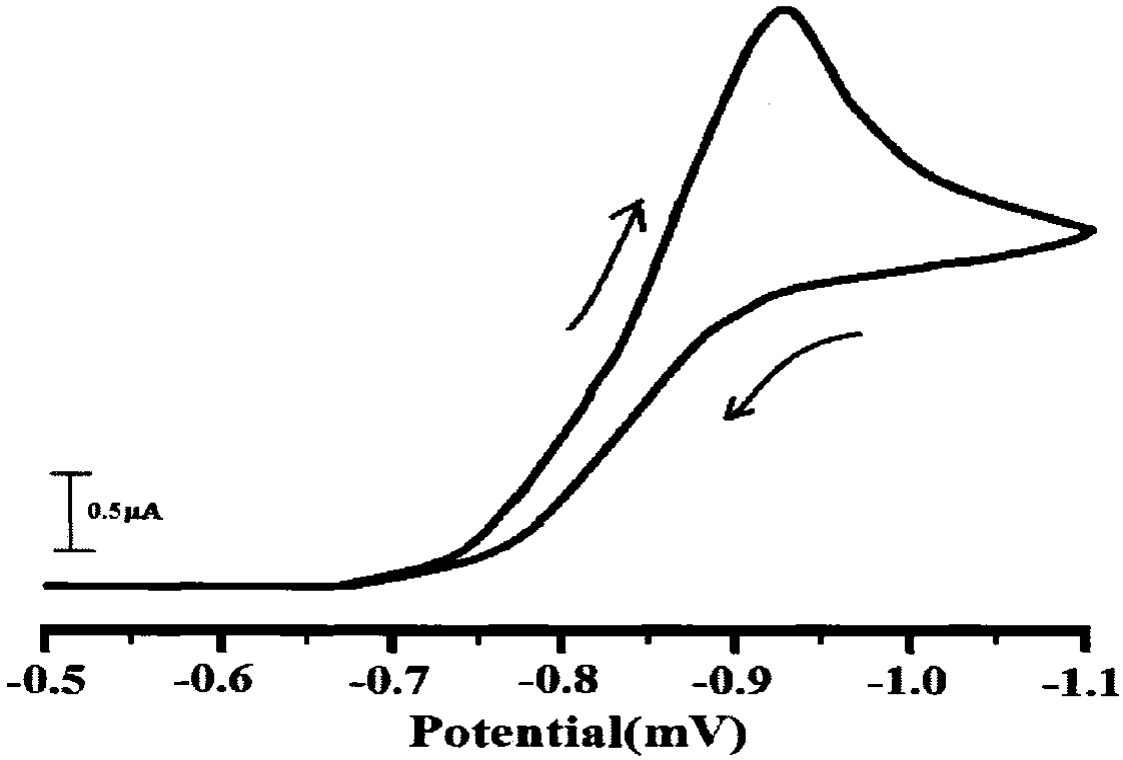

Figure 1.8. Typical voltammogram for an irreversible process [11].

For an irreversible process, only forward oxidation or reduction peak is observed (Fig. 1.8). This process is usually due to slow electron exchange or slow chemical reactions at the electrode surface [17]. In an irreversible electrode process, the mass transfer step is very fast as compared to the charge transfer step.

For an Irreversible reaction, the peak current is given by [18]

$$i_p = (2.99 \times 10^5) n\,(\alpha n)^{1/2} A\, D_o^{1/2}\, \nu^{1/2}\, C_o^* \qquad (1.8)$$

$$(\alpha n_a) = \frac{47.7}{E_p - E_{p/2}} \qquad (1.9)$$

The value of E_p, the difference between the cathodic and anodic peak is given by equation 1.9. The peak separation E_p is a factor determining the reversibility or irreversibility of an electrode reaction.

Quasi Reversible Electron Transfer process

Quasi-reversible process is intermediate between reversible and irreversible systems (Fig. 1.9). The current due to quasi-reversible processes is controlled by both mass transport and charge transfer kinetics [19]. The process occurs when the relative rate of electron transfer with respect to that of mass transport is insufficient to maintain Nernst equilibrium at the electrode surface. In the quasi-reversible region both forward and backward reactions contribute to the observed current. The equation by Nicholson is normally used to calculate electron transfer rate constants [20].

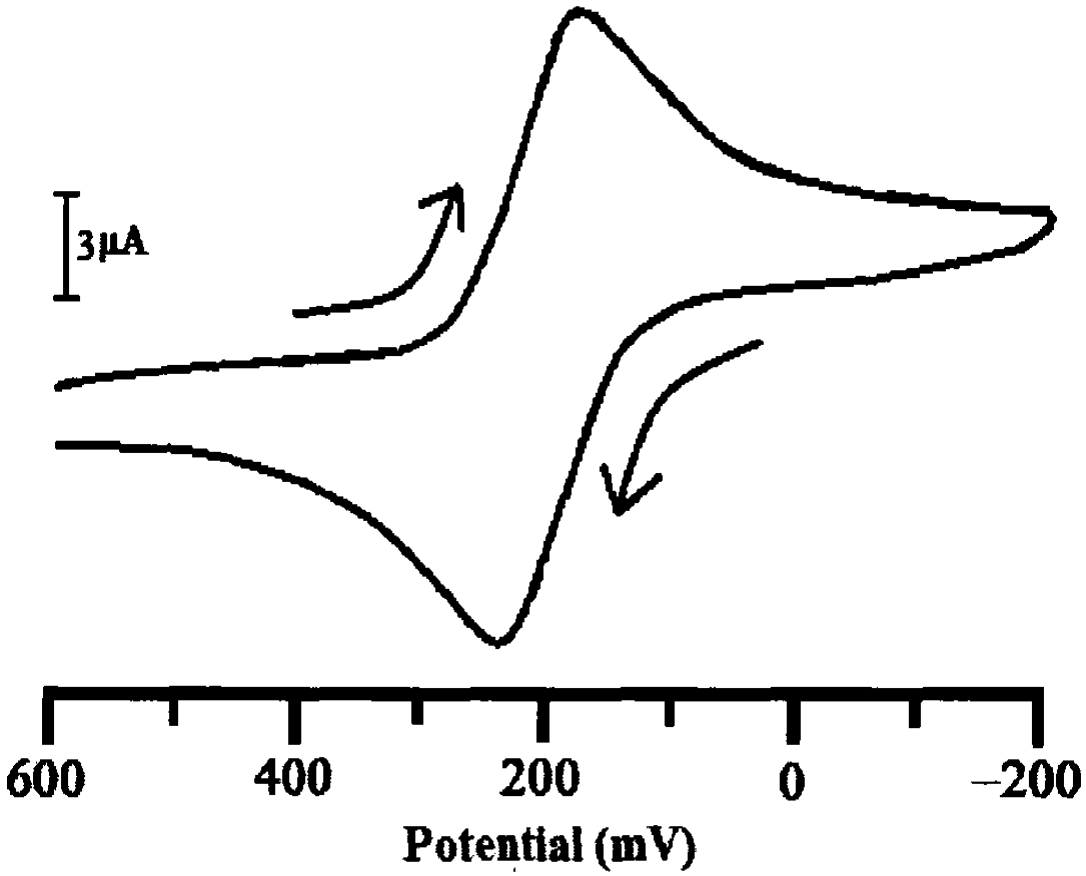

Figure 1.9. Typical voltammogram for a quasi-reversible process [11].

1.4. Electrocatalysis at nanomaterials

Nanomaterials are solid materials that have dimensions at the nanoscale. In general, nanomaterials are fabricated either by size reduction of bulk materials, the so called top-down, or, starting from the atomic level and build up the nanomaterials, the so-called bottom-up approach. The former one is based on physical processes like crushing or grinding, and usually adopted by Engineers. Bulk material is ventured into the nanometer range via miniaturization. Using this approach, it is

difficult to prepare nanomaterials of uniform shapes. In addition, nanomaterials prepared by this approach suffers from imperfections and significant damage of the crystallographic orientation of the surface [21]. Synthesis of nanomaterials considering the route can be subdivided into top-down and bottom up, and in view of routes, it can be subdivided into physical and chemical methods. It can also be subdivided in terms of phase of medium for preparation into gas phase/ liquid phase/ aerosol phase and Solid phase. Selection of the route, of course, depends on the purpose of preparing the nanomaterials.

In the other hand, bottom –up approach includes the build-up of a material from the bottom: atom-by-atom, molecule-by-molecule or cluster-by-cluster. It utilizes the chemical and/or physical forces in assembling basic units into larger structures in the nano range. This approach avoids most of the problems encountered by the previous approach. In addition, it provides several alternative ways to control onto scale dimension. Thus, it is often used for fabricating nano-scale materials characterized by a uniform size, shape and distribution. This route is approached by chemical synthesis by which a tailored nanomaterial can be assembled.

1.5. Nanomaterials for the direct oxidation of glucose

Detection of glucose oxidation directly at an electrode is one of the most important research in non-enzymatic glucose sensors. However, there are several limitations in it such as the need for a large applied potential and slow reaction kinetics, which decreases specificity [22]. Nanomaterials have helped to overcome these limitations and thereby have allowed the development of direct-oxidation glucose sensors as replacements for biological recognition sensors.

1.6. Glucose

It is a simple sugar with the molecular formula $C_6H_{12}O_6$. Glucose is the most abundant monosaccharide, a subcategory of carbohydrates. Glucose is mainly made by plants and most algae during photosynthesis from water and carbon dioxide, using energy from sunlight. In energy metabolism, glucose is the most important source of energy in all organisms. Glucose for metabolism is partially stored as a polymer, in plants mainly as starch and amylopectin and in animals as glycogen. Glucose circulates in the blood of animals as blood sugar. The naturally occurring form of glucose is D-glucose, while L- glucose is produced synthetically in comparatively small amounts and is of lesser importance. Glucose is a monosaccharide containing six carbon atoms and an

aldehyde group and is therefore referred to as an aldohexose. The glucose molecule can exist in an open-chain (acyclic) and ring (cyclic) form, the latter being the result of an intramolecular interaction between the aldehyde C atom and the C-5 hydroxyl group to form an intramolecular hemiacetal [23].

1.6.1. Chemical properties

With six carbon atoms, it is classed as a hexose, a subcategory of the monosaccharides. D-Glucose is one of the sixteen aldohexose stereoisomers. The D-isomer, D-glucose, also known as dextrose, occurs widely in nature, but the L-isomer, L- glucose, does not. Glucose can be obtained by hydrolysis of carbohydrates such as milk sugar (lactose), cane sugar (sucrose), maltose, cellulose, glycogen, etc. All forms of glucose are colorless and easily soluble in water, acetic acid, and several other solvents. They are only sparingly soluble in methanol and ethanol.

1.6.2. Practical applications

Electrochemical oxidation of glucose has generated much interest over the years. It has been extensively studied for applications in glucose sensors, [23] whose optimization (in terms of response time, lifetime, sensitivity and selectivity) is required to improve the treatment of Diabetes Mellitus, a chronic disease affecting millions of people around

the world [24]. Most studies on this subject have involved the use of the enzymes to catalyze the oxidation of glucose to δ-gluconolactone [23]. Although enzymatic detection usually shows good selectivity and high sensitivity, the enzyme is easily denatured during its immobilization process. The most serious problem of such sensors is the inherent lack of stability due to the sensitive nature of enzymes, especially in implantable devices that represent the new frontier in diabetes management. Non-enzymatic glucose sensors have been studied in order to develop effective enzyme-free sensors. Much attention has also been paid to the electrocatalytic oxidation of glucose for the construction of glucose-air biofuel cells and abiotically catalyzed fuel cells. In comparison with other fuel cells, this new type is powered with glucose derived from degradable biomass. Moreover, the direct glucose fuel cell is of high energy-density. Theoretically, glucose can be completely oxidized to CO_2 and H_2O, releasing 24 electrons per glucose molecule [25].

1.7. Mechanism of glucose oxidation on electrode surface

The glucose oxidation rate and its detection are mainly influenced by the electrochemical factors on the surface of the electrode. The glucose oxidation mechanism on the surface of the electrode is unclear, but two main models have been proposed to explain them [26-28].

The first model, discovered by the researcher Pletecher [29]. This model is known as chemisorption activator. The mechanism occurs by forming a part of the glucose bond with the surface of the electrode through the process of adsorption with the help of electric balls. At the same time, the hydrogen atom is extracted in the part of the glucose (see Figure 1.10), which is attached to hemiacetal carbon [26,27,30].

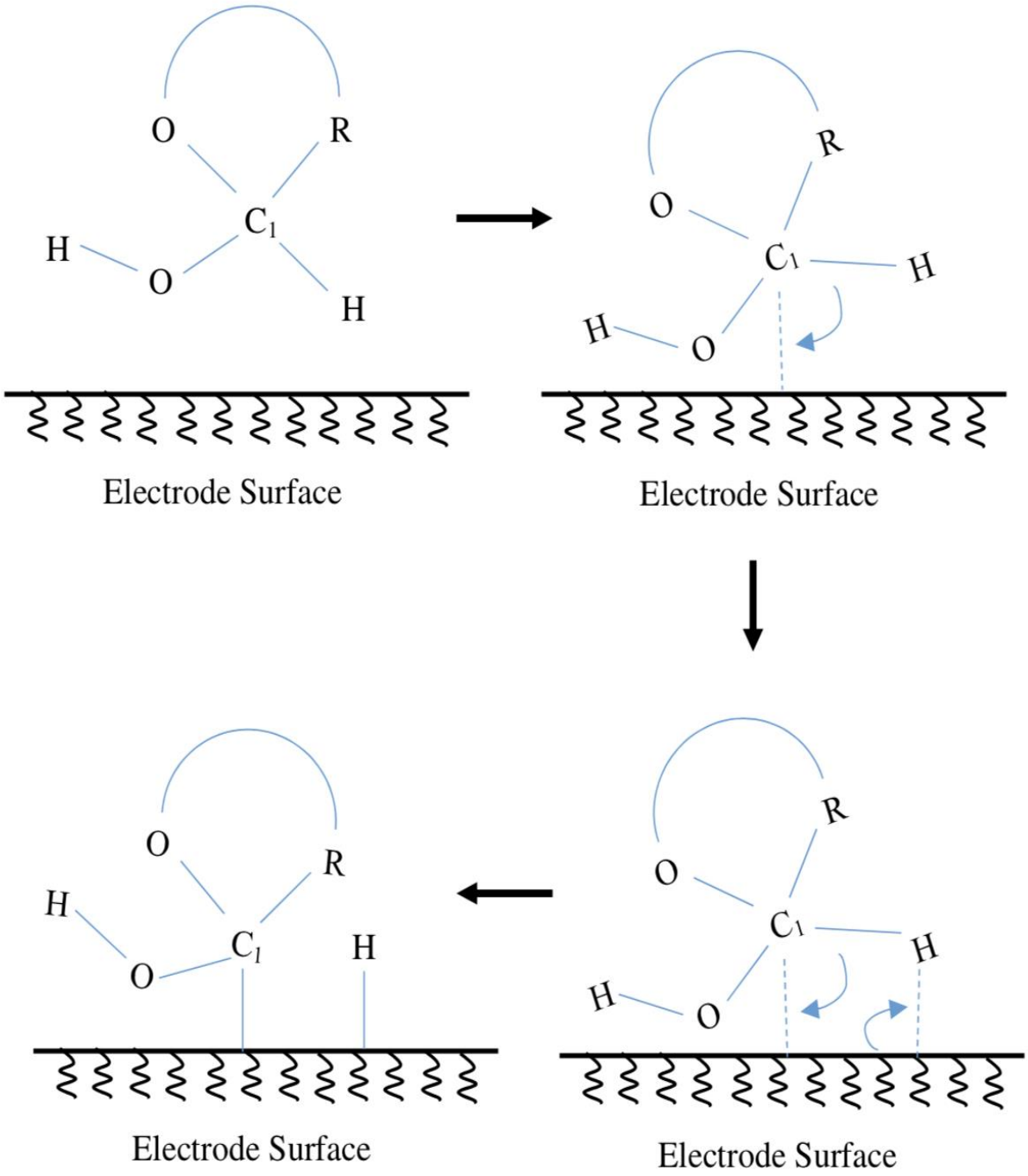

Figure 1.10. An example of the concentric adsorption theory with adjacent adsorption sites proposed by Pletcher. C1: hemiacetalic carbon atom. R: the other parts of the glucose molecule [31]

After extraction the hydrogen atom is associated with the electrode surface and the link is near the selected glucose. There is a change in the interaction of the glucose with the metal because of the change in the case of oxidation of the part of the glucose at the metal electrode. So, the effect of the strength of the link between the glucose and the metal occurs, which leads to the adsorption of the part of the glucose on the surface of the electrode. A strong intermediate bond is needed in the electro-catalytic process to form and break the bonds on the surface of the electrode and on the glucose molecules. Therefore, a strong, intermediate bonding force must be available in this method, and this association helps to adsorption (Formation of the bonds) and operations of desorption (break the bonds).

The second model, discovered by the researcher Burke and named "incipient hydrous oxide adatom mediator" (IHOAM) [28,32]. This model was originally suggested based on the observation that there are active metallic atoms on the electrode surface that have low lattice stability and improved interaction [26,32,33]. Where the metal atoms are subjected to premonolayer oxidation step through which the formation of the primary water oxide, OH_{ads} is formed. This layer is believed to mediate the oxidation of glucose on the electrode surface [33]. Figure 1.11 shows a schematic illustration of the IHOAM model.

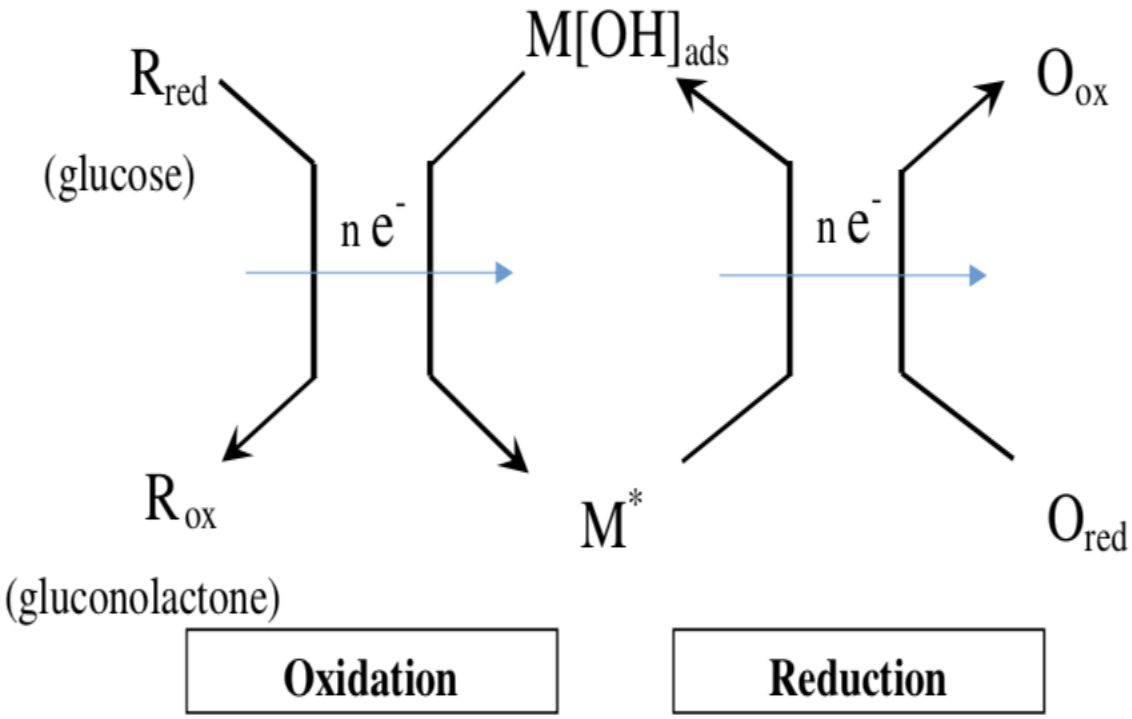

Figure1.11. A schematic illustration of the IHOAM model [31].

1.8. Literature survey

Glucose electro-oxidation is of potential importance in many fields including for example the diagnosis of diabetes mellitus, food preparation and for the development of a category of fuel cells [34-38]. Glucose electrooxidation is realized by catalysis either enzymatically (enzyme-based) or non-enzymatically (enzymeless-based) methods. In the enzymatically based methods, the used enzyme can be utilized in a free state or in an immobilized one.

Enzyme-based electrooxidation is characterized by;

i. High selectivity

ii. It is the widely accepted approach since 1967 [39].

iii. Most of enzymatic sensing electrodes need electron shuttle, i.e., mediators or catalysts [40,41].

In this case, the enzyme converts analyte into electroactive species. However, enzymatic detection of glucose suffers from some restrictions;

i. The prerequisite of a biocompatible matrix as support

ii. Limited stability.

iii. Oxygen deficit under low oxygen pressure.

iv. The difficult immobilization of the enzyme [42,43].

Glucose oxidase (GOD)-based sensor depends on reaction conversion of glucose to gluconic acid, liberating hydrogen peroxide

(H_2O_2). Thus, the glucose was sensed either by measuring the consumption of oxygen or the liberated H_2O_2 [43].

$$\text{Glucose} + O_2 + H_2O \xrightarrow{GOD} \text{gluconic acid} + H_2O_2 \qquad (1.10)$$

Enzyme-based electrodes have been fabricated by several approaches including reversible and irreversible immobilization (Fig.1. 12)

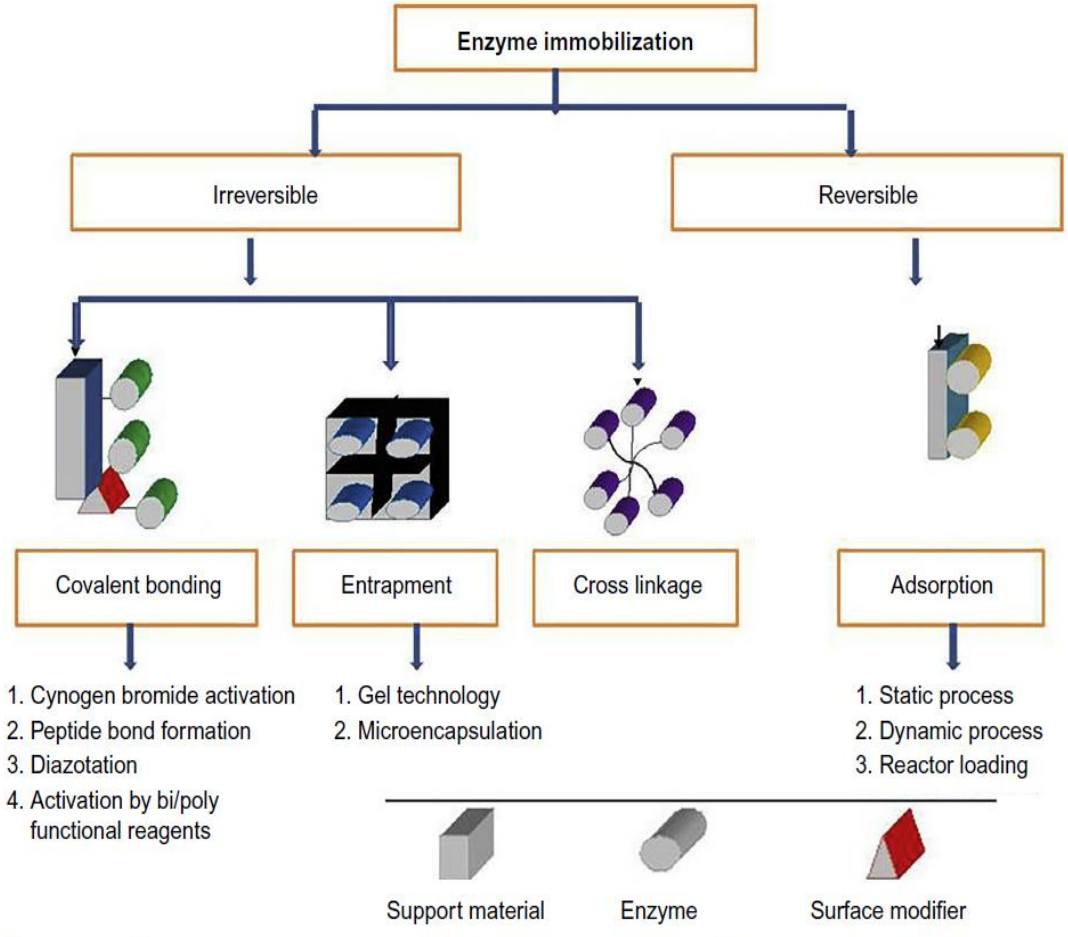

Figure1.12. Classification and representation of different enzyme immobilization techniques.

Reversible immobilization occurs via adsorption which includes the enzyme molecule bounding to the carrier matrix either by hydrogen bonding, van der Waals forces, electrostatic and hydrophobic interactions. This strategy of adsorption fulfills several advantages as for instance simplicity, cost effective and is generally non-destructive toward enzyme activity. However, it suffers several drawbacks as the bound of the enzyme to the carrier matrix is loose. Changes in temperature, pH or ionic strength may result in enzyme desorption. Enzyme leaching from the carrier can be prevented by compounds such as silicone [44].

Irreversible immobilization includes covalent bonding, entrapment and cross- inking. In immobilization via covalent bonding, stable complexes between functional groups on enzyme molecules and a support matrix are formed, taking in consideration that the included functional group of the enzyme in the covalent bond is not essential for enzymatic activity. The enzyme functional groups that could be utilized in covalent coupling include: amino group, carboxylic group, phenolic group, sulfhydryl group, thiol group, imidazole group, indole group and hydroxyl group [45].

In entrapment immobilization, enzyme is entrapped within a polymeric network. Entrapment immobilization process is conducted via mixing the enzyme with a monomer solution, and the subsequent

polymerization of monomer solution either chemically or electrochemically. This method improves enzyme stability and minimize enzyme leaching and denaturation. However, a limitation of the method is the mass transfer resistance occurred as polymerization extension tends to increase the gel matrix thickness [46].

In cross linking immobilization, a bifunctional chemical cross-linker is used. This had several drawbacks such as low activity retention, low mechanical stability, poor reproducibility, and difficulties in handling the gelatinous cross-linked enzymes [47].

Immobilized enzymes, compared with free enzymes, can be operated in a continuous manner and present good stability and wider working concentration range of analytes [48-50], but the lifetime of the enzyme-based sensors is limited [51,52]. Immobilization of the enzymes onto metallic substrates through a thin film of self-assembled monolayer and conducting polymers [53-57] were introduced to increase the life time of enzyme- based sensors. Also, nanostructured materials have been used as an underlying platform for enzymes immobilization because of their large surface-to-volume ratio and high catalytic and surface reaction activity. Using nanomaterials as substrates require some strategies to prevent enzyme leaching from electrode surface [58].

1.8.1. Enzymeless glucose sensors

Enzymeless glucose sensors can overcome the above-mentioned problems, and thus have been uses as a promising alternative for enzyme-based analysis [59]. Electrocatalysts designed for sensing or electrocatalysis of glucose oxidation usually use a single or binary catalyst of metal and/or metal oxides. Noble metals have been extensively used for the purpose of enzymeless electroanalysis of glucose owing to their biocompatibility, good electrocatalytic activity and strong stability [60,61].

Platinum was the first discovered material that demonstrated electrocatalytic activity for glucose oxidation [62]. However, Pt electrode suffer from required large polarization as well as the poisoning by adsorbed intermediates and interfering species. As a result, the sensitivity is low and selectivity is very poor [63-67]. To solve these problems, researchers used another metal as a co-catalyst with Pt with the aim to decrease poisoning. It has been reported that using a sacrificial metal with Pt increase the life time of Pt [68,69]. Pt-based electrocatalysts, PtM (M = Ru, Pd, Au, Ni, Ag, Bi, Pb) received much attention regarding glucose oxidation. They provide rapid response, good stability, and high catalytic efficiency [70-88].

Gold electrode is characterized by oxidizing glucose at relatively low anodic potential, both in neutral and alkaline media, and so shows high selectivity as well as sensitivity towards glucose oxidation. However, the electro-oxidation of glucose at Au electrodes has been faced with two main problems. First is the interference from ascorbic acid (AA), and the other one is the deactivation of the electrode activity by Cl^- ions [89,90]. Chlorides, getting adsorbed at gold active sites inhibit the glucose oxidative-adsorption, which is the first and key step of the failure of the oxidation mechanism [91]. Toghill and Compton reported this problem earlier in 2010 [59]. After that, a number of approaches have been reported including that of gold-modified electrodes [92-96]. Au electrode surfaces with porous structures have been successfully used to eliminate interference from AA [97-102]. Several strategies have been explored for the preparation of nanostructured Au-modified electrodes in recent years. Nanoporous gold electrodes have been prepared mainly by de-alloying [102,103] and anodization [104-107]. Pd coated nanoporous gold films [108] enhanced the catalytic activity and stability of gold electrode for glucose oxidation [109,110]. Pd nanoparticles have been dispersed on a variety of substrates such as indium tin oxide, carbon nanotubes [111,112], epoxy-silver [113], graphene nanohybrids [114], boron-doped diamond [115], and polymers [116-118]. In this correspondence, Au-based bimetallic catalysts, AuM (M = Pt, Pd, Ag)

have been reported [119,120]. Other bimetallic catalysts have been reported albeit not extensively as those of the combination of either Pt or Au with other metals [121].

Cu-modified electrodes, characterized by their low cost and ease of fabrication, have received considerable attention due to their electrocatalytic activity for glucose oxidation [122]. The effect of the underlying substrate on the electrocatalytic properties of copper-modified electrodes has also been reported [123,124]. Recently, combining copper-based materials with carbon nanotubes for glucose detection has been widely investigated. This has been achieved by sputtering cupric oxide on multi-walled carbon nanotubes (MWCNTs) [125,126], electrodepositing copper nanocubes onto vertically-well-aligned MWCNTs [127], electrochemical deposition of copper oxide nanoparticles on horizontally-aligned single-walled carbon nanotubes (SWCNTs) [128], seed-mediated growth synthesis of copper nanoparticles on carbon nanotubes (CNTs) [129], copper oxide nanoleaves decorated CNTs [130] and nanospindle-like cuprous oxide/straight CNT nanohybrids [131].

1.8.2. Metal oxides

Recently, large numbers of transition metal oxides replaced costly noble metals as non-enzymatic electrocatalysts for glucose

electrooxidation [132-142]. Among these oxides, NiOx and CuOx received substantial attention because of their low cost and environmental safety [143-158].

Copper oxides (CuO, Cu_2O), as an important class of p-type semiconductor metal oxides, have attracted considerable attention for use in enzyme free glucose sensors due to their high electrocatalytic activity resulting from the multi-electron oxidation mediated by surface metal oxide layers [159-160]. Since the catalytic activities of the nanoscale materials are shapes dependent, the electrochemical behavior of glucose at nanostructured copper oxides with various morphologies have been studied [161-167].

Electrocatalytic materials containing nickel redox couple Ni(II)/Ni(III) received much interest devoted to investigations of the electrochemistry of a nickel hydroxide/oxyhydroxide couple [168-171]. Nickel oxyhydroxide has high affinity for the adsorption of some organic substances and electrocatalyze their oxidation via mediation electron-transfer processes in alkaline solutions. The electrocatalytic activity of Ni-based nanomaterials originating from the redox couple of Ni(II)/Ni(III) formed on the electrode surface in alkaline medium [172-176].

1.8.3. Details regarding nickel

- ***Electrocatalytic oxidation of glucose at Nicke.***

Nickel-modified glassy carbon electrode prepared by galvanostatic deposition has been used for the electrocatalytic oxidation of glucose in alkaline solutions utilized several electrochemical techniques. In cyclic voltammetry studies, in the presence of glucose an increase in the peak current of the oxidation of nickel hydroxide is followed by a decrease in the corresponding cathodic current. The oxidation of glucose has been reported to follow mediated electron transfer in which the nickel hydroxide layer comprising nickel ions of various valence states play the role of a mediator. The reaction followed a Cottrellian behavior and the diffusion coefficient of glucose was found to be $8 \times 10^{-6} cm^2 s^{-1}$ and was in consistency with the value determined hydrodynamic voltammetry [177].

Also, Nickel based materials such as nickel, its oxides, hydroxides as well as oxyhydroxides exhibited excellent electrocatalysis performances toward many small molecules. Electrocatalyis by these modifiers are proposed from three aspects such as $Ni(OH)_2$/NiOOH mediated electrolysis, direct electrocatalysis of $Ni(OH)_2$ or NiOOH. The transformation from nickel or its oxides to hydroxides or oxyhydroxides enhanced in the strong alkaline solution under the

cyclic scanning at relatively high positive potential. The redox transition between $Ni(OH)_2$ and NiOOH is also contributed to the electrocatalytic oxidation of Ni and its oxides toward small molecules in alkaline media [178].

Nickel based modified electrodes have been utilized for highly sensitive and selective non-enzymatic detection of glucose. A novel disposable electrochemical sensor based on three-dimensional (3D) porous nickel nanostructures. The enzyme-free sensor was fabricated through in situ growing porous nickel networks on a homemade screen-printed carbon electrode substrate via electrochemically reducing the Ni^{+2} precursor, along with continuously liberating hydrogen bubbles. The resulting nickel-modified electrode was morphologically and electrochemically characterized Under optimized condition. The enzymeless sensor exhibited excellent performance for glucose analysis selectively, offering a much wider linear range (from 0.5 μM to 4 mM), an extremely low detection limit (0.07 μM, signal-to-noise ratio (S/N) of 3), and an ultrahigh sensitivity of 2.9 mA/(cm^2 mM). Application of the proposed sensor in monitoring blood glucose was also demonstrated [179].

Modification of nickel in the form of foam by low-cost methods has been also reported and applied for non-enzymatic glucose sensing.

The Ni nanofoam was converted to the catalytic $Ni(OH)_2$/NiOOH – necessary for non-enzymatic glucose oxidation – by cyclic voltammetry (CV) in NaOH electrolyte. The electrode fabricated on conducting glass substrate showed a glucose sensitivity of 2.37 mA/cm^2 mM, a linear range of 0.01–0.7 mM, a limit of detection (LOD) of 5 μM, a fast response time (1 s), and resistance to chloride poisoning. The glucose sensor also exhibited an excellent long-term stability (4% decrease in sensitivity after 64 days) and selectivity in the presence of common interfering species. The versatility of the preparation method was demonstrated in the fabrication of a flexible (plastic substrate) sensor with a sensitivity of 1.43 mA/cm^2 mM. The ease of fabrication and the excellent properties of Ni nanofoam in glucose sensing make it promising for low-cost and wearable sensing applications [180].

Nickel nanoparticles (NPs) modified glassy carbon electrode, characterized morphologically and electrochemically, prepared by potentiostatic electrodeposition has been also reported and applied for glucose electro-oxidation in alkaline medium. Amperometric response of the electrocatalytic oxidation to glucose at the potential of 500 mV presents a linear dependence in the glucose concentration range of 5 μM-1.155 mM, with a 1 μM detection limit. The biologic compounds

probably existed in human serum sample, such as ascorbic acid, uric acid, and dopamine, do not disturb the determination of glucose. The relative standard deviation (RSD) of the determination of practical serum samples is less than 7 % compared with the results obtained from clinical examination. The proposed sensor exhibits excellent electrocatalytic activity toward the oxidation of glucose, which is a good candidate for glucose quantification [181].

- ***Electrocatalytic oxidation of glucose at Nickel oxide***

The electrochemical pretreatment of the glassy carbon prior to the electrodeposition of nickel largely affected the response of the modified electrode as has been reported. Different shape and size of NiO_X nanoparticles were reported when NiO_X is deposited on anodically oxidized GC electrode. Glucose electrooxidation is conducted in alkaline medium at GC/NiO_X (GC is untreated) and GC_{OX}/NiO_X (GC is treated) electrodes. The GC_{OX}/NiO_X shows an excellent electrocatalytic activity toward glucose oxidation compared to GC/NiO_X. The enhancement of the electrocatalytic activity obtained at the GC_{OX}/NiO_X is discussed in the light of the obtained differences

in characteristics of GC_{OX} /NiO_X and increase in the surface concentration of C–O functional groups [182].

Preparation method has been reported to largely affect the electrocatalytic activity. Nickel oxide nanoparticles (nano-NiO_X) of peculiar shape were prepared by sole gel technique and its electrocatalytic activity was evaluated at different conditions. The prepared nanoparticles were annealed at three different temperatures, i.e., 200, 400 and 600 C and anchored on glassy carbon (GC) electrode. Nano-NiO_X modified GG (nano-NiO_X/GC) electrodes are subjected to surface analysis techniques such as field emission scanning electron microscopy (FE-SEM) high resolution transmission electron micrograph (TEM) and X-ray diffraction (XRD). Electrochemical characterizations were performed using cyclic voltammetry and chronoamperometric techniques. The effects of annealing temperature on the morphological structure, surface concentration and subsequently on the electrochemical properties of nano-NiO_X/GC were examined. Experimental results indicated that the grain size and electrochemical characteristics of the nano-NiO_X/GC are significantly affected by the annealing temperature. The electrocatalytic oxidation of glucose at nano-NiO_X/GC electrode is

significantly enhanced especially with nano-NiO_X annealed at 200 C compared to those annealed at 400 and 600 C. Nano-NiO_X is applied for the electrocatalytic oxidation of glucose [183].

Impacts of the synthesis route on the structural and electrochemical properties of NiO_X nanoparticles modified glassy carbon electrode (nano-NiO_X/GC) have been reported. Nanoparticles of nickel oxide (nano-NiO_X) have been synthesized using electrochemical and sol-gel routes. Cyclic voltammetry (CV), field emission scanning electron microscopy (FE-SEM), X-ray diffraction and transmission electron microscopy (TEM) were used for the characterization of nano-NiO_X/GC. The size of the particles using the sol-gel technique (NiO_X-SG) is uniform and have smaller particle size (~20 nm) than that obtained using the electrochemical route (NiO_X-El, ~80 nm). The specific activity (given in mA per mg of the NiO_X) of the $Ni(OH)_2$/NiOOH redox couple of the NiO_X-SG is higher with higher reversibility compared with the NiO_X-EL. Impacts of the synthesis route on the electrocatalytic properties of the NiO_X-SG and NiO_X-El are tested by the glucose oxidation in alkaline solution as a probing reaction for the electrocatalytic activity [184].

Assembled NiO nanosheets have been successfully prepared using graphene oxide (GO) film as template, where the Ni^{2+} ion was firstly adsorbed in GO film, followed by calcination in N_2 to form NiO-based materials and calcination in air to remove carbon-based template. The morphology, structure, and electrochemical activities of these NiO nanosheets were characterized by X-ray diffraction (XRD), transmission electron microscope (TEM) and electrochemical techniques, respectively. It has been found that the NiO nanosheets thus obtained electrochemically catalyzed glucose oxidation in 0.1 M NaOH, leading to fabrication of non-enzymatic glucose sensor. The glucose sensor based on NiO nanosheets exhibits detection limit of 0.18 μM, and linear range from 1 μM to 0.4 mM with the sensitivity of 1138 μA mM^{-2} cm^{-2}. Furthermore, such glucose sensor also shows excellent selectivity for detection of glucose, compared to the commonly interfering species, such as ascorbic acid, dopamine, and uric acid [185].

Substitution of carbon substrate reflected on the electrocatalytic activity of deposited nickel. Nickel oxide (NiO) nanofilm electrodeposited on a bare Cu electrode for glucose oxidation has been reported. Electrochemical deposition was assisted with cetyl

trimethylammonium bromide (CTAB) as a template. Scanning electron microscopy (SEM) was applied to observe the surface morphology of the modified electrode. Cyclic voltammetry (CV) and amperometry techniques were used to study the electrocatalytic behavior of NiO porous film in glucose and methanol detection. The electrode showed a linear relationship in the concentration range of 0.01-2.14 mM with a low limit of detection (LOD) 1.7 µM. Moreover, high sensitivities of 4.02 mA mM^{-1} cm^{-2} and 0.38 mA mM^{-1} cm^{-2} respectively in glucose and methanol monitoring suggested the modified electrode as an excellent sensor. The NiO-Cu modified electrode was relatively insensitive to common biological interferers. The sensor possessed good poison resistance towards chloride ions, and long-term stability and significant selectivity towards glucose and methanol. The proposed sensor was successfully applied for determination of glucose in human blood serum samples [186].

The aqueous NiOOH nanosheets were also synthesized using a hydrothermal method via a surfactant template under mild reaction conditions. The as-prepared products were characterized by atomic force microscopy (AFM), X-ray diffraction (XRD) and scanning electron microscopy (SEM), the results of which indicated that ultrathin and porous NiOOH nanosheets with a thickness of only

several nanometers have been obtained. The obtained NiOOH nanosheets were subsequently assembled on electrochemically pretreated glassy carbon (EPGC) electrode through a simple physical bath deposition method to form NiOOH/EPGC electrode. SEM, energy dispersive X-ray spectroscopy (EDX) and electrochemical impedance spectroscopy (EIS) proved the successful assembly of NiOOH on EPGC surface. They explained the effective deposition of NiOOH electrocatalyst based the higher surface area and higher surface concentration of C-O functional groups existing on EPGC surface. The modified electrode was applied for glucose and methanol oxidation [187].

- ***Electrocatalytic oxidation of glucose at Nickel composite***

A non-enzymatic potentiometric glucose sensor was developed by modifying a glass carbon electrode with Ni/NiO decorated nitrogen doped carbon spheres (Ni/NiO/NCSs). The Ni/NiO/NCSs were prepared with in situ growth of Ni/NiO on the nitrogen doped carbon spheres. The amperometric measurement revealed that the sensor had wide linear regions of 2 mM-600 mM and 800 mM-2500 mM with a sensitivity of 219.19 mA $mM^{-1}\,cm^2$ and 87.88 mA $mM^{-1}cm^2$ respectively. Moreover, the Ni/NiO/NCS composites also exhibited

good selectivity by adding certain amount of urea, NaCl, L-proline, L-valine, L-Leucine and ascorbic acid into 0.1 M NaOH solution. The excellent electro- catalytic performance was attributed to the synergistic effect of nitrogen doping and Ni loading, which may result in the increase of electron density and the enhancement of surface conductivity of the composite electrode materials [188].

- ***Electrocatalytic oxidation of glucose by nickel oxides composite***

A novel binary electrocatalyst fabricated from manganese and nickel oxides nanoparticles (MnO_X and NiO_X), prepared by electrodeposition, has neen proposed as an anode for an amplified electrochemical oxidation of glucose in NaOH solutions. Cyclic voltammetry and scanning electron microscopy images were used to characterize these electrocatalysts. It has been found that the electrocatalytic activity critically depends on the order of the deposition of the two oxides. The NiO_X/MnO_X/GC electrode (MnO_X deposited first) showed a superior electrocatalytic activity towards glucose oxidation compared to NiO_X/GC, MnO_X/GC or MnO_X/NiO_X/GC electrodes (NiO_X deposited first). The extraordinary activity obtained at the NiO_X/MnO_X/ GC electrode is attributed to the compilation of the better adsorption of glucose molecules on the

MnO_X sites and the increase of conductivity of the NiO_X due to the increase of Ni^{3+} content. A synergism between the two oxides towards the electrooxidation of glucose was proposed for explaining the extraordinary electroactivity [189].

Modification of glassy carbon electrode (GCE) with graphene oxide (GO), NiO nanofibers (NiONFs) and Nafion (NA) were also reported for the oxidation of glucose. NiONFs were prepared by the facile electrospinning technique followed by calcination. The modified electrode was pretreated by the electrochemical reduction. The sensor was characterized by scanning electron microscopy (SEM), energy dispersive X-ray spectroscopy (EDX), X-ray photoelectron spectroscopy (XPS) and electrochemical impedance spectroscopy (EIS). The sensor exhibited high sensitivity (1100 μ A mM^{-1} cm^{-2}), fast response time (less than 5 s), low detection limit of 0.77 μM (S/N = 3), long term stability, and excellent anti-fouling ability for glucose determination. The sensor was further applied to detection of glucose in human blood serum sample, and the results accorded with those of commercial test [190].

1.9. REFERENCES

1. Brett CM and Brett O (1993). Electrochemistry, A. M., *Principles, methods and applications.*
2. JO'M B and Minevski ZS (1994). Electrocatalysis: past, present and future. *Electrochim. Acta*, 39(11-12), 1471-1479.
3. Mkwizu and Samwel Peter (2015). Electrochemical Synthesis and Characterization of Multi metallic Nanostructured Electrocatalysts. *Diss. University of Pretoria*.
4. Chorkendorff I and Niemantsverdriet JW (2003). Concepts of modern catalysis and kinetics. *Weinheim: Wiley-VCH*.
5. Lu GQ and Wieckowski A (2000). Heterogeneous electrocatalysis: a core field of interfacial science. *Curr. Opin. Colloid Interface Sci*.,5(1-2), 95–100.
6. Bard A and Faulkner LR, (2001). Electrochemical methods: Fundamentals and Applications. *John-Wiley & Sons*, New York.
7. Girault HH (2004). *Analytical and physical electrochemistry*. CRC Press.
8. Speiser B, Bard AJ, Stratmann M, Unwin PR (2003). Encyclopedia of Electrochemistry. *Wiley-VCH: Weinheim*, p. 81-104.
9. Fischer AC (1996). Electrode Dynamics, *Oxford University Press*, NewYork.

10. Christensenand PA and Hamnett A (1994). Techniques and Mechanismsin Electrochemistry, *Chapman & Hall, London*.

11. Hibbert DB (1993), Introduction to Electrochemistry, *Macmillan, London Eds*.

12. Randles JE (1948). A cathode ray polarograph. Part II.—The current-voltage curves. *Trans. Faraday Soc*., 44, 327-338.

13. Kaifer AE and Kaifer MG, (1999). Supramolecular Electrochemistry. *Willey, VCH, New York Eds*.

14. Bard AJ and Faulkner LR (1996). Electrochemical Methods: Fundamentals and Applications. *John Willey & Sons Eds*.

15. Brown ER and Large RF (1971). Techniques of Chemistry, Vol. 1, Part II A," *Electrochemical Methods*", chapter 6.

16. Renault JP, Bernard A, Bietsch A, Michel B, Bosshard HR, Delamarche E, Wild UP (2003). Fabricating arrays of single protein molecules on glass using microcontact printing. *J. Phys. Chem. B, 107*(3), 703-711.

17. Bockris J.O.M and Shaded U. M. K. (1993). Surface Electrochemistry: *a Molecular Level Approach Plenum Press*. New York, *78*.

18. Van Benschoten JJ, Lewis JY, Heineman WR, Roston DA, Kissinger PT (1983). Cyclic voltammetry experiment. *J. Chem. Educ.*, *60*(9), 772.

19. Domb AJ, Kost J, Wiseman D (1998). *Handbook of biodegradable polymers*. CRC press.

20. Nicholson RS and Shain I (1964). Theory of stationary electrode polarography. Single scan and cyclic methods applied to reversible, irreversible, and kinetic systems. *Anal. Chem.*, *36*(4), 706-723.

21. Kulkarni and Sulabha K. (2015). Nanotechnology: Principles and Practices. *Springer*.

22. Shamsipur M, Najafi M, Hosseini M. R. M (2010). Highly improved electrooxidation of glucose at a nickel(II) oxide/multi-walled carbon nanotube modified glassy carbon electrode. *Bioelectrochem.*, 77(2), 120–124.

23. Heller A and Feldman B (2008). Electrochemical glucose sensors and their applications in diabetes management. *Chem. Rev.*, *108*(7), 2482-2505.

24. Ekoé JM, Rewers M, Williams R, Zimmet P (Eds.) (2008). *The epidemiology of diabetes mellitus*. John Wiley & Sons.

25. Kerzenmacher S, Ducrée J, Zengerle R, Von Stetten F (2008). Energy harvesting by implantable abiotically catalyzed glucose fuel cells. *J. Power Sources*, *182*(1), 1-17.

26. Nikolaeva NN, Khazova OA, Vasilev YB (1983). Main principles of the electrooxidation of glucose on a gold electrode. *Soviet. Electrochem.*, *19*(8), 934-940.

27. Wang J (1999). Amperometric biosensors for clinical and therapeutic drug monitoring: a review. *J. pharm. Biomed. Anal.*, 19(1-2), 47-53.

28. Rahman M, Ahammad AJ, Jin JH, Ahn SJ, Lee JJ (2010). A comprehensive review of glucose biosensors based on nanostructured metal -oxides. *Sensors*, 10(5), 4855-4886.

29. Si P, Huang Y, Wang T, Ma J (2013). Nanomaterials for electrochemical non-enzymatic glucose biosensors. *RSC Adv.*, 3(11), 3487-3502.

30. Pletcher D (1984). Electrocatalysis: present and future. *J. Appl. Electrochem.*, 14(4):403-15.

31. Tian K, Prestgard M, Tiwari A (2014). A review of recent advances in nonenzymatic glucose sensors. *Mater. Sci. Eng., C*, 41:100-18.

32. Burke LD (1994). Premonolayer oxidation and its role in electrocatalysis. *Electrochim. Act*a, 39(11-12):1841-8.

33. Ernst S, Heitbaum J, Hamann CH (1980). The electrooxidation of glucose in phosphate buffer solutions: kinetics and reaction mechanism. *Berichte der Bunsengesellschaft für physikalische Chemie*. ,84(1):50-5.

34. Bankar SB, Bule MV, Singhal RS, Ananthanarayan L (2009). Glucose oxidase—an overview. *Biotechnol. Adv.*, 27, 489.

35. Quan H, Park SU, Park J (2010). Electrochemical oxidation of glucose on silver nanoparticle-modified composite electrodes. *Electrochim. Acta, 55*(7), 2232-2237.

36. Newman JD and Turner AP (2005). Home blood glucose biosensors: a commercial perspective. *Biosens. Bioelectron., 20*(12), 2435-2453.

37. Wilson GS and Gifford R (2005). Biosensors for real-time in vivo measurements. *Biosens. Bioelectron., 20*(12), 2388-2403.

38. Ramanavicius A, Kausaite A, Ramanaviciene A (2005). Biofuel cell based on direct bioelectrocatalysis. *Biosens. Bioelectron., 20*(10), 1962-1967.

39. Updike SJ and Hicks GP (1967). The enzyme electrode. *Nature, 214*(5092), 986-988.

40. Wang J and Pamidi PV (1997). Sol− gel-derived gold composite electrodes. *Anal. Chem., 69*(21), 4490-4494.

41. Patolsky F, Weizmann Y, Willner I (2004). Long-range electrical contacting of redox enzymes by SWCNT connectors. *Angew. Chem. Int. Ed., 43*(16), 2113-2117.

42. Wang J (2008). Electrochemical glucose biosensors. *Chem. Rev., 108*(2), 814-825.

43. Park S, Boo H, Chung TD (2006). Electrochemical non-enzymatic glucose sensors. *Anal. Chim. Acta, 556*(1), 46-57.

44. Zhang Y, Chang G, Liu S, Lu W, Tian J, Sun X (2011). A new preparation of Au nanoplates and their application for glucose sensing. *Biosens. Bioelectron.*, *28*(1), 344-348.

45. Hanachi P, Jafary F, Motamedi S (2015). Immobilization of the alkaline phosphatase on collagen surface via cross-linking method. *Iran. J. Biotechnol*. 13 (2), 31–38.

46. Nawaz MA, Rehman HU, Bibi Z, Aman A, Qader S.A.U (2015). Continuous degradation of maltose by enzyme entrapment technology using calcium alginate beads as a matrix. *Biochem. Biophys*. *Rep.*, 4, 250–256.

47. Dwevedi A (2016). Enzyme Immobilization Advances in Industry, Agriculture, Medicine, and the Environment. *Springer*.

48. Chen T, Friedman KA, Lei I, Heller A (2000). In situ assembled mass-transport controlling micromembranes and their application in implanted amperometric glucose sensors. *Anal. Chem.*, *72*(16), 3757-3763.

49. Guo G, Chen Q, Chen X (2011). Electrochemiluminescence glucose biosensor based on glucose dehydrogenase functionalized Ru (bpy) 3 2+ doped silica nanoparticles. *Sci. China Chem.*, *54*(11), 1777-1781.

50. Guo G, Wang X, Zhou T, Chen X (2010). Extended detection range for an optical enzymatic glucose sensor coupling with a novel data-processing method. *Sci. China Chem.*, *53*(6), 1385-1390.

51. Kausaite-Minkstimiene A, Mazeiko V, Ramanaviciene A, Ramanavicius A (2010). Enzymatically synthesized polyaniline layer for extension of linear detection region of amperometric glucose biosensor. *Biosens. Bioelectron*., 26, 790.

52. Cosnier S (1999). Biomolecule immobilization on electrode surfaces by entrapment or attachment to electrochemically polymerized films. A review. *Biosens. Bioelectron.*, *14*(5), 443-456.

53. Heller J and Heller A (1998). Loss of activity or gain in stability of oxidases upon their immobilization in hydrated silica: significance of the electrostatic interactions of surface arginine residues at the entrances of the reaction channels. *J. Ame. Chem. Soc.*, *120*(19), 4586-4590.

54. Ratner BD (1995). Surface modification of polymers: chemical, biological and surface analytical challenges. *Biosens. Bioelectron.*, *10*(9-10), 797-804.

55. Chaudhury MK (1995). Self-assembled monolayers on polymer surfaces. *Biosens. Bioelectron.*, *10*(9-10), 785-788.

56. Gooding JJ and Hibbert DB (1999). The application of alkanethiol self-assembled monolayers to enzyme electrodes. *TrAC Trends Anal. Chem.*, *18*(8), 525-533.

57. Willner I, Katz E, Willner B (1997). Electrical contact of redox enzyme layers associated with electrodes: routes to amperometric biosensors. *Electroanalysis*, *9*(13), 965-977.

58. Ferretti S, Paynter S, Russell DA, Sapsford KE, Richardson DJ (2000). Self-assembled monolayers: a versatile tool for the formulation of bio-surfaces. *TrAC Trends Anal. Chem.*, *19*(9), 530-540.

59. Toghill KE and Compton RG (2010). Electrochemical non-enzymatic glucose sensors: a perspective and an evaluation. *Int. J. Electrochem. Sci.*, *5*(9), 1246-1301.

60. Hu Y, Song Y, Wang Y, Di J (2011). Electrochemical synthesis of gold nanoparticles onto indium tin oxide glass and application in biosensors. *Thin Solid Films*, *519*(19), 6605-6609.

61. Atta NF, Galal A, Ekram H (2012). Gold nanoparticles-coated poly (3, 4-ethylene-dioxythiophene) for the selective determination of sub-nano concentrations of dopamine in presence of sodium dodecyl sulfate. *Electrochim. Acta*, *69*, 102-111.

62. Park S, Chung TD, Kim HC (2003). Nonenzymatic glucose detection using mesoporous platinum. *Anal. Chem.*, *75*(13), 3046-3049.

63. Yuan JH, Wang K, Xia XH (2005). Highly ordered platinum-nanotubule arrays for amperometric glucose sensing. *Adv. Funct. Mater.*, *15*(5), 803-809.

64. Guo MQ, Hong HS, Tang XN, Fang HD, Xu XH (2012). Ultrasonic electrodeposition of platinum nanoflowers and their application in nonenzymatic glucose sensors. *Electrochim. Acta*, *63*, 1-8.

65. Wang J, Thomas DF, Chen A (2008). Nonenzymatic electrochemical glucose sensor based on nanoporous PtPb networks. *Anal. Chem.*, *80*(4), 997-1004.

66. Song YY, Zhang D, Gao W, Xia XH (2005). Nonenzymatic glucose detection by using a three-dimensionally ordered, macroporous platinum template. *Chem. –A Euro. J.*, *11*(7), 2177-2182.

67. Shen Q, Jiang L, Zhang H, Min Q, Hou W, Zhu JJ (2008). Three-dimensional dendritic Pt nanostructures: sonoelectrochemical synthesis and electrochemical applications. *J. Phys. Chem. C*, *112*(42), 16385-16392.

68. Ryu J, Kim K, Kim HS, Hahn HT, Lashmore D (2010). Intense pulsed light induced platinum–gold alloy formation on carbon nanotubes for non-enzymatic glucose detection. *Biosens. Bioelectron.*, *26*(2), 602-607.

69. Safavi A and Farjami F (2011). Electrodeposition of gold–platinum alloy nanoparticles on ionic liquid–chitosan composite film and its application in fabricating an amperometric cholesterol biosensor. *Biosens. Bioelectron.*, *26*(5), 2547-2552.

70. Bai Y, Sun Y, Sun C (2008). Pt–Pb nanowire array electrode for enzyme-free glucose detection. *Biosens. Bioelectron.*, *24*(4), 579-585.

71. Bo X, Bai J, Qi B, Guo L (2011). Ultra-fine Pt nanoparticles supported on ionic liquid polymer-functionalized ordered mesoporous carbons for nonenzymatic hydrogen peroxide detection. *Biosens. Bioelectron.*, *28*(1), 77-83.

72. Ding Y, Liu Y, Parisi J, Zhang L, Lei Y (2011). A novel NiO–Au hybrid nanobelts based sensor for sensitive and selective glucose detection. *Biosens. Bioelectron.*, *28*(1), 393-398.

73. Li LH, Zhang WD, Ye JS (2008). Electrocatalytic oxidation of glucose at carbon nanotubes supported PtRu nanoparticles and its detection. *Electroanalysis*, *20*(20), 2212-2216.

74. Xiao F, Li Y, Gao H, Ge S, Duan H (2013). Growth of coral-like PtAu–MnO2 binary nanocomposites on free-standing graphene paper for flexible nonenzymatic glucose sensors. *Biosens. Bioelectron. 41*, 417-423.

75. Liu Y, Ding Y, Zhang Y, Lei Y (2012). Pt–Au nanocorals, Pt nanofibers and Au microparticles prepared by electrospinning and calcination for nonenzymatic glucose sensing in neutral and alkaline environment. *Sens. Actuators, B, 171*, 954-961.

76. Chen J, Wiley B, McLellan J, Xiong Y, Li ZY, Xia Y (2005). Optical properties of Pd− Ag and Pt− Ag nanoboxes synthesized via galvanic replacement reactions. *Nano lett.*, *5*(10), 2058-2062.

77. Guo S, Dong S, Wang E (2010). Ultralong Pt-on-Pd bimetallic nanowires with nanoporous surface: nanodendritic structure for enhanced electrocatalytic activity. *Chem. Commun.*, *46*(11),1869-1871.

78. Basu D and Basu S (2011). Synthesis, characterization and application of platinum based bi-metallic catalysts for direct glucose alkaline fuel cell. *Electrochim. Acta*, *56*(17), 6106-6113.

79. Basu D, and Basu S (2010). A study on direct glucose and fructose alkaline fuel cell. *Electrochim. Acta*, *55*(20), 5775-5779.

80. Liu Z, Huang L, Zhang L, Ma H, Ding Y (2009). Electrocatalytic oxidation of d-glucose at nanoporous Au and Au–Ag alloy electrodes in alkaline aqueous solutions. *Electrochim. Acta*, *54*(28), 7286-7293.

81. Jin C and Taniguchi I (2007). Electrocatalytic activity of silver modified gold film for glucose oxidation and its potential application to fuel cells. *Mater. Lett.*, *61*(11-12), 2365-2367.

82. Cuevas-Muñiz FM, Guerra-Balcázar M, Castaneda F, Ledesma-García J, Arriaga LG (2011). Performance of Au and AuAg nanoparticles supported on Vulcan in a glucose laminar membraneless microfuel cell. *J. Power Sources*, *196*(14), 5853-5857.

83. Zhu C, Guo S, Dong S (2012). PdM (M= Pt, Au) Bimetallic Alloy Nanowires with Enhanced Electrocatalytic Activity for Electro-oxidation of Small Molecules. *Adv. Mater.*, *24*(17), 2326-2331.

84. Cui HF, Ye JS, Liu X, Zhang WD, Sheu, FS (2006). Pt–Pb alloy nanoparticle/carbon nanotube nanocomposite: a strong electrocatalyst for glucose oxidation. *Nanotechnol.*, *17*(9), 2334.

85. Sun Y, Buck H, Mallouk TE (2001). Combinatorial discovery of alloy electrocatalysts for amperometric glucose sensors. *Anal. Chem.*, *73*(7), 1599-1604.

86. Tonda-Mikiela P, Napporn TW, Morais C, Servat K, Chen A, Kokoh KB (2012). Synthesis of gold-platinum nanomaterials using bromide anion exchange-synergistic electroactivity toward CO and glucose oxidation. *J. Electrochem. Soc.*, *159*(11), H828.

87. Gao H, Xiao F, Ching CB, Duan H (2011). One-step electrochemical synthesis of PtNi nanoparticle-graphene nanocomposites for nonenzymatic amperometric glucose detection. *ACS Appl. Mater. Interfaces*, *3*(8), 3049-3057.

88. Hermans S, Deffernez A, Devillers M (2011). Au–Pd/C catalysts for glyoxal and glucose selective oxidations. *Appl. Catal., A*, *395*(1-2), 19-27.

89. Cho S, Shin H, Kang C (2006). Catalytic glucose oxidation on a polycrystalline gold electrode with an amalgamation treatment (TM 05092). *Electrochim. Acta*, *51*(18), 3781-3786.

90. Seo B, Choi S, Kim J (2011). Simple electrochemical deposition of Au nanoplates from Au (I) cyanide complexes and their electrocatalytic activities. *ACS Appl. Mater. Interfaces*, *3*(2), 441-446.

91. Pasta M, La Mantia F, Cui Y (2010). A new approach to glucose sensing at gold electrodes. *Electrochem. Commun.*, *12*(10), 1407-1410.

92. Habrioux A, Servat K, Girardeau T, Guérin P, Napporn TW, Kokoh KB (2011). Activity of sputtered gold particles layers towards glucose electrochemical oxidation in alkaline medium. *Curr. Appl. Phys.*, *11*(5), 1149-1152.

93. Oztekin Y, Yazicigil Z, Ramanaviciene A, Ramanavicius A (2011). Polyphenol-modified glassy carbon electrodes for copper detection. *Sens. Actuators, B*, *152*(1), 37-48.

94. Jeong H and Kim J (2012). Electrochemical oxidation of glucose at nanoporous black gold surfaces in the presence of high concentration of chloride ions and application to amperometric detection. *Electrochim. Acta*, *80*, 383-389.

95. Liu A, Ren Q, Xu T, Yuan M, Tang W (2012). Morphology-controllable gold nanostructures on phosphorus doped diamond-like

carbon surfaces and their electrocatalysis for glucose oxidation. *Sens. Actuatros, B, 162*(1), 135-142.

96. Wang Q, Min F, Zhu J (2013). Preparation of gold nanowires and its application in glucose biosensing. *Mater. Lett., 91*, 9-11.

97. Li Y, Song YY, Yang C, Xia XH (2007). Hydrogen bubble dynamic template synthesis of porous gold for nonenzymatic electrochemical detection of glucose. *Electrochem. Commun.*, *9*(5), 981-988.

98. Cho S and Kang C (2007). Nonenzymatic glucose detection with good selectivity against ascorbic acid on a highly porous gold electrode subjected to amalgamation treatment. *Electroanalysis*, *19*(22), 2315-2320.

99. Bai Y, Yang W, Sun Y, Sun C (2008). Enzyme-free glucose sensor based on a three-dimensional gold film electrode. *Sens. Actuators, B, 134*(2), 471-476.

100. Xia Y, Huang W, Zheng J, Niu Z, Li Z (2011). Nonenzymatic amperometric response of glucose on a nanoporous gold film electrode fabricated by a rapid and simple electrochemical method. *Biosens. Bioelectron.*, *26*(8), 3555-3561.

101. Hyun M, Choi S, Kim J (2010). Simple Fabrication of Porous Gold-Film Electrodes and Their Electroanalytical Applications. *Anal. Sci.*, *26*(1), 129-132.

102. Liu Z, Du J, Qiu C, Huang L, Ma H, Shen D, Ding Y (2009). Electrochemical sensor for detection of p-nitrophenol based on nanoporous gold. *Electrochem. Commun.*, *11*(7), 1365-1368.

103. Seo B and Kim J (2010). Electrooxidation of glucose at nanoporous gold surfaces: structure dependent electrocatalysis and its application to amperometric detection. *Electroanalysis*, *22*(9), 939-945.

104. Deng Y, Huang W, Chen X, Li Z (2008). Facile fabrication of nanoporous gold film electrodes. *Electrochem. Commun.*, *10*(5), 810-813.

105. Nishio K and Masuda H (2011). Anodization of gold in oxalate solution to form a nanoporous black film. *Angew. Chem. Int. Ed.*, *50*(7), 1603-1607.

106. Zhao W, Xu JJ, Shi CG, Chen HY (2006). Fabrication, characterization and application of gold nano-structured film. *Electrochem. Commun.*, *8*(5), 773-778.

107. Qiu H and Huang X (2010). Effects of Pt decoration on the electrocatalytic activity of nanoporous gold electrode toward glucose and its potential application for constructing a nonenzymatic glucose sensor. *J. Electroanal. Chem.*, *643*(1-2), 39-45.

108. Tavakkoli N and Nasrollahi S (2013). Non-enzymatic glucose sensor based on palladium coated nanoporous gold film electrode. *Aust. J. Chem.*, *66*(9), 1097-1104.

109. Bai H, Han M, Du Y, Bao J, Dai Z (2010). Facile synthesis of porous tubular palladium nanostructures and their application in a nonenzymatic glucose sensor. *Chem. Commun.*, *46*(10), 1739-1741.

110. Chen XM, Cai ZM, Lin ZJ, Jia TT, Liu HZ, Jiang YQ, Chen X (2009). A novel non-enzymatic ECL sensor for glucose using palladium nanoparticles supported on functional carbon nanotubes. *Biosens. Bioelectron.*, *24*(12), 3475-3480.

111. Meng L, Jin J, Yang G, Lu T, Zhang H, Cai C (2009). Nonenzymatic electrochemical detection of glucose based on palladium− single-walled carbon nanotube hybrid nanostructures. *Anal. Chem.*, *81*(17), 7271-7280.

112. Zhang WJ, Bai L, Lu LM, Chen Z (2012). A novel and simple approach for synthesis of palladium nanoparticles on carbon nanotubes for sensitive hydrogen peroxide detection. *Colloids. Surf., B*, *97*, 145-149.

113. Gutes A, Carraro C, Maboudian R (2011). Nonenzymatic glucose sensing based on deposited palladium nanoparticles on epoxy-silver electrodes. *Electrochim. Acta*, *56*(17), 5855-5859.

114. Lu LM, Li HB, Qu F, Zhang XB, Shen GL, Yu RQ (2011). In situ synthesis of palladium nanoparticle–graphene nanohybrids and their application in nonenzymatic glucose biosensors. *Biosens. Bioelectron.*, *26*(8), 3500-3504.

115. Szunerits S and Boukherroub R (2008). Investigation of the electrocatalytic activity of boron-doped diamond electrodes modified with palladium or gold nanoparticles for oxygen reduction reaction in basic medium. *CR CHIM*, *11*(9), 1004-1009.

116. Atta NF and El-Kady MF (2009). Poly (3-methylthiophene) /palladium sub-micro-modified sensor electrode. Part II: Voltammetric and EIS studies, and analysis of catecholamine neurotransmitters, ascorbic acid and acetaminophen. *Talanta*, *79*(3), 639-647.

117. Liao F, Wang Z, Guo T, Zhang T, Wu Z (2012). Synthesis of well dispersed palladium nanoparticles-decorated poly (o-phenylenediamine) colloids with excellent performance for hydrazine oxidation. *J. Electroanal. Chem.*, *673*, 38-42.

118. Santhosh P, Manesh KM, Uthayakumar S, Komathi S, Gopalan AI, Lee KP (2009). Fabrication of enzymatic glucose biosensor based on palladium nanoparticles dispersed onto poly (3, 4-ethylenedioxythiophene) nanofibers. *Bioelectrochem.*, *75*(1), 61-66.

119. Reyter D, Odziemkowski M, Bélanger D, Roué L (2007). Electrochemically Activated Copper Electrodes Surface

Characterization, Electrochemical Behavior, and Properties for the Electroreduction of Nitrate. *J. Electrochem. Soc.*, *154*(8), K36-K44.

120. Jin C and Taniguchi I (2007). Electrocatalytic activity of silver modified gold film for glucose oxidation and its potential application to fuel cells. *Mater. Lett.*, *61*(11-12), 2365-2367.

121. Cuevas-Muñiz FM, Guerra-Balcázar M, Castaneda F, Ledesma-García J, Arriaga LG (2011). Performance of Au and AuAg nanoparticles supported on Vulcan in a glucose laminar membraneless microfuel cell. *J. Power Sources*, *196*(14), 5853-5857.

122. Zhu C, Guo S, Dong S (2012). PdM (M= Pt, Au) Bimetallic Alloy Nanowires with Enhanced Electrocatalytic Activity for Electro-oxidation of Small Molecules. *Adv. Mater.*, *24*(17), 2326-2331.

123. Zhao J, Wei LM, Peng CH, Su YJ, Yang Z, Zhang LY, Wei H, Zhang YF (2013). A non-enzymatic glucose sensor based on the composite of cubic Cu nanoparticles and arc-synthesized multi-walled carbon nanotubes. *Biosens. Bioelectron.*, 47, 86.

124. Zhao Y, Zhao JZ, Ma DC, Li. YL, Hao XL, Li LZ, Yu CZ, Zhang L, Lu Y, Wang ZC (2012). Synthesis, growth mechanism of different Cu nanostructures and their application for non-enzymatic glucose sensing. *Colloids Surf., A*, 409, 105.

125. Jiang LC and Zhang WD (2010). A highly sensitive nonenzymatic glucose sensor based on CuO nanoparticles-modified carbon nanotube electrode. *Biosens. Bioelectron.*, 25, 1402.

126. Wu, H. X., Cao, W. M., Li, Y., Liu, G.,Wen, Y., Yang, H. F. and Yang, S-P. (2010). In situ growth of copper nanoparticles on multiwalled carbon nanotubes and their application as non-enzymatic glucose sensor materials. *Electrochim. Act*a, 55, 3734.

127. Yang JA, Zhang WD, Gunasekaran S (2010). An amperometric non-enzymatic glucose sensor by electrodepositing copper nanocubes onto vertically well-aligned multi-walled carbon nanotube arrays. *Biosens. Bioelectron.*, 26, 279.

128. Jiang F, Wang S, Lin JJ, Jin HL, Zhang LJ, Huang SM, Wang J (2011). Aligned SWCNT-copper oxide array as a nonenzymatic electrochemical probe of glucose**.** *Electrochem. Commun.*, 13, 363-365, 2011.

129. Lu LM, Zhang XB, Shen GL, Yu RQ (2012). Seed-mediated synthesis of copper nanoparticles on carbon nanotubes and their application in nonenzymatic glucose biosensors. *Anal. Chim. Act*a, 715, 99.

130. Yang Z, Feng J, Qiao J, Yan Y, Yu Q, Sun K (2012). Copper oxide nanoleaves decorated multi-walled carbon nanotube as platform for glucose sensing. *Anal. Methods*, 4, 1924.

131. Zhou X, Nie H, Yao Z, Dong Y, Yang Z, Huang S (2012). Facile synthesis of nanospindle-like Cu2O/straight multi-walled carbon nanotube hybrid nanostructures and their application in enzyme-free glucose sensing. *Sens. Actuators, B,* 168, 1.

132. Yang GC, Liu EJ, Khun NW, Jiang SP (2009). Copper oxide nanoleaves decorated multi-walled carbon nanotube as platform for glucose sensing. *J. Electroanal. Chem*., 627, 51.

133. Li C, Liu Y, Li L, Du Z, Xu S, Zhang M, Yin X, Wang T (2008). A novel amperometric biosensor based on NiO hollow nanospheres for biosensing glucose, *Talanta*, 77, 455.

134. Xia C and Ning W (2010). A novel non-enzymatic electrochemical glucose sensor modified with FeOOH nanowire. *Electrochem. Commun*., 12, 1581.

135. Das D, Sen P, Das K (2006). Electrodeposited MnO 2 as electrocatalyst for carbohydrate oxidation. *J. Appl. Electrochem*., 36, 685.

136. Shim J, Kang M, Lee Y, Lee C (2012). A nanoporous ruthenium oxide framework for amperometric sensing of glucose and potentiometric sensing of pH. *Microchim. Act*a, 177, 211.

137. Zhang L, Li H, Ni Y, Li J, Liao K, Zhao G (2009). Porous cuprous oxide microcubes for non-enzymatic amperometric hydrogen peroxide and glucose sensing. *Electrochem. Commun*.,11, 812.

138. Ding Y, Wang Y, Su L, Bellagamba M, Zhang H, Lei Y (2010). Electrospun Co3O4 nanofibers for sensitive and selective glucose detection. *Biosens. Bioelectron.*, 26, 542.

139. Bai Y, Sun Y, Sun C (2008). Pt–Pb nanowire array electrode for enzyme-free glucose detection. *Biosens. Bioelectron.*, 24, 579.

140. Lei Y, Yan X, Zhao J, Liu X, Song Y, Luo N, Zhang Y (2011). Improved glucose electrochemical biosensor by appropriate immobilization of nano-ZnO. *Colloids Surf., B*, 82, 168.

141. Berchmans S, Gomathi H, Rao GP (1995). Electrooxidation of alcohols and sugars catalysed on a nickel oxide modified glassy carbon electrode. *J. Electroanal. Chem.*, 394, 267.

142. Lyons ME, Fitzgerald CA, Smyth MR (1994). Glucose oxidation at ruthenium dioxide-based electrodes, *Anal.*, 119, 855.

143. Chen JW, Zhang D, Ye JS (2008). Nonenzymatic electrochemical glucose sensor based on MnO2/MWNTs nanocomposite. *Electrochem. Commun.*, 10, 1268.

144. Noorbakhsh A and Salimi A (2009). Amperometric detection of hydrogen peroxide at nano-nickel oxide/thionine and celestine blue nanocomposite-modified glassy carbon electrodes. *Electrochim. Acta*, 54, 6312.

145. Nam, K. W. and Kim, K. B. (2002). A study of the preparation of NiO x electrode via electrochemical route for supercapacitor

applications and their charge storage mechanism. *J. Electrochem. Soc*., 149, A346.

146. Zhang Y, Xu FG, Sun YJ, Shi Y, Wen ZW, Li Z (2011). Assembly of Ni (OH) 2 nanoplates on reduced graphene oxide: a two-dimensional nanocomposite for enzyme-free glucose sensing. *J. Mater Chem*.,21, 16949.

147. Li X, Liu J, Ji X, Jiang J, Ding R, Hu Y, Huang X (2010). Ni/Al layered double hydroxide nanosheet film grown directly on Ti substrate and its application for a nonenzymatic glucose sensor. *Sens. Actuators, B, 147*(1), 241-247.

148. Zhang YC, Su L, Manuzzi D, Jia WJ, Huo DQ, Hou CJ, Lei Y (2012). Ultrasensitive and selective non-enzymatic glucose detection using copper nanowires. *Biosens. Bioelectron*., 31, 426.

149. Li S, Zheng YJ, Qin GW, Ren YP, Pei WL, Zuo L (2011). Enzyme-free amperometric sensing of hydrogen peroxide and glucose at a hierarchical Cu2O modified electrode. *Talanta,* 85,1260.

150. Cherevko S and Chung CH (2010). The porous CuO electrode fabricated by hydrogen bubble evolution and its application to highly sensitive non-enzymatic glucose detection. *Talanta*, 80, 1371.

151. Tong SF, Jin HY, Zheng DF, Wang W, Li X, Xu YH, Song WB (2009). Investigations on copper–titanate intercalation materials for amperometric sensor. *Biosens. Bioelectron*., 24, 2404.

152. Luo J, Jiang SS, Zhang HY, Jiang JQ, Liu XY (2012). A novel non-enzymatic glucose sensor based on Cu nanoparticle modified graphene sheets electrode. *Anal. Chim. Acta*,709. 47.

153. Li X, Zhu Q, Tong S, Wang W, Song W (2009). Self-assembled microstructure of carbon nanotubes for enzymeless glucose sensor. *Sens. Actuators, B,* 136, 444.

154. Luque G, Rodríguez M, Rivas G (2005). Glucose biosensors based on the immobilization of copper oxide and glucose oxidase within a carbon paste matrix. *Talanta*, 15, 467.

155. Tong S, Xu Y, Zhang Z, Song W (2010). Dendritic bimetallic nanostructures supported on self-assembled titanate films for sensor application. *J. Phys. Chem. C,* 114, 20925.

156. Luo P, Prabhu SV, Baldwin RP (1990). Constant potential amperometric detection at a copper-based electrode: electrode formation and operation. *Anal. Chem*., 62, 752.

157. Luo PF and Kuwana T (1994). Nickel-titanium alloy electrode as a sensitive and stable LCEC detector for carbohydrates. *Anal. Chem*., 66, 2775.

158. Casella IG, Desimoni E, Cataldi TR (1991). Study of a nickel-catalysed glassy carbon electrode for detection of carbohydrates in liquid chromatography and flow injection analysis. *Anal. Chim. Acta*, 248, 117.

159. Lu B, Bai J, Bo X, Zhu L, Guo L (2010). A simple hydrothermal synthesis of nickel hydroxide–ordered mesoporous carbons nanocomposites and its electrocatalytic application. *Electrochim. Acta*, 55, 8724.

160. El Khatib KM, Hameed RA (2011). Development of Cu2O/Carbon Vulcan XC-72 as non-enzymatic sensor for glucose determination. *Biosens. Bioelectron*., 26, 3542.

161. Wang W, Zhang L, Tong S, Li X, Song W (2009). Three-dimensional network films of electrospun copper oxide nanofibers for glucose determination. *Biosens. Bioelectron*., 25, 708.

162. Zhang X, Wang G, Liu X, Wu J, Li M, Gu J, Liu H, Fang B (2008). Different CuO nanostructures: synthesis, characterization, and applications for glucose sensors. *J. Phys. Chem., A*, 112, 16845.

163. Wang X, Hu C, Liu H, Du G, He X, Xi Y (2010). Synthesis of CuO nanostructures and their application for nonenzymatic glucose sensing. *Sens. Actuators, B*, 144, 220.

164. Li C, Su Y, Zhang S, Lv X, Xia H, Wang Y (2010). An improved sensitivity nonenzymatic glucose biosensor based on a CuxO modified electrode. *Biosens. Bioelectron.*, 26, 903.

165. Zhuang Z, Su X, Yuan H, Sun Q, Xiao D, Choi MM (2008). An improved sensitivity non-enzymatic glucose sensor based on a CuO nanowire modified Cu electrode. *Anal.*,133, 126.

166. Li JY, Xiong S, Pan J, Qian Y (2010). Hydrothermal Synthesis and Electrochemical Properties of Urchin-Like Core− Shell Copper Oxide Nanostructures. *J. Phys. Chem. C*, 114, 9645.

167. Reitz E, Jia W, Gentile M, Wang Y, Lei Y (2008). CuO nanospheres based nonenzymatic glucose sensor. *Electroanal*ysis, 20, 2482.

168. Fleischmann M, Korinek K, Pletcher D (1971). The oxidation of organic compounds at a nickel anode in alkaline solution. *J. Electroanal. Chem.*,31, 39.

169. Vertes G and Horanyi G (1974). Some problems of the kinetics of the oxidation of organic compounds at oxide-covered nickel electrodes. *J. Electroanal. Chem.*, 52, 47.

170. Robertson PM (1980). On the oxidation of alcohols and amines at nickel oxide electrodes: mechanistic aspects. *J. Electroanal. Chem*., 111, 97.

171. Wolf JF, Yeh LR, Damjanovic A (1981). Anodic oxide films at nickel electrodes in alkaline solutions—I. Kinetics of growth of the β-Ni (OH) 2 phase. *Electrochim. Acta*, 26, 4.

172. Nie H, Yao Z, Zhou X, Yang Z, Huang S (2011). Nonenzymatic electrochemical detection of glucose using well-distributed nickel nanoparticles on straight multi-walled carbon nanotubes. *Biosens. Bioelectron*., 30, 28.

173. You T, Niwa O, Chen Z, Hayashi K, Tomita M, Hirono S (2003). An amperometric detector formed of highly dispersed Ni nanoparticles embedded in a graphite-like carbon film electrode for sugar determination. *Anal.Chem*., 75, 5191.

174. Mu Y, Jia D, He Y, Miao Y, Wu HL (2011). Nano nickel oxide modified non-enzymatic glucose sensors with enhanced sensitivity through an electrochemical process strategy at high potential. *Biosens. Bioelectron*., 26, 2948.

175. Safavi A, Maleki N, Farjami E (2009). Fabrication of a glucose sensor based on a novel nanocomposite electrode. *Biosens. Bioelectron*., 24, 1655.

176. De Mele MF, Videla HA, Arvia AJ (1983). The electrooxidation of glucose on platinum electrodes in buffered media. *J. Electroanal. Chem. Interfacial Electrochem*.,155:239-49.

177. Danaee I, Jafarian M, Forouzandeh F, Gobal F (2012). Kinetic studies of glucose electrocatalytic oxidation on GC/Ni electrode. *Int. J. Chem. Kinet.*, *44*(11), 712-721.

178. Miao Y, Ouyang L, Zhou S, Xu L, Yang Z, Xiao M, Ouyang R (2014). Electrocatalysis and electroanalysis of nickel, its oxides, hydroxides and oxyhydroxides toward small molecules. *Biosens. Bioelectron.*, *53*, 428-439

179. Niu X, Lan M, Zhao H, Chen C (2013). Highly sensitive and selective nonenzymatic detection of glucose using three-dimensional porous nickel nanostructures. *Anal. Chem.*, *85*(7), 3561-3569

180. Iwu KO, Lombardo A, Sanz R, Scirè S, Mirabella S (2016). Facile synthesis of Ni nanofoam for flexible and low-cost non-enzymatic glucose sensing. *Sens. Actuators, B*, *224*, 764-771.

181. Guo H, Huang Z, Zheng Y, Weng S (2015). Electrodeposition of nickel nanoparticles modified glassy carbon electrode for nonenzymatic glucose biosensing. *Int. J. Electrochem. Sci.*, *10*, 10703-10712.

182. Ghonim AM, El-Anadouli BE, Saleh MM (2013). Electrocatalytic glucose oxidation on electrochemically oxidized glassy carbon modified with nickel oxide nanoparticles. *Electrochim. Acta*, *114*, 713-719.

183. Danial AS, Saleh MM, Salih SA, Awad MI (2015). On the synthesis of nickel oxide nanoparticles by sol–gel technique and its electrocatalytic oxidation of glucose. *J. Power Sources*, *293*, 101-108.

184. Danial AS, Awad MI, Al-Odail FA, Saleh MM (2017). Effect of different synthesis routes on the electrocatalytic properties of NiOX nanoparticles. *J. Mol. Liq.*, *225*, 919-925.

185. Zhang H and Liu S (2017). Nanoparticles-assembled NiO nanosheets templated by graphene oxide film for highly sensitive non-enzymatic glucose sensing. *Sens. Actuators, B, 238*, 788-794.

186. Hasanzadeh M and Sabzi R (2015). Preparation and characterization of nickel oxide nanoparticles and their application in glucose and methanol sensing. *Curr. Chem. Lett.*, *4*(2), 45-54.

187. Qiao N and Zheng J (2012). Nonenzymatic glucose sensor based on glassy carbon electrode modified with a nanocomposite composed of nickel hydroxide and graphene. *Microchim. Acta*, *177*(1-2), 103-109.

188. El-Refaei SM, Saleh MM, Awad MI (2013). Enhanced glucose electrooxidation at a binary catalyst of manganese and nickel oxides modified glassy carbon electrode. *J. power sources*, *223*, 125-128.

189. Zhang Y, Wang Y, Jia J, Wang J (2012). Nonenzymatic glucose sensor based on graphene oxide and electrospun NiO nanofibers, *Sens. Actuators, B., 171*, 580-587.

190. El-Refaei SM, Awad MI, El-Anadouli BE, Saleh MM (2013). Electrocatalytic glucose oxidation at binary catalyst of nickel and manganese oxides nanoparticles modified glassy carbon electrode: Optimization of the loading level and order of deposition. *Electrochim. Acta, 92*, 460-467.

CHAPTER II

EXPERIMENTAL

CHAPTER II

EXPERIMENTAL

This Chapter of dissertation would introduce the materials, synthesis of nanoparticles, morphological, and electrochemical characterization techniques employed along with a brief overview of the techniques.

2.1. Chemicals and solutions

All chemicals used in the present work were analytical grade. Reagent grade Sulphuric acid (H_2SO_4, OmniTrace Ultra), glucose ($C_6H_{12}O_6$, 99.9 % purity) were purchased from (Sigma-Aldrich). Sodium hydroxide NaOH (99. 8% purity), Boric acid, and Nickel sulphate were purchased from (BDH). Nickel chloride was purchased from (M&B). In this work, all chemicals were used as received without any further purification.

All solutions were prepared with deionized water and bubbled with nitrogen whenever needed. A nickel oxide (NiO_x) nanoparticles electrocatalyst was prepared by electrodeposition from a nickel bath (0.02 M $NiSO_4$ + 0.03 M $NiCl_2$ + 0.03M H_3BO_3) in the presence or absence of a suitable additive, typically glucose, dissolved in deionized water. Details are mentioned in chapter III.

Glucose was prepared by taking the right amount of glucose using a micropipette and mix it with the appropriate electrolyte. All the glassware (Conical flask, volumetric flask, pipette, measuring cylinder, etc.) were cleaned by distilled water, rinsed with de-ionized water, and air dried before use.

2.1.1. Electrolyte

Deionized water was used to prepare all aqueous solutions and for rinsing. The electrolyte solutions consisting of 0.5 M NaOH were prepared with de-ionized water for glucose oxidation experiments in alkaline medium.

2.2. Electrochemical measurements

To determine the chemical behavior of nickel oxide (NiO_x) nanoparticles for the electrooxidation of glucose, cyclic voltametery, chronoamperometry, chronocoulometry and Tafel techniques were used.

2.2.1. Electrodes

In this thesis, two working electrodes, i.e., gold (Au) electrode and glassy carbon (GC) electrodes, platinum spiral wire as the counter electrode and silver/ silver chloride Ag/AgCl (KCl sat.) as reference electrode.

2.2.2. Pretreatment of working electrodes

The electrode was prepared in such a manner to make sure its surface is reproduced before each experiment. These may be as simple as mechanical polishing and may include pre-scanning across a certain potential range or exposure to a solvent or chemical species to "activate" the electrode.

Polishing procedure was used in this work to prepare the working electrodes **(**Au and GC electrodes**)**. The electrode was polished until the surface is visually smooth with sandpaper. Polishing start from Grit 1500 to 3000 and rinsed with de-ionized water. Then, using alumina powder (down to 0.06 μm) and then ultrasonically cleaned in pure De-ionized water for 15 min for removing any physically adsorbed species.

2.2.2.1. Electrochemical pretreatment

Au electrode was electrochemically pretreated [1] in 0.5 M H_2SO_4 solution by repeating the potential scan in the potential ranges of – 0.2 to 1.5 V vs. Ag/AgCl (KCl sat.) at three steps. First step called (before treatment), in this step one potential scan in the potential ranges of – 0.2 to 1.5 V vs. Ag/AgCl (KCl sat.) at scan rate 100 mV/s^{-1}. is conducted. Second step called (treatment step), this step takes ~800 potential scan by cyclic voltammetry (CV) at 10 V/s^{-1}. in the potential ranges of – 0.2 to 1.5 V vs. Ag/AgCl (KCl sat.). Third step called (after treatment), in this

step one scan by CV measured in the potential ranges of –0.2 to 1.5 V vs. Ag/AgCl (KCl sat.) at a scan rate 100 mV/s^{-1}. to make sure that the cyclic voltammetric (CV) characteristic of a clean Au electrode was obtained.

GC electrode was electrochemically activated in 0.5 M H_2SO_4 solution by repeating the potential scan in the potential ranges of – 0.2 to 2.0 V vs. Ag/AgCl (KClsat.) at a scan rate 100 mV/s^{-1}. for a suitable number of potential cycles [2].

2.2.3. Modification of graphene on glassy carbon electrode (GC_{ox}/Gr)

Graphene was prepared (figure 2.1) in ultrasonicating for 30 min by using 0.1 mg of graphene with 5 ml of ethanol according to literature [3]. Then, 10 μl of prepared graphene is dropped on the surface of glassy carbon electrode then left to dry room temperature.

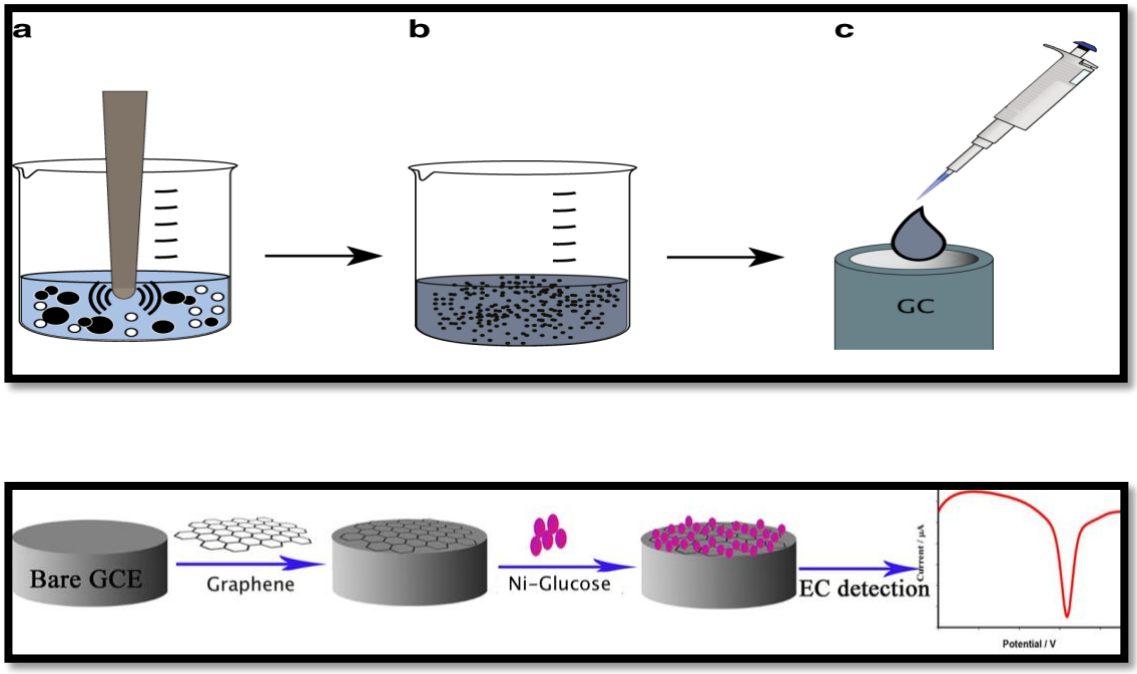

Figure 2.1: Steps of the preparation of GC_{ox}/Gr electrode.

2.2.4. Assembling of NiOx nanoparticles on gold and glassy carbon electrodes

In cell 1 the electrochemical behavior of GC_{ox} electrode and Au electrode are recorded in 0.5 M H_2SO_4. The electrode was then transferred to cell II where the deposition of the nickel oxide (NiO_x) nanoparticles from a nickel bath (0.02 M $NiSO_4$ + 0.03 M $NiCl_2$ + 0.03M H_3BO_3) containing a suitable additive, typically glucose, using five potential cycles at range from 0.0 to -1.0 V vs. Ag/AgCl (KCl sat.).

2.3. Measurements

The voltammetric measurements are conducted in a conventional three-electrode cell of around 20 ml, shown in (Fig. 2.2). Potentiostat/galvanostat/ZRA model the Reference 600 ™ machine (Fig 2.3) was used for voltammetric experiments. Counter and reference electrode used in the all experiments were a platinum spiral wire and Ag/AgCl (KCl sat.), respectively. A 3 mm glassy carbon disc (SigradurR-G, Sigri Electrographite GMBH, Germany) bound in a Teflon tube via araldite (Fig. 2.4) and gold was used as working electrode. All electrochemical measurements were performed at the room temperature.

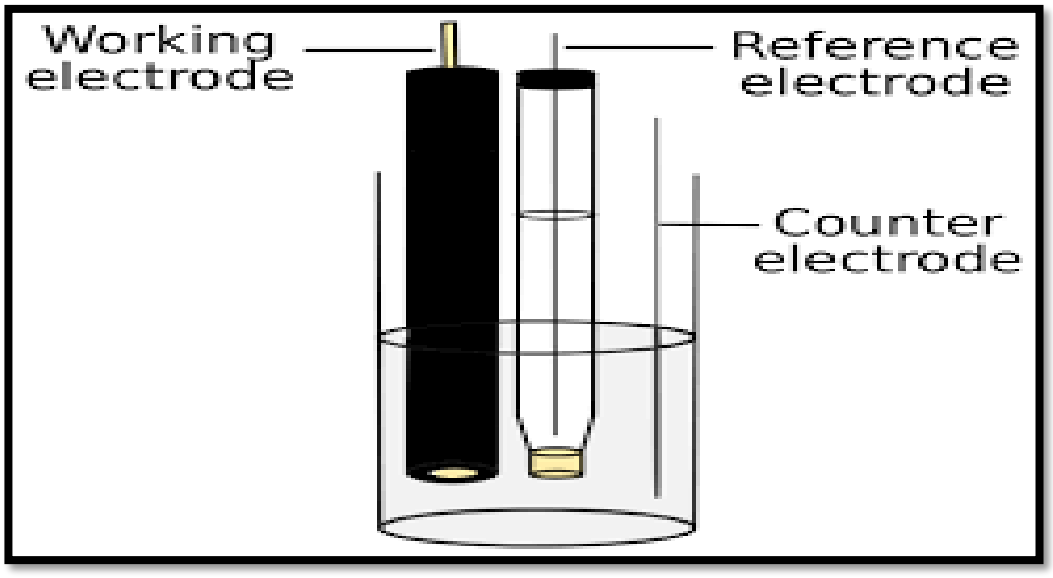

Figure 2.2. One compartment cell.

Figure 2.3. Potentiostat /galvanostat/ZRA model Reference 600 ™.

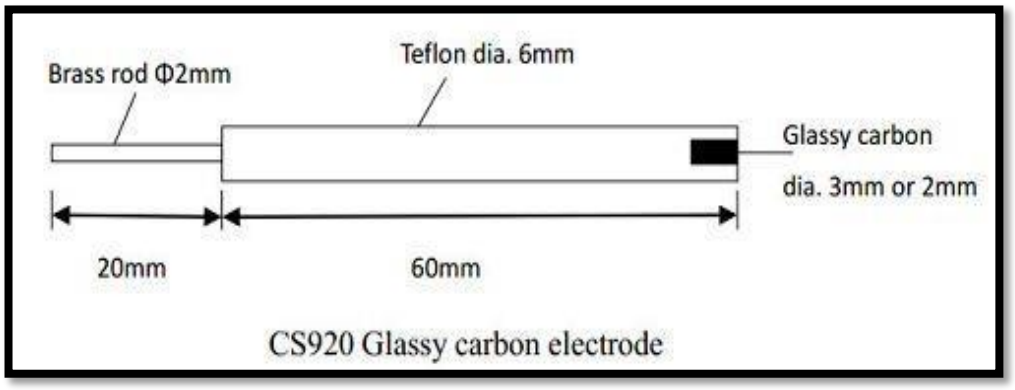

Figure 2.4. Glassy Carbon (GC) electrode.

2.4. Electrochemical characterization

2.4.1. Cyclic Voltammetry

After assembling of nickel oxide (NiO_x) nanoparticles by potential cycling, the modified electrode was subjected to measuring cyclic

voltammetry under different conditions, both in the presence and absence of glucose.

2.4.2. Tafel

After recording the CV of the modified electrode in 0.5M NaOH, the electrode has been transferred to another cell (containing 5 mM glucose) and Tafel plot has been obtained at potential scan rate of 5 mV/s^{-1}.

2.4.3. Current-decay measurements

After recording the voltammogram of the modified electrode in 0.5M NaOH, the electrode the current decay measurements were measured over a period of ~3000 sec.

2.5. Surface Characterization of modified electrode

Several qualitative and quantitative methods were employed for structural characterization, probing morphology of modified electrodes.

2.5.1. Scanning electron microscopy (SEM)measurements

Scanning Electron Microscopy (SEM) is a type of electron microscope technique that utilizes back scattered and secondary electrons to produces images by scanning the surface of the sample

with focused beam of a tiny electrons. At the same time, the generated signals are being recorded, and an image is formed pixel by pixel.

It also has the ability to accurately measure and evaluate materials, molecules and fibers. SEM is a useful tool in terms of industry and research because it is a strong tool for characterization in many fields. For example, pollution problems, identification of unknown particles, component testing, study of interaction between materials and their substrates.

High-resolution images can be obtained by applying SEM to both catalysts, plastics, raw materials, food, surfaces, contaminants, films, coatings, metals, biological tissues or unknown materials.

A Scanning Electron Microscope (SEM) Model (JEOL JSM 5410 JAPAN) was used to investigate the surface morphology and composition of the metal nanoparticles on glassy carbon electrodes, before and after modification with catalysts.

2.5.2. XRD Characterization

X-ray diffraction (XRD) is a powerful and non-destructive technique for the characterization of crystalline materials. Many information is obtained about the preferred crystalline orientations (texture), phases and other structural parameters and structures. For example, strain, grain size, crystal and crystal defects. Each set of lattice planes occurs by the

constructive interference of a monochromatic beam of x-rays diffraction at specific angles from which X-ray diffraction peaks are produced. Bragg's law is used for evaluation of crystal structure, which can be modeled as constructive interference by two waves reflected from rows of atoms. Fig. 2.5. shows the model of reflection from two planes of atoms in a solid. If the wavelength (λ) of the incident X-rays and the incident angle (θ) are known, then the interplanar spacing (d) can be determined by Bragg‟s equation as:

$$2d\sin(\theta) = n\lambda \qquad (2.1)$$

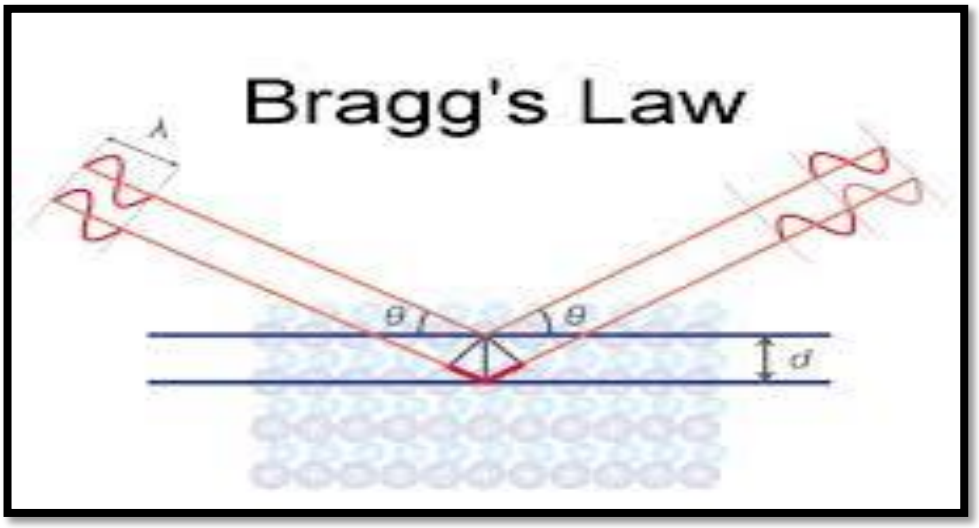

Figure 2.5. Diffraction of X-ray by rows of atoms in a crystal lattice

This technique is characterized by giving a certain material the fingerprint of periodic atomic arrangements.

In this work, the X-ray diffraction studies were recorded with using a Philips PW 105 diffractometer using Nifiltered Cu Kα radiation at a grazing incidence angle of 1.540 A˚ with a step size of 0.1° and counting time of 15 s per step. A scanning range recorded in the 2θ of extending from 10° to 85°.

2.5.3 EDAX Characterization

There are many x-ray techniques, including Energy Dispersive X-Ray Analysis EDX, referred to as EDS or EDAX, which are used to determine the initial structure of the elements by identifying the atomic ratios in the electrocatalysts synthesized.

EDX gives the sample data that is analyzed in the form of spectra to determine their true composition by showing the peaks corresponding to the elements in the sample and mapping them first by measuring the characteristic X-rays energies emitted during the transferring process (a transition of the outer shell electrons to inner shell). Also, a high energy incident electron beam makes an electron hole in the inner shell and causes the transition of an outer shell electron. As well as, the energy of the X-rays emitted is characteristic of the element, an accurate estimation of elemental compositions can be obtained using this technique. Elemental composition of the catalyst on the electrode surface was determined using energy dispersive x-ray

(EDAX), horida-ex-200, Japan. The incident electron energies were kept constant at 10 keV for all the samples.

2.6. REFERENCES

1. Casella IG, Guascito MR, Sannazzaro MG (1999). Voltammetric and XPS investigations of nickel hydroxide electrochemically dispersed on gold surface electrodes. *J. Electroanal. Chem*., 462(2):202-10.

2. Ghonim AM, El-Anadouli BE, Saleh MM (2013). Electrocatalytic glucose oxidation on electrochemically oxidized glassy carbon modified with nickel oxide nanoparticles. *Electrochim. Acta,*114:713-9.

3. Hummers Jr, William S, Offeman RE (1958). Preparation of graphitic oxide. *J. Am. Chem. Soci*., 80(6):1339-1339.

CHAPTER

III

RESULTS

AND

DISCUSSION

PART 1

CHAPTER III (PRAT 1)

RESULTS AND DISCUSSION

Electrocatalytic oxidation of glucose at nickel oxide modified gold electrode

3.1.1. Abstract

Nickel oxides (NiOx) modified gold electrodes (Au) was suggested as efficient and durable anode for glucose oxidation reaction. It was fabricated from (Watts Nickel) in the presence, designated as Au/NiOx(Glu), and in absence, designated as Au/NiOx, of suitable additive (Glucose). Moreover, Au/NiOx(Glu) electrode showed the best electrocatalytic activity for electrooxidation of glucose compared to Au/NiOx electrode. These outstanding enhancements are attributed to adding of glucose in the deposition bath. The electrocatalytic activity of the various prepared electrodes towards electrooxidation of glucose was evaluated by cyclic voltammetry (CV) and chronoamperometry in alkaline media. Furthermore, scanning electron microscopy (SEM) and energy-dispersive X-ray spectroscopy (EDX), mapping EDX techniques were used to characterize the electrocatalysts. Enhancement of electrooxidation of glucose is discussed in the light of the difference in structural and electrochemical characteristics of both electrodes.

3.1.2. Introduction

In the clinical field it was estimated that 2.8% of the world population, around 171 million people, were affected by diabetes in 2000. It is expected to be around 4.4% by the year 2030, approximately 366 million people [1]. Most of the studies involved for the glucose sensor are the enzymatic reaction between the glucose and glucose oxidase.

Glucose oxidase catalyzes the oxidation of glucose to gluconolactone in the presence of redox mediators and metallic nanoparticles coated on the electrode. However, the cost of the enzyme, mediator, and electrode are expensive. In addition, electrode fouling might occur due to the thermal environment, pH change, lack of chemical stability, and fair toxicity [2-4]. Hence, the enzymeless glucose sensors are dramatically developed due to the low fabrication cost, overpotential reduction, and low detection limit with selectivity, sensitivity, and stability [5-10]. The noble metals and their oxides used as the redox mediators for the non-enzymatic glucose sensors have been reported [11-17].

In the present work nickel oxide (NiOx) film modified gold electrode (Au) is applied for electrocatalysis of glucose. NiOx become popular for sensor devices because of its electrocatalytic activities [18-22].

3.1.3. Experimental

3.1.3.1. Chemicals

All chemicals used in this work were of analytical grade and were purchased from Sigma Aldrich and they were used as received without further purification. All solutions were prepared using deionized water.

3.1.3.2. Electrochemical measurements

Potentiostat/galvanostat/ZRA model the Reference 600 ™ machine were used for the electrochemical measurements. A conventional cell with a three-electrode configuration was used in this work. An Ag/AgCl/KCl (sat.) as a counter electrode and a platinum spiral wire as reference electrodes were utilized. The working electrode was gold electrode. It was cleaned by mechanical polishing with aqueous slurries of successively finer alumina powder then washed thoroughly with deionized water.

3.1.3.3. Fabrication of modified electrode

Au electrode was electrochemically pretreated in 0.5 M H_2SO_4 solution by repeating the potential scan in the potential ranges of – 0.2 to 1.5 V vs. Ag/AgCl (KCl sat.) at scan rate 100 mV/S^{-1} to make sure the cyclic voltammetric (CV) characteristic of a clean Au electrode was obtained. Then, Au electrode was transferred to cell II containing the nickel bath, either

containing glucose as additive or not, where the deposition of the nickel oxide (NiO_x) using cyclic voltammetry in potential range from 0.0 to -1.0 V vs. Ag/AgCl (KCl sat.) is conducted.

3.1.3.4. surface characterization

A field emission scanning electron microscope, FE-SEM, (QUANTA FEG 250) was used to identify the structure of the nano-NiO_X Energy. Also, dispersive X-Ray Analysis (EDX) analysis, referred to as EDS or EDAX, (PANalytical, X'Pert PRO) operated with Cu target (λ = 1.54 Å) were used to identify the crystallographic structure of the nano-NiO_X at bare Au, Au/NiOx electrodes, and Au/ NiOx(Glu) electrode.

3.1.4. Results and Discussion

3.1.4.1. Morphological characterization

Fig. 3.1 shows (A, C and E) SEM images and (B, D and E) EDX taken for (A,B) bare Au, (C,D) Au/NiOx and (E,F) Au/NiOx(Glu) electrodes. Electrodes were prepared as mentioned in the experimental section. In image (A) a relatively smooth surface is shown and in EDX (plot B), an intense peak for Au obtained at 2.2 KeV is revealed. In the case of Au/NiOx (image C), a nickel film is revealed. The formation of non-porous nickel film is confirmed from the EDX (plot D) in which the peak of the gold is almost disappeared

along with the formation of an intense peak for Ni at 0.9, 7.6, 8.2 KeV in addition of another peak at 0.4 KeV for oxygen. Probably the last peak is formed as a result of the oxidation of nickel in NaOH as explained in the experimental section. In image E, obtained at Au/NiOx(Glu) electrode; i.e., at nickel oxide deposited onto Au from a nickel bath containing glucose as an additive, a deposition of NiO_x is observed, as revealed from the EDX (plot F) in which peaks for nickel appeared at 0.9 , 7.6, 8.2 KeV, are observed [23,24]. In this case the peaks of the Au, obtained at 0.8, 2.2, 8.4, and 9.8 KeV are also revealed. This may point to that the deposited of nickel film is porous.

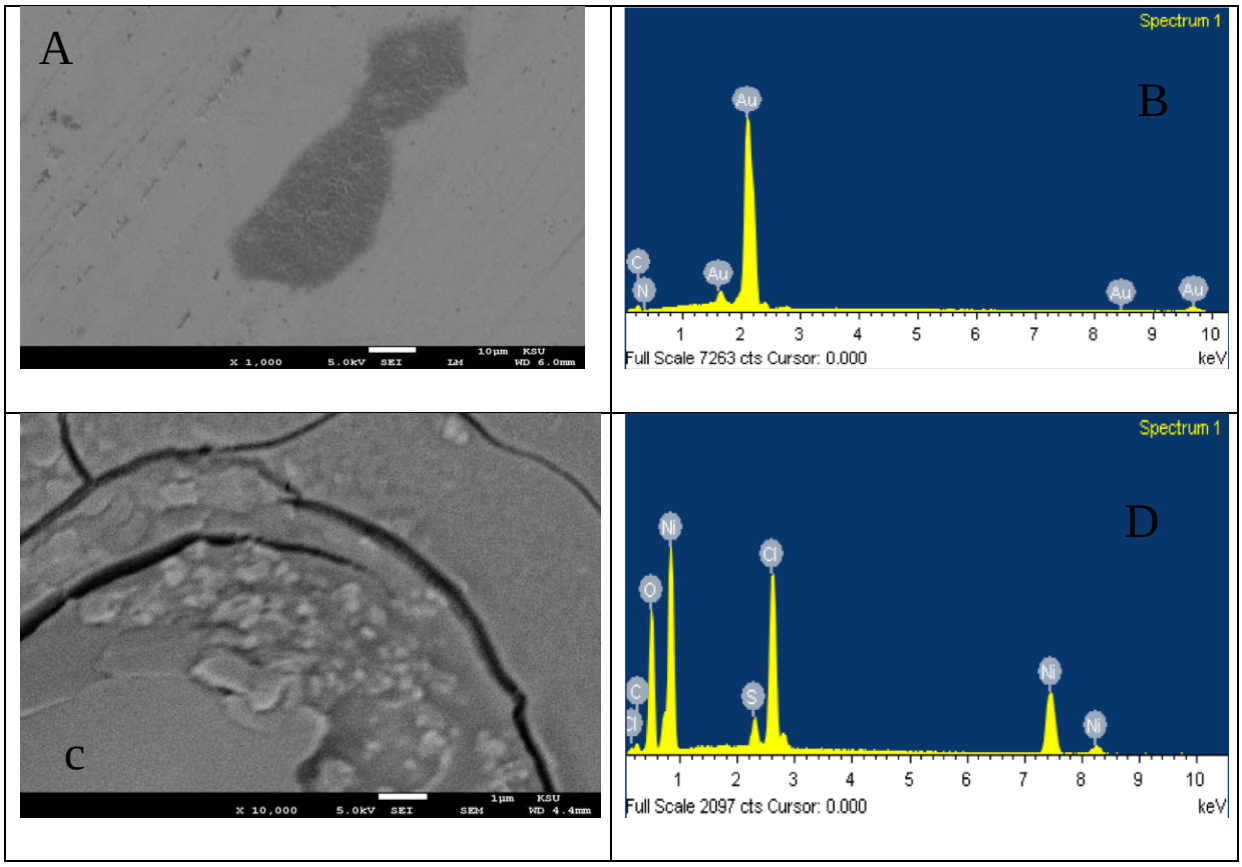

Figure 3.1. SEM (A,C,E) and EDX (B,D,F) of (A,B) Au, (C,D) Au/NiOx , and(E,F) Au/NiOx(Glu) electrodes.

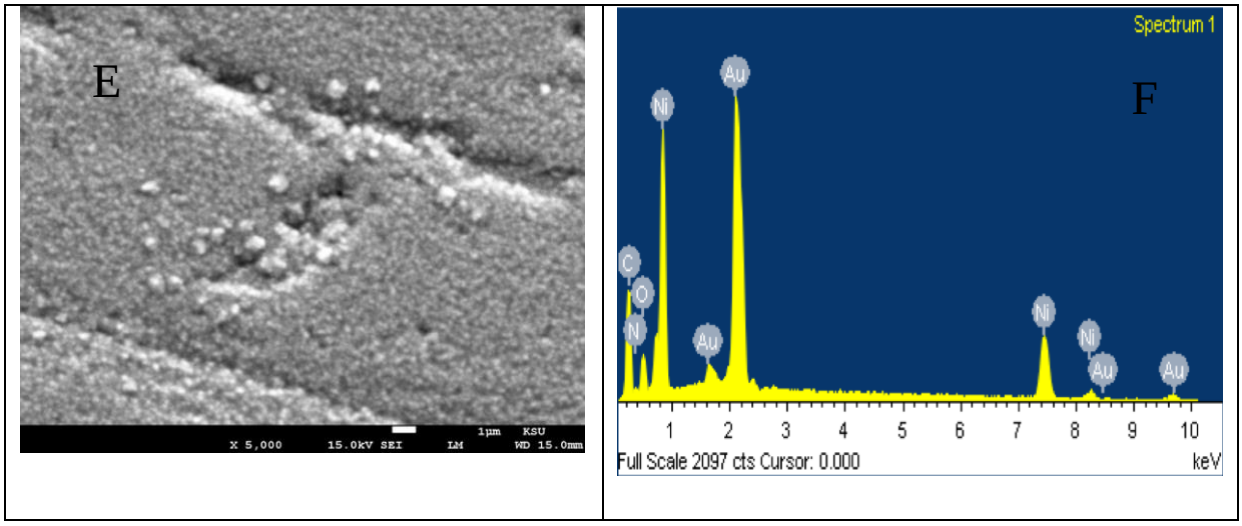

Figure 3.1. (Continued).

3.1.4.2. Cyclic Voltammetry

Fig. 3.2. shows CVs obtained at (a) bare Au, (b) Au/NiOx and (c) Au/NiOx(Glu) electrodes in 0.5 M NaOH solution. In curve a, the well-known response of Au electrodes is obtained; the broad peak started at 0.45 V which coupled by a cathodic peak, centered at 0.18 V, for the reduction of gold oxide formed in the anodic scan is revealed. In the case of Au/NiOx (curve b) the gold/gold oxide couple disappeared and another new couple appeared. Probably this couple, at 0.35 and 0.39 V corresponds to nickel oxidation/ reduction couple, consistently with the reported values [25]. In the case of Au/NiOx(Glu) in which nickel was deposited from nickel bath containing glucose as additive the response for the nickel couple is intensified and became sharper than for Au/NiOx, which is prepared from nickel bath free of glucose. One more point to be focused is the successful deposition of nickel as indicated from the

enhancement of oxygen evolution at large anodic potential. The oxygen evolution at bare Au is not revealed within the studied potential range. It is well reported that Nickel is more active than gold towards oxygen evolution [26]. The absence of gold response at both modified electrodes points to the complete coverage of the underlying substrate with deposited nickel.

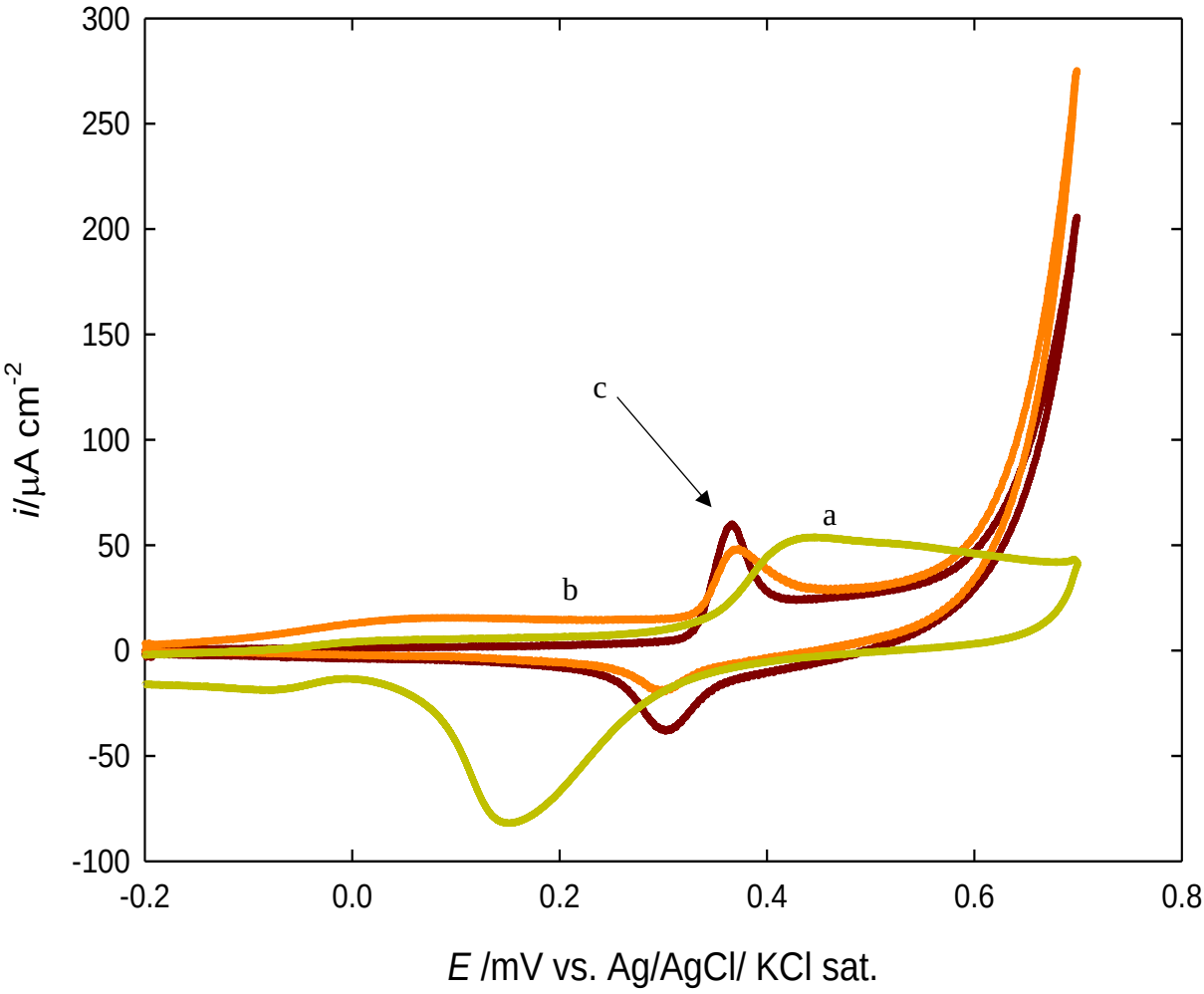

Figure 3.2. CV obtained at (a) bare Au, (b) Au/NiOx, (c) Au/NiO$_x$(Glu) electrodes in 0.5 M NaOH.

Fig. 3.3 shows the cyclic voltammograms obtained at the Au/NiOx(Glu) in 0.1 M NaOH solution at different potential scan rates. The anodic and cathodic peak currents directly proportional to the potential scan rate (Fig. 3.4). This can be attributed to an electrochemical activity of an immobilized redox

couple at the surface (Eq. (3.1)). A direct proportion points to a surface confined species [26,27,28]. From the slope of this line and using (Eq. (3.2)) [29,30]:

$$Ni(OH)_2 + OH^- \rightleftarrows NiOOH + H_2O + e^- \qquad (3.1)$$

$$I_p = n^2F^2\upsilon A\,\Gamma^*/4RT \qquad (3.2)$$

where I_p, A and Γ^* are peak current, electrode surface area and surface coverage of the redox species, respectively, and taking the average of both cathodic and anodic currents, the total surface coverage of the immobilized active substance of about 2.01×10^{-8} mol cm^{-2} was derived.

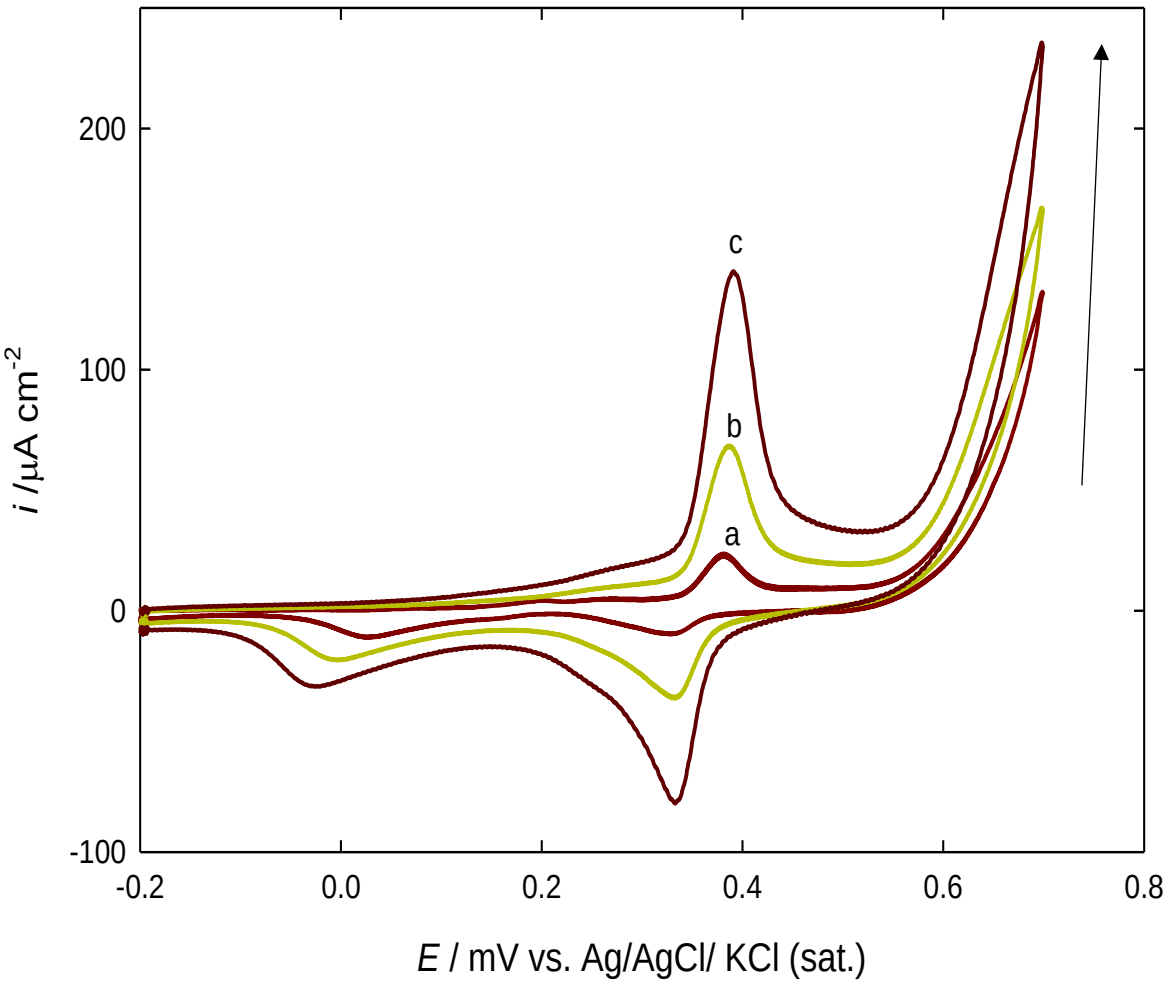

Figure 3.3. CV obtained at Au/NiO_x (Glu) electrode in 0.5 M NaOH at different scan rates (a) 20, (b) 50, and (c) 100 mV/s.

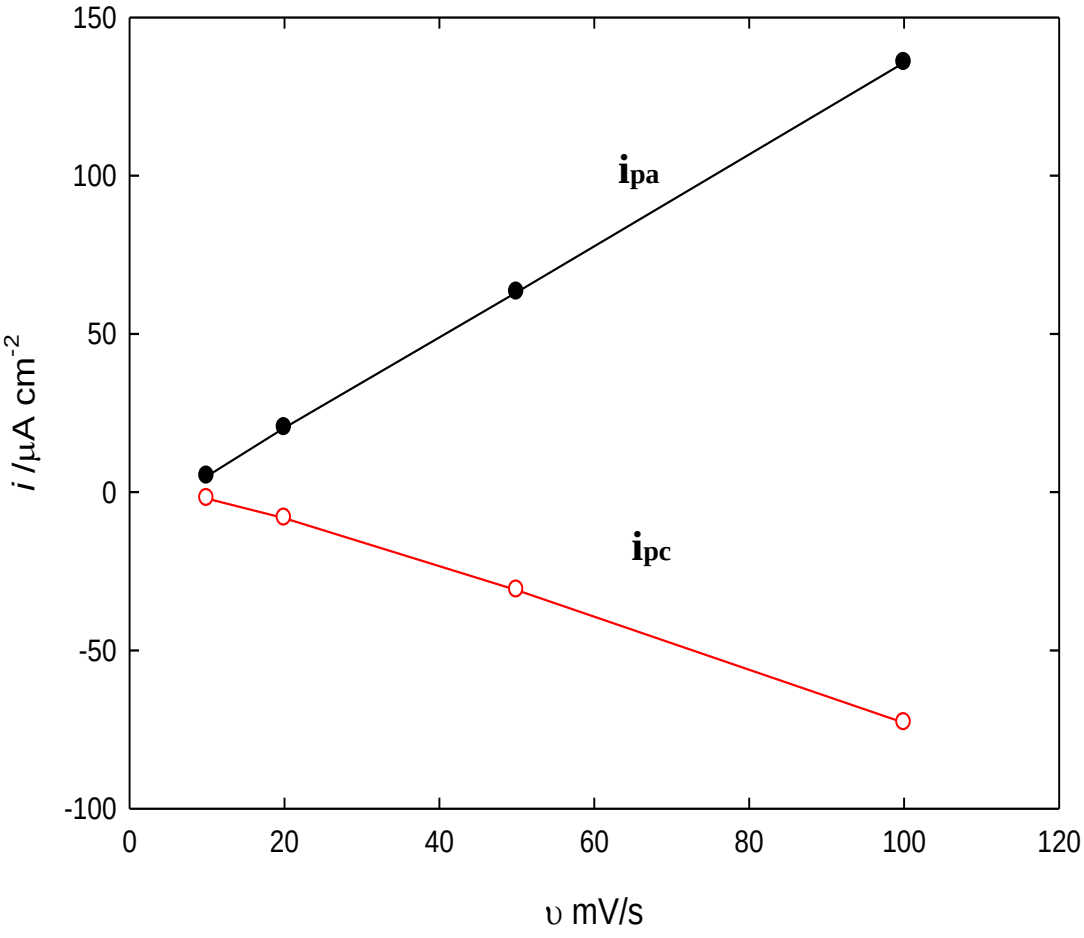

Figure 3.4. A plot of Ip with the scan rate obtained at Au/NiOx(Glu) in 0.5 M NaOH, for both anodic (i_{pa}) and cathodic (i_{pa}) peaks.

Fig. 3.5 shows CVs responses obtained (a) Au/NiOx and (b) Au/NiOx(Glu) electrodes in 0.5 M NaOH solution containing 2.5 mM glucose. As clearly shown, in the response at Au/NiOx(Glu) electrode (curve b) is significantly enhanced compared with the one obtained at Au/NiOx electrode. While a well-defined oxidation peak is obtained at Au/NiOx(Glu) electrode at relatively less positive potential, a weak peak is obtained at larger positive potential at Au/NiOx electrode. This confirms the prominent role of glucose in

the deposition bath for the subsequent oxidation of glucose at the modified electrode. In addition to the enhancement of glucose oxidation, the oxygen evolution at Au/NiOx(Glu) electrode is largely retarded compared with Au/NiOx electrode, a point which is very useful in the analysis of glucose.

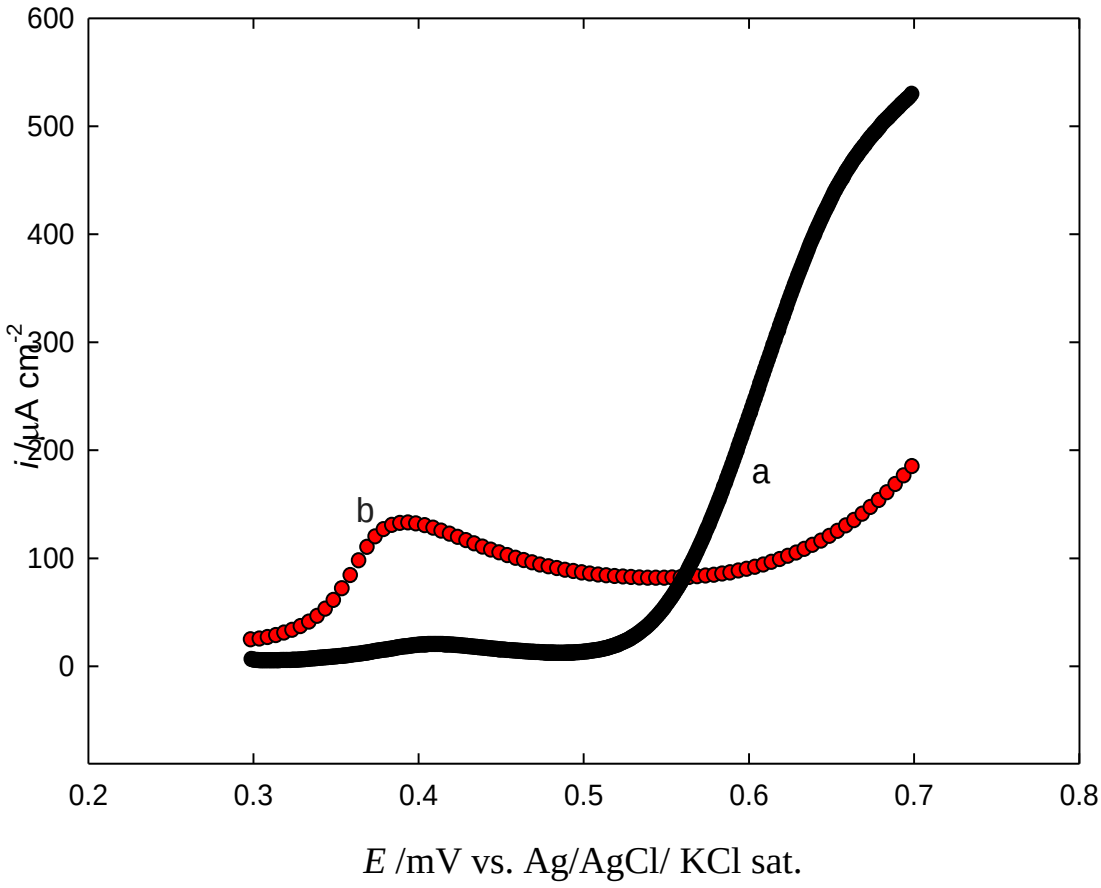

Figure 3. 5. CV obtained at (a) Au/NiO$_x$ and (b) Au/NiO$_x$(Glu) in 0.5 M NaOH containing 2.5 mM glucose, scan rate 100 mV/s.

Cyclic voltammograms of the Au/NiOx(Glu) in the presence of 2.5 mM glucose at various potential scan rates were recorded in Fig. 3.6. It can be seen from this figure that glucose oxidation peaks potentials slightly shift to more positive values with increasing of potential scan rates, suggesting a kinetic limitation. This reveals that the catalytic oxidation of glucose on the modified electrode is not a rapid reaction. The catalytic behavior is pointed by the increase of the anodic peak current, at ca. 0.42 V on the expense of the reduction peak obtained at ca. 0.35 V.

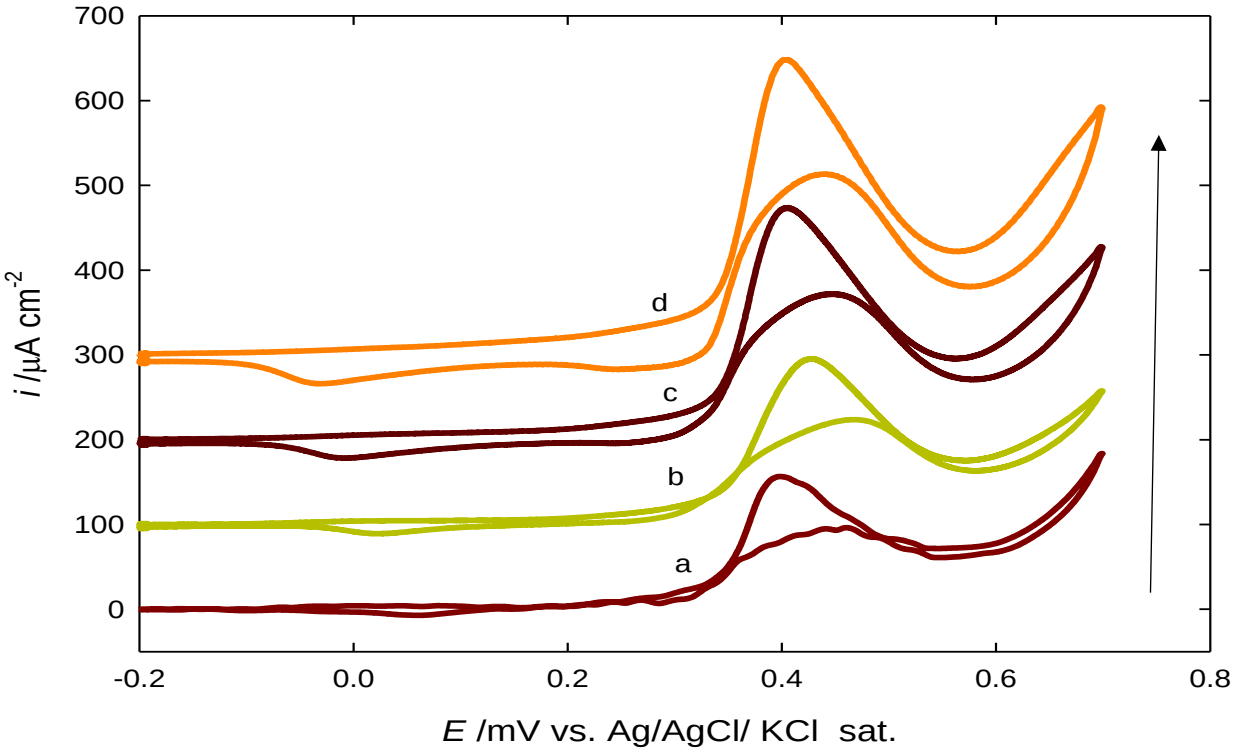

Figure 3.6. CV obtained at Au/NiOx(Glu) electrode in 0.5 M NaOH containing 2.5 mM glucose at different scan rates (a) 10, (b) 20, (c) 50, and (d) 100 mV/s.

The value of diffusion coefficient (D, cm^2/s) were obtained by the Randles-Sevcik equation (Eq. 3.3) for irreversible systems using the slope (of Fig. 3.7) of scan rates study (Ip vs. $\nu^{1/2}$).

$$I_p = (2.99 \times 10^5)\alpha^{\frac{1}{2}} AC^* D^{\frac{1}{2}} \nu^{\frac{1}{2}} \qquad (3.3)$$

where A is the electrode surface area (cm^2) and ν is the scan rate (V s^{-1}) C* is the bulk concentration of glucose in 0.05 M NaOH in terms of molar (mol/cm^3) solution. In this study the obtained D value is 2.6 x $10^{-6} cm^2/s$ from the slope value of Fig. 3.7, consistent with literature [31].

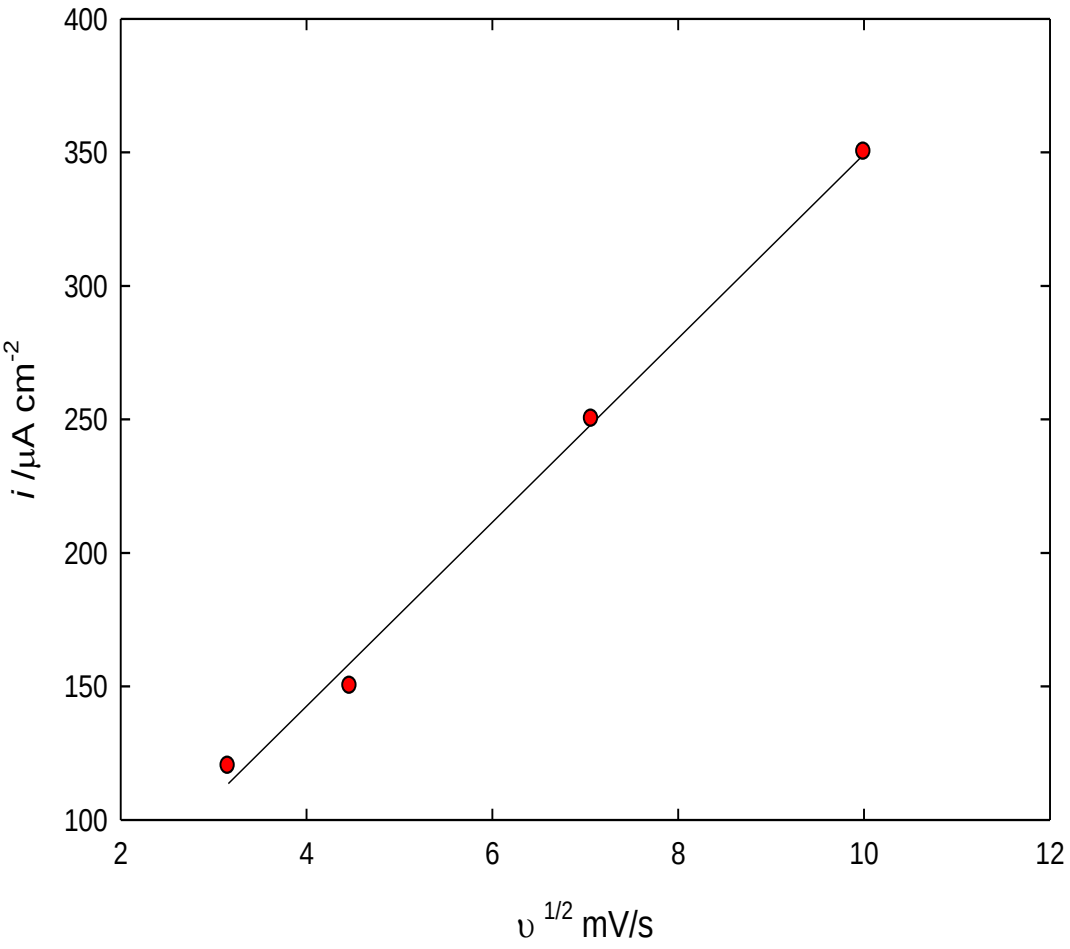

Figure 3.7. A plot of peak height (Ip) against square root of scan rate ($\nu^{1/2}$), in range of 10-100 mVs^{-1}, at Au/NiO_x(Glu) electrode in 0.5 M NaOH containing 2.5 mM glucose.

Fig. 3.8 shows the dependence of the function (Ip/$\nu^{1/2}$),) with *v* obtained at the Au/NiOx(Glu) electrode. As can be seen at scan rate higher than 40 mV s^{-1}, Ip/$\nu^{1/2}$ does not change significantly with the scan rate. This behavior is reported as a characteristic of catalytic reactions [33,34], i.e., EC mechanism, represented by Eqs. (3.4), and (3.5).

$$NiOOH + [Glucose]_{ads} \longrightarrow Ni(OH)_2 + \text{radical intermediate.} \quad (3.4)$$

$$\text{Radical intermediate} + 2NiOOH \longrightarrow 2Ni(OH)_2 + \text{gluconolactone} + 2e^- \quad (3.5)$$

The glucose oxidation is mediated by Ni couple, and that the inclusion of glucose in the deposition bath significantly modify deposited nickel oxide in such a manner that glucose oxidation is enhanced.

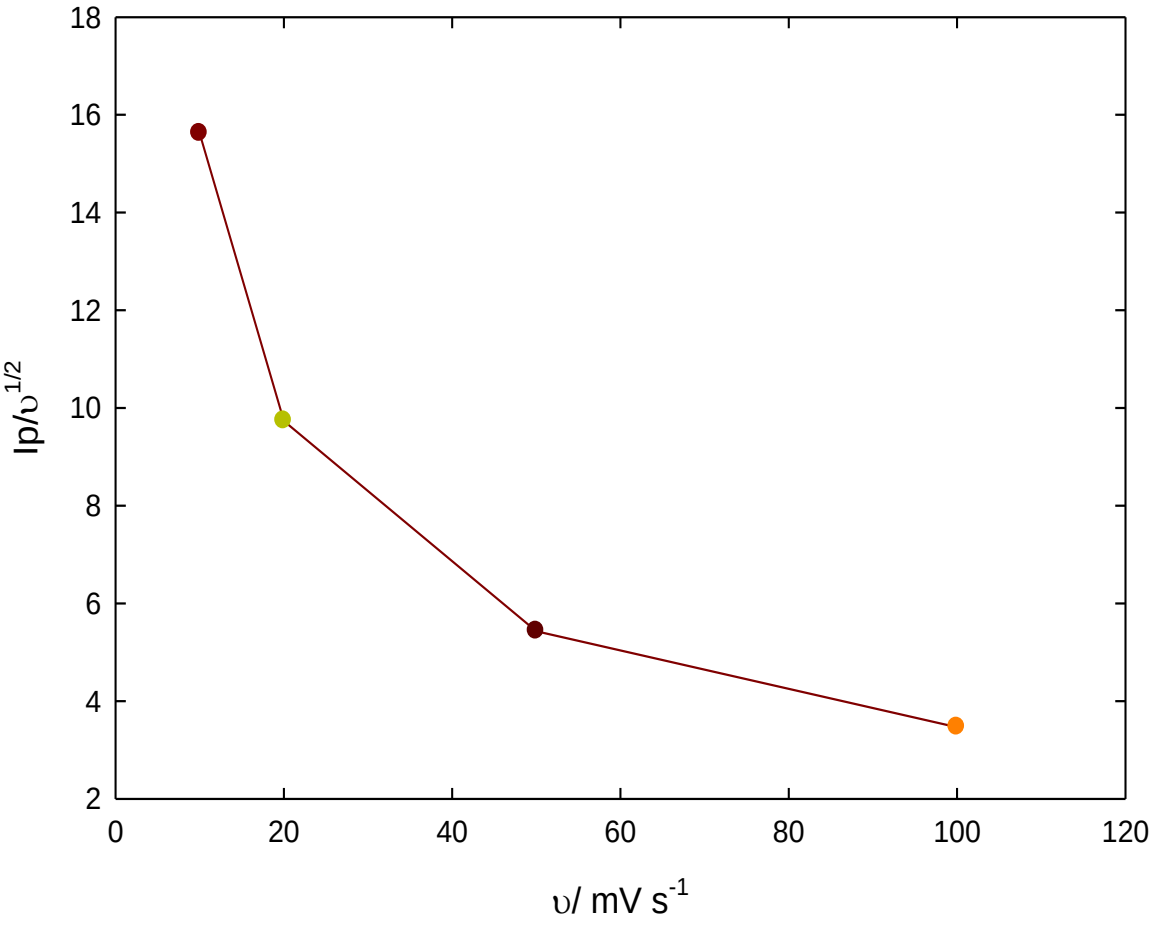

Figure 3.8. Variation of Ip/$\nu^{1/2}$ with ν for glucose electrooxidation obtained at Au/NiO_x(Glu) in 0.5 M NaOH containing 2.5 mM glucose.

3.1.4.3. Effect of loading of NiOx

Fig. 3.9 shows the effect of increasing loading of NiOx on the glucose oxidation. Parameters obtained from this figure are shown in Table 3.1. With increase of the time of deposition the current peak of glucose oxidation regularly increases with the larger current obtained at the deposition time of 400 s (at -1V). Thus, the deposition time of 400 s will be used as the optimum one. As clearly shown, the effect on the peak potential is negligible, while the effect on the peak current is significant.

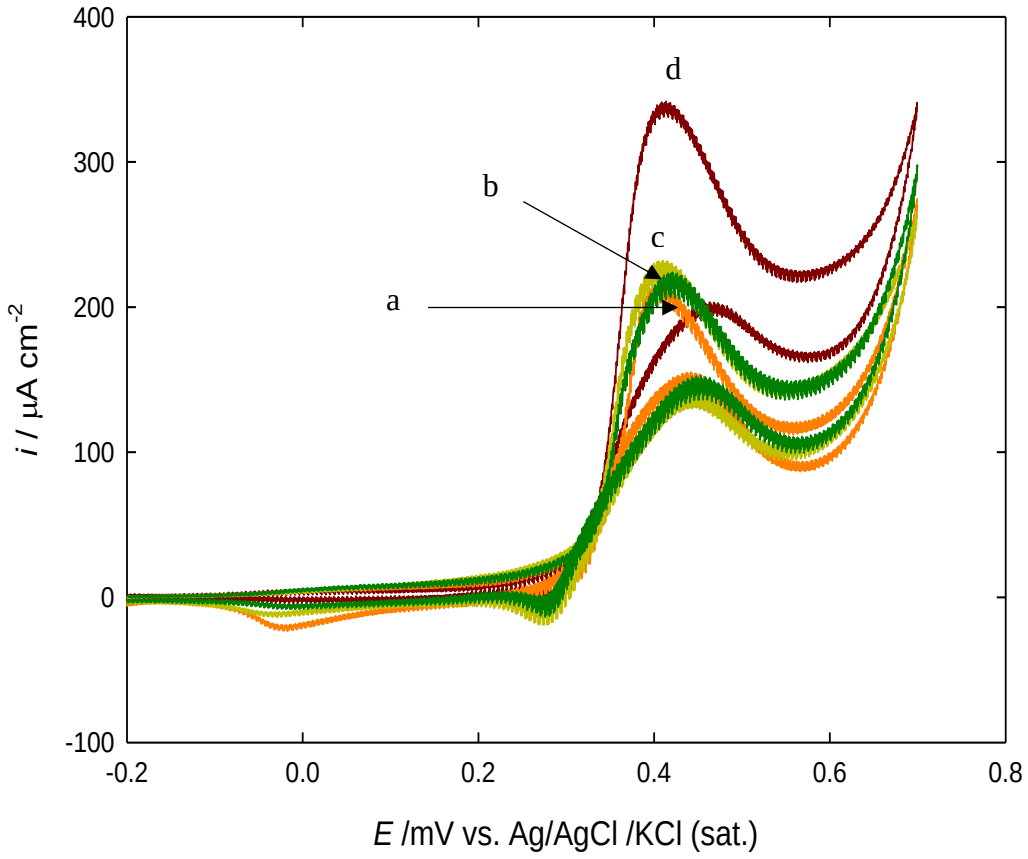

Figure 3.9.CV obtained at Au/NiO_x(Glu) in 0.5 M NaOH containing 2.5 mM glucose, with different loading of NiO_x obtained by various time of deposition: at (a) 50, (b) 150, (c) 200, (d) 400s. at SR = 100 mV/S.

Table 3.1. Glucose peak current, peak potential obtained at (a) Au/NiOx(Glu) electrode with different loading of NiOx.

Deposition time / s	Peak current / μA cm^{-2}	Peak potential /mV
50	211.9	0.39
150	213.9	0.4
200	223.4	0.4
400	336.7	0.4

3.1.4.4. Effect of concentration of glucose

Fig. 3.10. shows behavior of the modified electrode in the presence of different glucose concentrations. It is observed that as glucose concentration increases, the anodic peak height increases linearly with glucose concentration (Fig. 3.11).

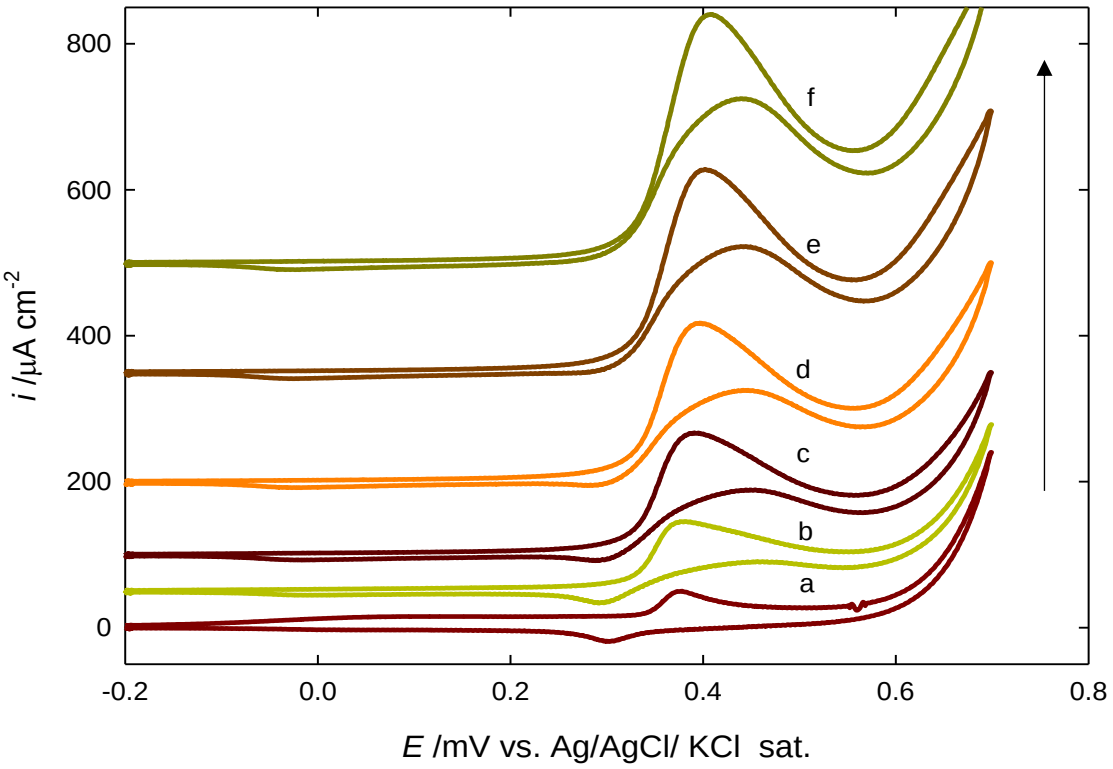

Figure 3.10. CV obtained at Au/NiO_x(Glu) electrode in 0.5 M NaOH containing 2.5 mM glucose at different concentrations of glucose (a) blank, (b) 0.001M, (c) 0.002 M, (d) 0.004 M, (e) 0.008 M, (f) 0.012 M.

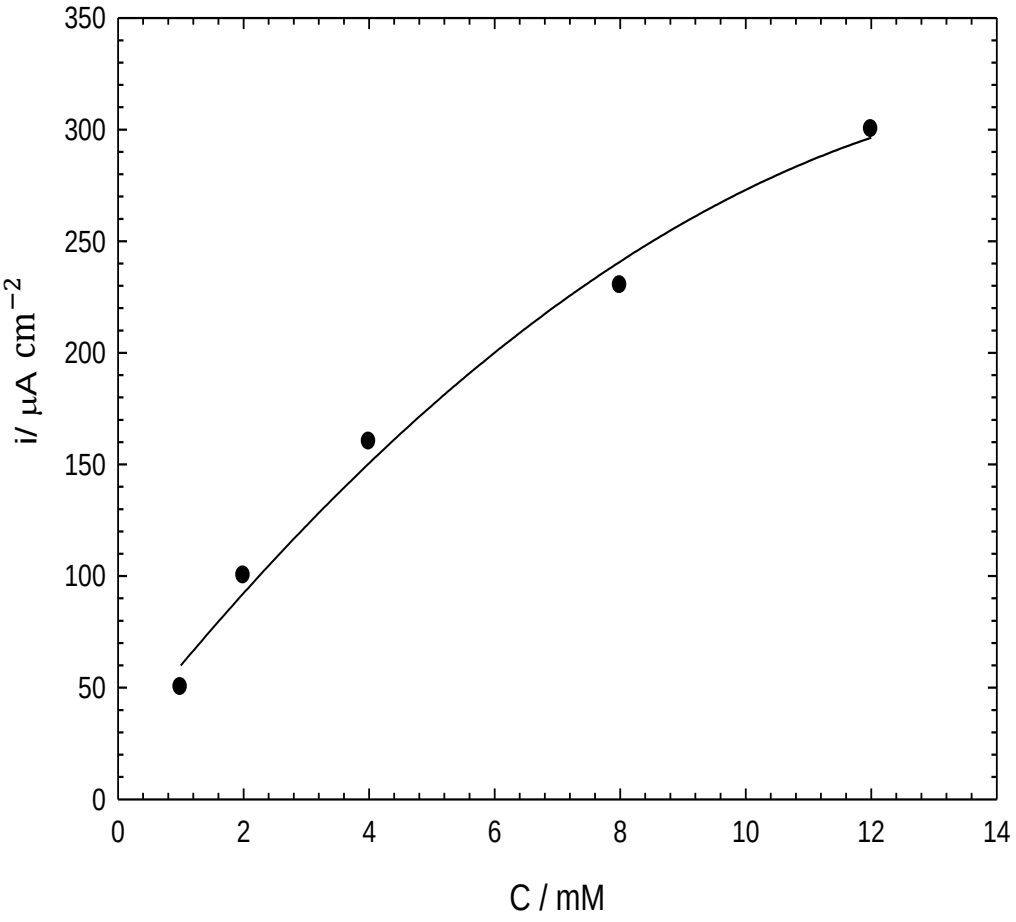

Figure 3.11. Peak current dependence for glucose. Data obtained from Figure 3.10.

3.1.4.5. Tafel plots

In order to get further insight and obtain information about the rate determining step the Tafel plots at (a) Au/NiOx, (b) Au/NiO$_x$(Glu) in 0.5 M NaOH containing 2.5 mM glucose at SR = 5 mV/S was obtained and shown in Fig. 3.12. Tafel slopes were obtained using the following Eq. (3.6) [29].

$$\eta = a + b \log i \qquad (3.6)$$

where η is the overpotential, "a" and "b" are Tafel constants

Tafel plots of ca. 119 and 110 mV/dec obtained at Au/NiOx(Glu) and Au/NiOx, respectively. This slope indicates that a one electron transfer process is the rate determining step (RDS) [32].

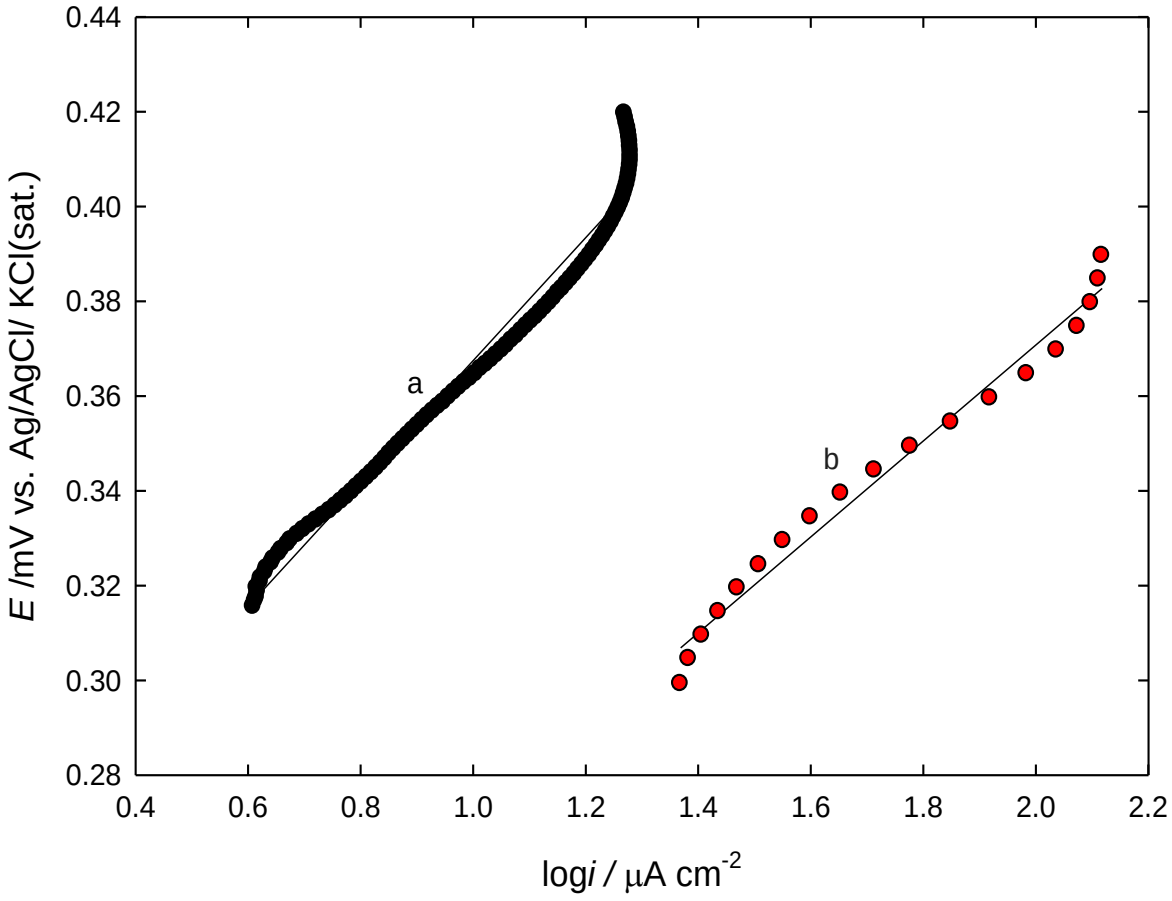

Figure 3.12. Tafel plots obtained at (a) Au/NiOx, (b) Au/NiOx(Glu) in 0.5 M NaOH containing 2.5 mM glucose at SR = 100 mV/S.

3.1.4.6. Chronoamperometry

One of the main objectives of using additive is to enhance the stability and catalytical activity of the NiO_x (the active oxide) modified electrode. So, to investigate the catalytical activity of the proposed catalysts, current–time curves were recorded for glucose oxidation and shown in Fig. 3.13 in which chronoampergram obtained at constant potential of 0.45 V for (a) Au/NiOx**,** (b) Au/NiOx(Glu) electrodes in 0.5 M NaOH containing 2.5 mM glucose. The obtained high current at the beginning was attributed to the charging of the double layer. The initial high current may be attributed to the increase in surface area. Then followed by a slight decrease which is indicative of a loss in the catalytic activity. Au/NiOx(Glu) electrode exhibits the highest initial currents and steady state currents compared with that obtained at Au/NiOx electrode in which Ni was deposited in the absence of glucose as additive. The order obtained using chronoamperometric measurements sustain that observed from cyclic voltammetry shown above. This confirmed the higher activity of the Au/NiOx(Glu) electrode, compared with Au/NiOx electrode towards glucose oxidation, and the prominent role of glucose in the deposition bath.

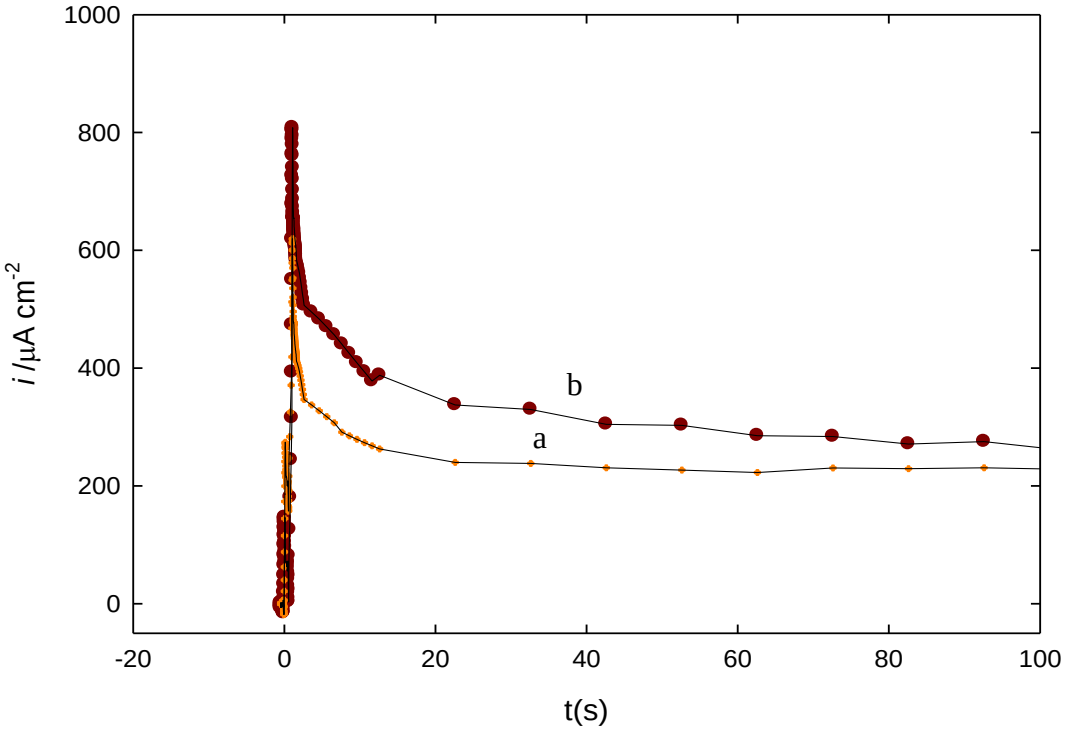

Figure 3.13. Chronoampergram obtained at constant potential of 0.45 V for (a) Au/NiOx, (b) Au/NiO$_x$(Glu) electrodes in 0.5 M NaOH containing 2.5mM glucose.

3.1.5. Conclusions

Au/NiOx(Glu) modified electrode displays high electrocatalytic activity for glucose oxidation compared with Au/NiOx electrode. This approved that glucose has dramatic effects on the electrodeposition of NiOx on Au electrode and on the catalytic oxidation of glucose from alkaline solutions. Au/NiOx(Glu) electrode has been studied at different scan rate. The relation between I_p and

$v^{1/2}$ gives the characteristic feature of a catalytic reactions. Further, the electrocatalytic activity of glucose oxidation was indicated by cyclic voltammetry for Au/NiOx(Glu) electrode at different concentrations. Tafel plots were used to give more insight and information about the rate determining step for Au/NiOx and Au/NiOx(Glu) electrodes. The rate determining step is found to be a one electron transfer process.

3.2.6. REFERENCES

1. Wild S, Roglic G, Green A, Sicree R, King H (2004). Global prevalence of diabetes: estimates for the year 2000 and projections for 2030. *Diabetes Care*, 27, 1047–1053
2. Casella IG, Cataldi TR, Salvi AM, Desimoni E (1993). Electrocatalytic oxidation and liquid chromatographic detection of aliphatic alcohols at a nickel-based glassy carbon modified electrode. *Anal. Chem.*, 65, 3143–3150
3. Heller A and Feldman B (2008). Electrochemical glucose sensors and their applications in diabetes management. *Chem. Rev.*, 108, 2482–2505.
4. Fang L and He J (2015). Nonenzymatic Glucose Sensors. *Prog. Chem.*,27. 585-593.
5. Ahmad R, Vaseem M, Tripathy N, Hahn YB (2013). Wide linear-range detecting nonenzymatic glucose biosensor based on CuO nanoparticles inkjet-printed on electrodes. *Anal. Chem*., 85, 10448–10454.
6. Pandya A, Sutariya PG, Menon SK (2013). A non enzymatic glucose biosensor based on an ultrasensitive calix[4]arene functionalized boronic acid gold nanoprobe for sensing in human blood serum. *Anal.*, 138, 2483–2490.
7. Pang H, Lu Q, Wang J, Li Y, Gao F (2010). Glucose-assisted synthesis of copper micropuzzles and their application as nonenzymatic glucose sensors. *Chem. Commun*., 46, 2010–2012.

8. Ibupoto ZH, Khun K, Beni V, Willander M (2013). Non-Enzymatic Glucose Sensor Based on the Novel Flower Like Morphology of Nickel Oxide. *SNL*., 3, 46–50.

9. Fang B, Gu A, Wang G, Wang W, Feng Y, Zhang C, Zhang X (2009). Silver Oxide Nanowalls Grown on Cu Substrate as an Enzymeless Glucose Sensor. *ACS Appl. Mater. Interfaces*, 1, 2829–2834

10. Wang J, Thomas DF, Chen A (2008). Nonenzymatic Electrochemical Glucose Sensor Based on Nanoporous PtPb Networks. *Anal. Chem.*, 80, 997–1004.

11. Jia-Hong H, Qiang X, Zhong-Rong S, Hai-Yan K (2010). Study on non-enzymatic glucose sensor based on a Ag2O nanoparticles self-assembled Ag electrode. *ICECE*, pp. 2109–2111.

12. Lei J, Liu Y, Wang X, Hua P, Peng X (2015). Au/CuO nanosheets composite for glucose sensor and CO oxidation. *RSC Adv*., 5, 9130–9137.

13. Thiagarajan S and Chen SM (2007). Preparation and characterization of PtAu hybrid film modified electrodes and their use in simultaneous determination of dopamine, ascorbic acid and uric acid. *Talanta*., 74, 212–222.

14. Feng D, Wang F, Chen Z (2009). Electrochemical glucose sensor based on one-step construction of gold nanoparticle–chitosan composite film. *Sens. Actuators, B*, 138, 539–544

15. Wang Z, Hu Y, Yang W, Zhou M, Hu X (2012). Facile One-Step Microwave-Assisted Route towards Ni Nanospheres/Reduced Graphene Oxide Hybrids for Non-Enzymatic Glucose Sensing. *Sensors*, 12, 4860–4869

16. Liu S, Yu B, Zhang T (2013). A novel non-enzymatic glucose sensor based on NiO hollow spheres. *Electrochim. Acta*, 102, 104–107

17. Kumar DR, Manoj D, Santhanalakshmi J (2014). Au–ZnO bullet-like heterodimer nanoparticles: synthesis and use for enhanced nonenzymatic electrochemical determination of glucose. *RSC Adv*., 4, 8943–8952.

18. Park B and Cairns EJ (2011). Electrochemical performance of TiO2 and NiO as fuel cell electrode additives. *Electrochem. Commun.*, 13, 75–77.

19. Needham SA, Wang GX, Liu HK (2006). Synthesis of NiO nanotubes for use as negative electrodes in lithium ion batteries. *J. Power Sources*, 159, 254–257.

20. Pang H, Lu Q, Zhang Y, Li Y, Gao F (2010). Selective synthesis of nickel oxide nanowires and length effect on their electrochemical properties. *Nanoscale*, 2, 920–922.

21. Ichiyanagi Y, Wakabayashi N, Yamazaki J, Yamada S, Kimishima Y, Komatsu E, Tajima H (2003). Magnetic properties of NiO nanoparticles. *Physica B*, 329, 862–863.

22. Ren S, Yang C, Sun C, Hui Y, Dong Z, Wang J, Su X (2012). Novel NiO nanodisks and hollow nanodisks derived from Ni(OH)2 nanostructures and

their catalytic performance in epoxidation of styrene. *Mater. Lett*., 80, 23–25.

23. El-Refaei SM, Saleh MM, Awad MI (2014). Tolerance of glucose electrocatalytic oxidation on NiO x/MnO x/GC electrode to poisoning by halides. *J. Solid State Electrochem.*, 18,5-12.
24. Ren Y and Gao L (2010). From three-dimensional flower-like α-Ni (OH) 2 nanostructures to hierarchical porous NiO nanoflowers: microwave-assisted fabrication and supercapacitor properties. *J. Am. Ceram. Soc.*, 93,3560.
25. Casella IG, Guascito MR, Sannazzaro MG (1999). Voltammetric and XPS investigations of nickel hydroxide electrochemically dispersed on gold surface electrodes. *J. Electroanal. Chem*.,18;462(2):202-10.
26. Sadiek IM, Mohammad AM, El-Shakre ME, El-Deab MS (2012). Electrocatalytic activity of nickel oxide nanoparticles-modified electrodes: Optimization of the loading level and operating pH towards the oxygen evolution reaction. *Int. J. Hydrogen Energy*,37(1):68-77.
27. Trafela Š, Zavašnik J, Šturm S, Rožman KŽ (2019). Formation of a Ni (OH) 2/NiOOH active redox couple on nickel nanowires for formaldehyde detection in alkaline media. *Electrochim. Acta*,20,309:346-53.
28. De Sá AC, Paim LL, Stradiotto NR (2014). Sugars electrooxidation at glassy carbon electrode decorate with multi-walled carbon nanotubes with nickel oxy-hydroxide. *Int. J. Electrochem. Sci*., 9,7746-62.

29. Bard AJ and Faulkner LR (2001). Fundamentals and applications. Electrochemical Methods. *Wiley and Sons*, New York, 2(482):580-632.

30. Ender B and Pakize C (2009). Electrochemical behaviuor of the antibiotic drug Novobiocin sodium on a mercury electrode. *Croat. Chem. Acta*, 82, 573–582.

31. Wei L, Feng MJ, Quangui G, Quan HY, Feiyu K (2012). DNA dispersed graphene/NiO hybrid materials for highly sensitive non-enzymatic glucose sensor. *Electrochim. Acta*, 73, 129–135

32. Golabi SM and Zare HR (1999). Electrocatalytic oxidation of hydrazine at a chlorogenic acid (CGA) modified glassy carbon electrode. *J. Electroanal. Chem.*, 465, 168–176.

33. Fleischmann M, Korinek K, Pletcher D (1971). The oxidation of organic compounds at a nickel anode in alkaline solution. *J. Electroanal. Chem. Interfacial Electrochem.*,31(1):39-49.

34. Zhao C, Shao C, Li M, Jiao K (2007). Flow-injection analysis of glucose without enzyme based on electrocatalytic oxidation of glucose at a nickel electrode. *Talanta*, 71(4):1769-73.

PART 2

CHAPTER III (PRAT 2)

3.2.1. Impact of Glucose as an Additive on the Deposition of Nickel: Application for Electrocatalytic Oxidation of Glucose

3.2.1.1 Abstract

A nickel oxide (NiO_x) nanoparticles modified glassy carbon (GC) electrode, designated as GC_{ox}/NiO_x(Glu), were fabricated from a nickel bath (0.02 M $NiSO_4$ + 0.03 M $NiCl_2$ + 0.03M H_3BO_3) containing a suitable additive, typically glucose. The GC was electrochemically pretreated prior to the deposition of nickel. The thus modified electrode was applied for the electrooxidation of glucose in alkaline medium. For the sake of comparison, a similar modification was conducted but in the absence of glucose as an additive, and the modified electrode is designated as GC_{ox}/NiO_x. The effect of loading of NiO_x was optimized. Cyclic voltammetry (CV), and chronoamperometry were used for the voltammetric characterization. Several surface techniques were used for probing the morphology and composition of the deposited modifier, including field emission scanning electron microscopy (FE-SEM), EDX and X-ray diffraction. The highest electrocatalytic activity towards glucose oxidation was obtained at GC_{ox}/NiO_x(Glu) using five potential cycles at range from 0.0 to -1.0 V vs. Ag/AgCl(Kcl sat.). Possible

reason(s) behind the enhancement of glucose electrocatalytic oxidation was (were) explored.

3.2.1.2. Introduction

Environmentally friendly materials have become very important at the moment, so research has turned to fuel with these specifications, leading researchers to use glucose to fuel cell work. There are three major types of glucose fuel cells, classified based on the type of catalyst used. First one, enzymatic glucose fuel cell, which uses biological enzymes such as glucose oxidase as catalysts. As such they have limited long-term stability. Second, microbial glucose fuel cell: these are fuel cells in which the catalysts are immobilized bacteria capable of oxidizing glucose. Bacterial and enzymatic fuel cells contain defects and complications so they can be replaced by non-enzymatic fuel cells counter or part for oxidation of glucose on the noble electrode. However, enzymes are unstable at high temperatures and aggressive environments. Many researches have been done to obtain non-enzymatic glucose sensors. Third, direct glucose fuel cell: they are fuel cell that use inorganic catalysts [1-4]. Out of the three types of cells, direct glucose fuel cells have the advantage that they are the most robust, and biocompatible. Commercializing glucose fuel cells face several problems; of these

problems the cost of the electrocatalyst and its susceptibility to poisoning are the dilemma. Oxidation of glucose to carbon dioxide yields very high energy (-2.87×10^6 J/mol) and 24 electrons are exchanged [5-8]. Theoretically, an open-circuit of 1.24 V voltage can be obtained from a direct glucose fuel cell [7,8]

Over the past decade, many studies have been conducted on the electrochemical oxidation of sugars resulting in the conclusion that single sugars such as glucose is oxidized by noble metal catalysts based on platinum and gold electrodes [9-11]. However, these electrodes showed their long term inefficiency due to several reasons: of these lack of selectivity and low sensitivity. A lot of research has been done on transition metal oxides to solve these problems either by replacing the costly platinum electrocatalyst or the co-deposition of a secondary catalyst [2,3]. Of these modifiers, nickel is the first choice as it is naturally active for glucose oxidation. Nickel and nickel oxide (NiO_x) electrodes have many technological applications which led to research in the past years. Of these applications: use in densities [12,13] alkaline batteries [14] biological sensors [15, 16] and energy conversion devices [17,18] .The electrooxidation rate of glucose in alkaline environments is facile than in neutral or acidic media [9,10, 19-22]. On the other hand, the use of nanoscale materials has led to the development of huge sensors,

particularly glucose sensors [2]. In the alkaline medium, the oxidation of glucose have been studied on the following electrodes Au, Pt ,Fe ,Ni ,Cu [23-27].

In this chaptre, the electrochemical fabrication of the electrode is based on the electro-oxidation of the glassy carbon electrode, and the subsequent deposition of nickel nanoparticles (nano-NiO_x) from solution containing nickel ions and glucose onto the thus oxidized glassy carbon electrode. Then, the deposited nickel is oxidized electrochemically in alkaline medium for the formation of NiO_x. The experimental parameters are optimized to sustain the highest electrocatalytic activity towards glucose oxidation.

3.2.1.3. Experimental

3.2.1.3.1. Electrochemical measurements

Potentiostat/galvanostat/ZRA model the Reference 600 ™ machine were used for the Electrochemical measurements. A conventional cell with a three-electrode configuration was used in this work. The electrochemical measurements were performed at room temperature (25 °C). The working electrode was glassy carbon (GC, d = 3.0 mm). It was cleaned by mechanical polishing with aqueous slurries of successively finer alumina powder then washed thoroughly with deionized water.

3.2.1.3.2. Fabrication of nickel oxide (NiO_x) nanoparticles.

Nickel oxide (NiOx) nanoparticles modified GC were prepared. First, the GC electrode was activated electrochemically designated as GC_{ox}. Second, (NiOx) nanoparticles were deposited in the GC_{ox} electrode further information were explained in experimental chapter. Then, the addressing of the electrocatalytic activity of the modified electrode toward glucose oxidation was conducted at different scan rates, different concentrations, different loading of nano-NiO_x. To prove reproducibility of the results the CVs were repeated several times.

3.2.1.4. Results and discussion.

3.2.1.4.1. Morphological characterizations.

Fig. 3.14 shows SEM images of nano-NiO_x prepared by a cyclic voltammetry technique described in the experimental section. Also, the atomic ratios of C/O/Ni from EDX test were examined. In image (a) a smooth surface is shown and in EDX (plot B), as expected, the weight of carbon element (97.07%) is large compared with oxygen. In case of GC_{Ox} (image C), the electrode surface becomes rougher, and as revealed from EDX (plot D) the percence of oxygen increased to 10 %. The increase in the percent of oxygen is attributed to the electrooxidation of

GC which results in the formation of several containing oxygen functional groups. In image E, obtained at GC_{ox}/NiO_x electrode; i.e., at nickel oxide deposited onto oxidized GCE, a deposition of NiO_x is observed, as revealed from the EDX (plot E) in which new peaks for nickel at 0.9 KeV, 7.4 KeV are observed [28]. At GC_{ox}/NiO_x(Glu) electrode which is fabricated similarly to GC_{ox}/NiO_x but in the presence of glucose in the deposition bath, EDX (plot H) presents a larger ratio of Ni at GC_{ox}/NiO_x-as revealed from the increase of intensities of peaks corresponds to nickel at 0.9, 7.6 ,and 8.2 KeV [29].

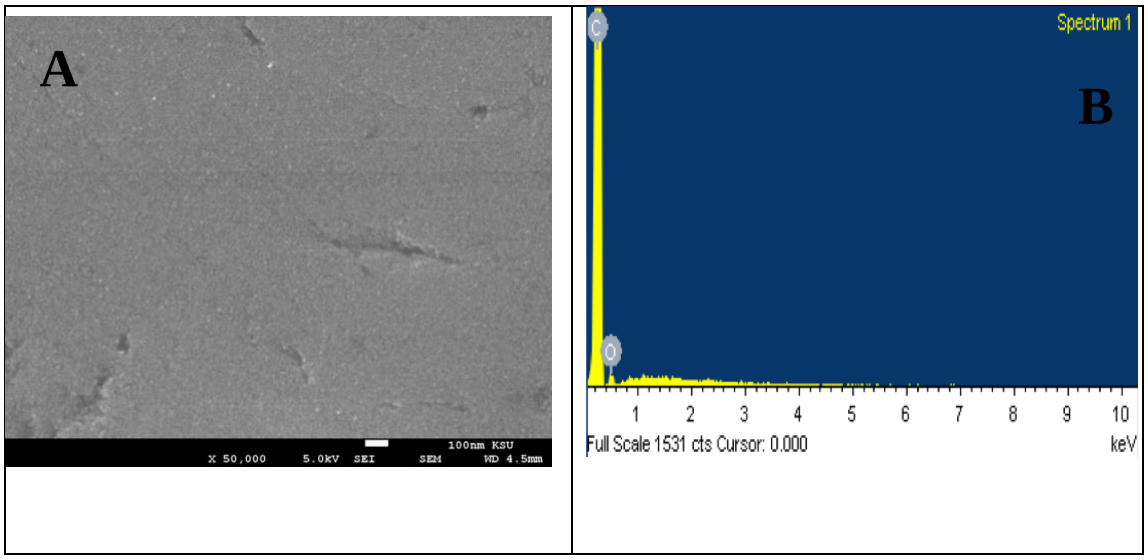

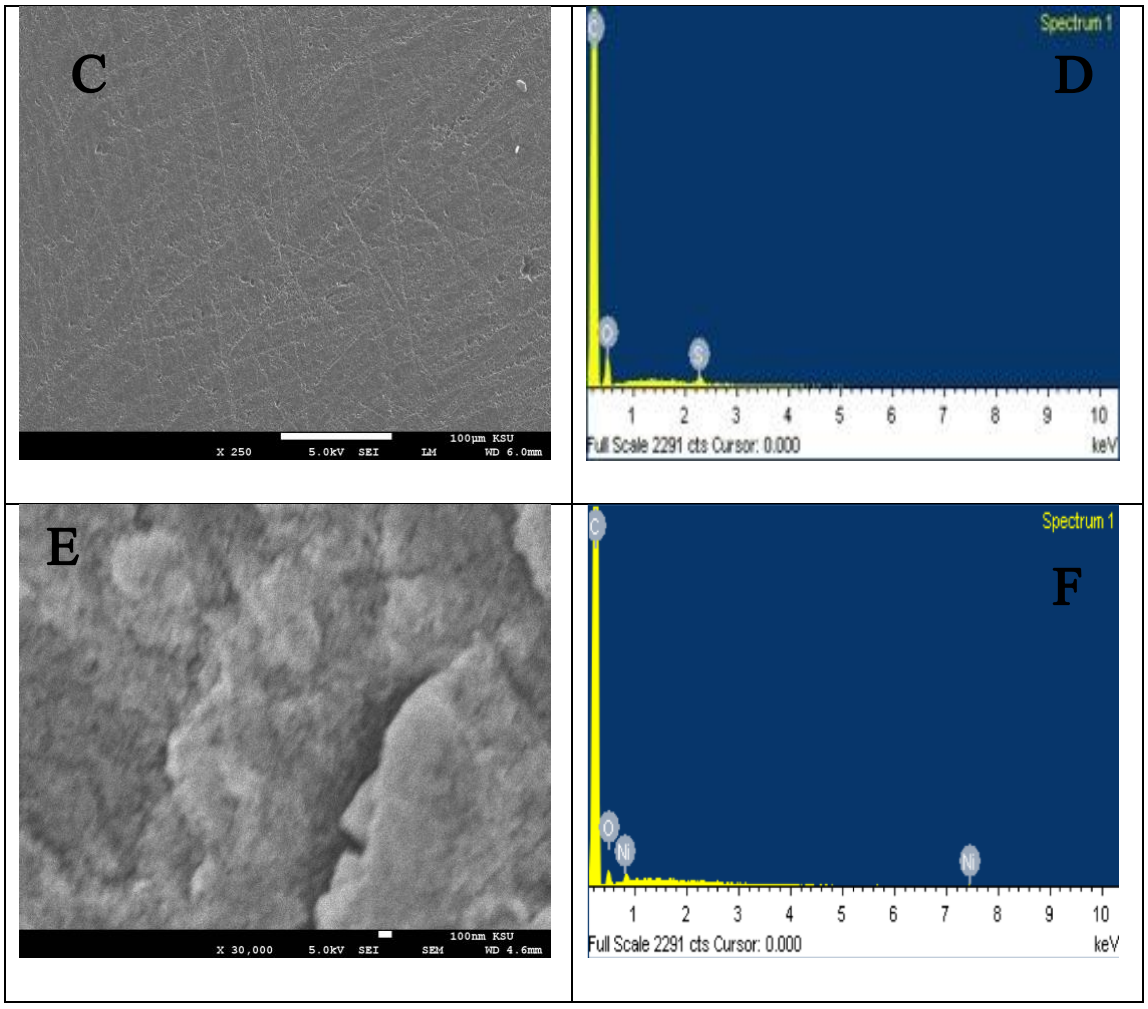

Figure 3.14. SEM (A,C,E,G) and EDX (B,D,F,H) of (A,B) GC, (C,D) GC_{ox} , (E,F) $GC_{ox}/NiOx$, and (G,H) $GC_{ox}/NiO_x(Glu)$ electrodes.

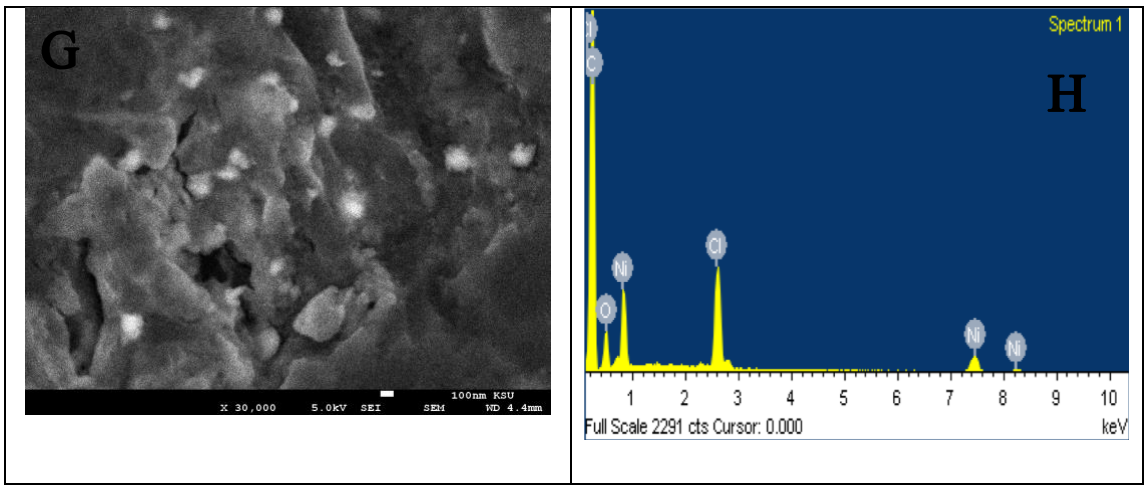

Figure 3.14. (Continued).

Fig. 3.15. shows XRD patterns obtained at (a) GC_{ox}, (b) GC_{ox}/NiO_x, and (C) GC_{ox}/NiO_x(Glu) electrodes. The sharp peak at 19° corresponds to the (002) diffraction of the glassy carbon underlying substrate. At GC_{ox}/NiO_x (curve b) and GC_{ox}/NiO_x(Glu) (curve c) electrodes, the XRD pattern of NiO showed several diffraction peaks at $2\theta = 37.20°$, 43.20°, 44.4°, 75.20° which are indexed as (101), (012), (111), (113) and (220) crystal planes of the NiOx, respectively. Those peaks are indexed to the face-centered cubic (FCC) crystalline structure of NiO_x in accordance with that of the standard spectrum (JCPDS, No. 04-0835) [30].

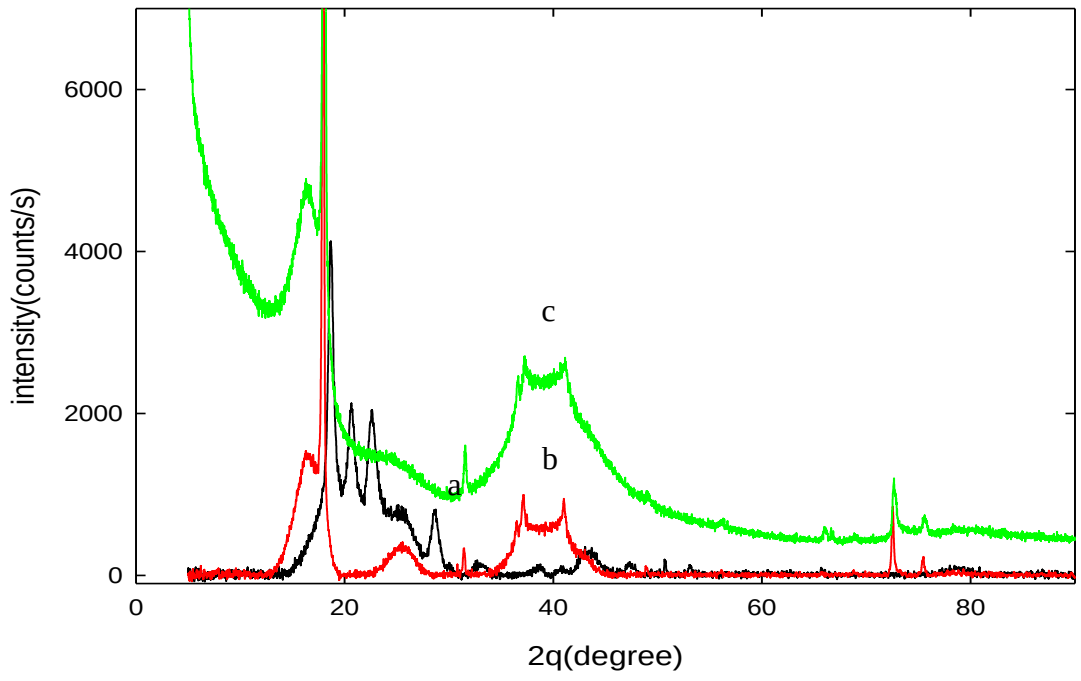

Figure 3.15. XRD of (a) GC, (b) GC_{ox}/NiO_x, and (C) GC_{ox}/NiO_x(Glu) electrodes.

3.2.1.4.2. Electrochemical characterizations.

The electrochemical oxidation of glucose has been an interesting topic for the last decade, especially at nickel modified electrodes, which presents a unique electrocatalytic properties. Nickel deposition is critically affected by the ingredient of the deposition bath [31]. Here, the effect of adding glucose, as an additive, in the deposition bath of nickel is examined. Fig. 3.16. shows CVs responses obtained at (a) GC, (b) GC/NiO_x(Glu), (c) GC_{ox}/NiO_x and (d) GC_{ox}/NiO_x(Glu) electrodes in 0.5 M NaOH. The same potential cycles were used to deposit Ni on the different electrodes. As clearly shown, in Fig. 3.16. (curve a), obtained at GC electrode, the CV is featureless. Curve b, obtained at GC/NiO_x(Glu) electrode in which nickel oxide was deposited, in the presence of glucose in the deposition bath, on GC electrode, a well-defined couple for nickel-nickel oxide is obtained. Curves C and d show CV responses obtained at GC_{ox}/NiO_x and GC_{ox}/NiO_x(Glu) electrodes, respectively. The peak current for nickel couple increases at both electrodes compared with that on the GC/NiO_x(Glu) (b). Probably, the functional groups of the underlying substrate participate in this enhancement. Comparing curves c

and d indicates that including glucose in the deposition bath (curve d) promotes the nickel-nickel oxide couple.

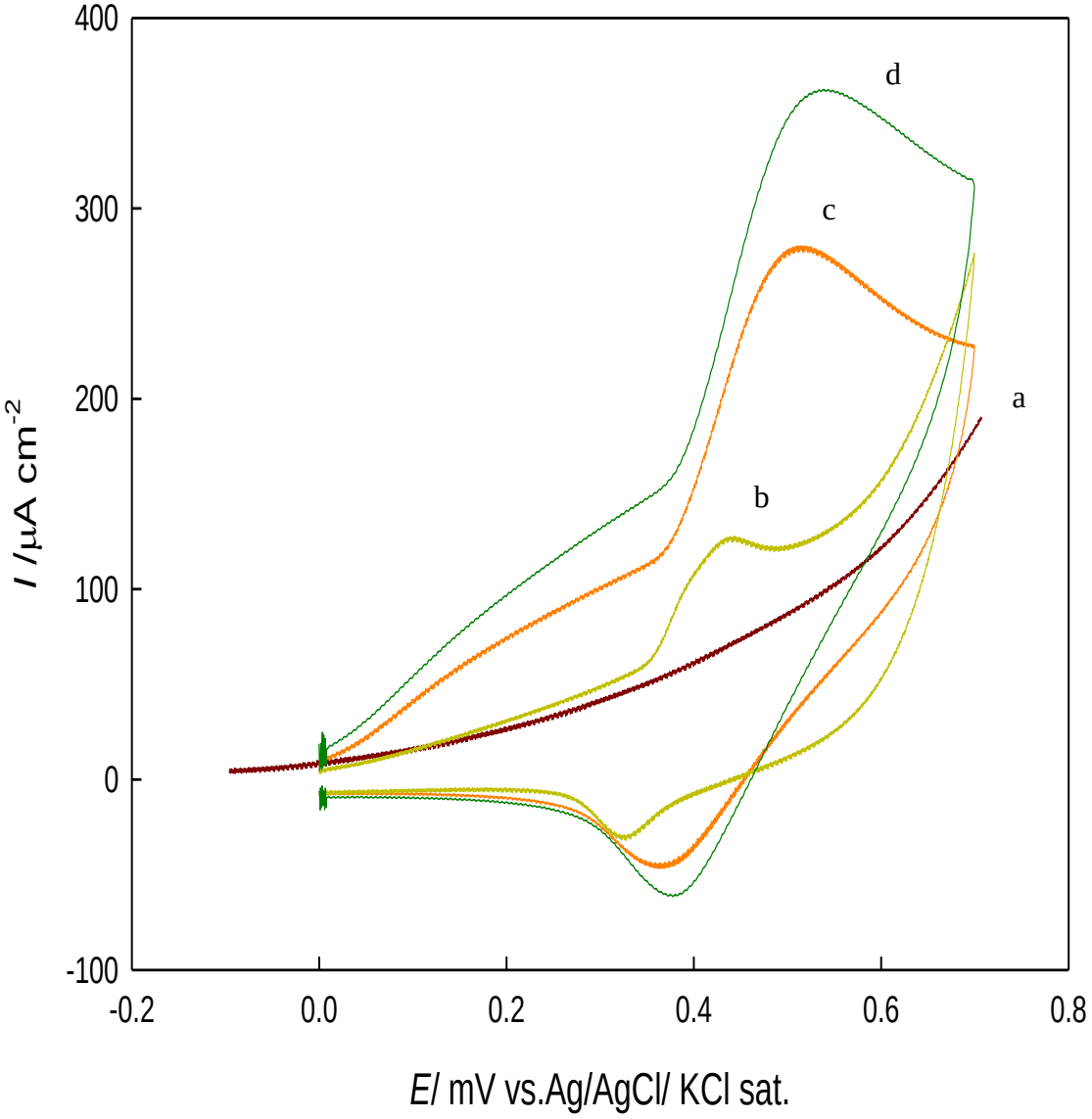

Figure 3. 16. CV obtained at (a) GC, (b) GC/NiO_x(Glu), (C) GC_{ox}/NiO_x and (d) GC_{ox}/NiO_x(Glu) electrodes in 0.5 M NaOH at SR = 100 mV/S.

Fig. 3.17. is similar to 3.16. but in the presence of glucose. Inspection of this figure reveals several interesting points;

i. GC is inactive towards glucose oxidation.

ii. At GC/NiO_x(Glu) (curve b), a well-defined oxidation response for glucose oxidation is obtained.

iii. At GC_{ox}/NiO_x (curve c) and GC_{ox}/NiO_x(Glu) (curve d), the oxidation of glucose is significantly enhanced, with the one at the latter is larger indicating the significant effect of the underlying substrate as well as the including of glucose in the deposition bath. The prominent role of the underlying substrate surface is proved by comparing curves b and d in which nickel was deposited from a bath containing glucose and the only difference is the case of the underlying substrate. It has been reported that anodic oxidation of GC in H_2SO_4 results in an increase of the percentage surface composition of functional groups bearing –OH group. The presence of –OH group adsorbed on the GC surface (i.e., OH_{ads}) promotes the electrocatalytic oxidation of glucose [32,33] and other small organic molecules such as methanol [34].

iv. The role of glucose in the deposition bath is confirmed by comparing curves c and d in which the modification of the underlying substrates is the same. Curve d was obtained for

GC_{ox}/NiOx(Glu) electrode, this electrode was fabricated in a similar way to GC_{ox}/NiO_x (curve c) with only one difference. In the former one, i.e., GC_{ox}/NiOx(Glu), glucose was added to the deposition bath. Interestingly, in this case the response for glucose oxidation is the largest among studied electrodes. It seems that a synergistic effect from the different conditions results in such increase along with the morphology presented in SEM images shown above. In previous study they assume [35], a part of the anodic current is due to glucose oxidation by NiOOH and a part of the current is due to glucose oxidation on the surface of oxide layer by direct electrooxidation.

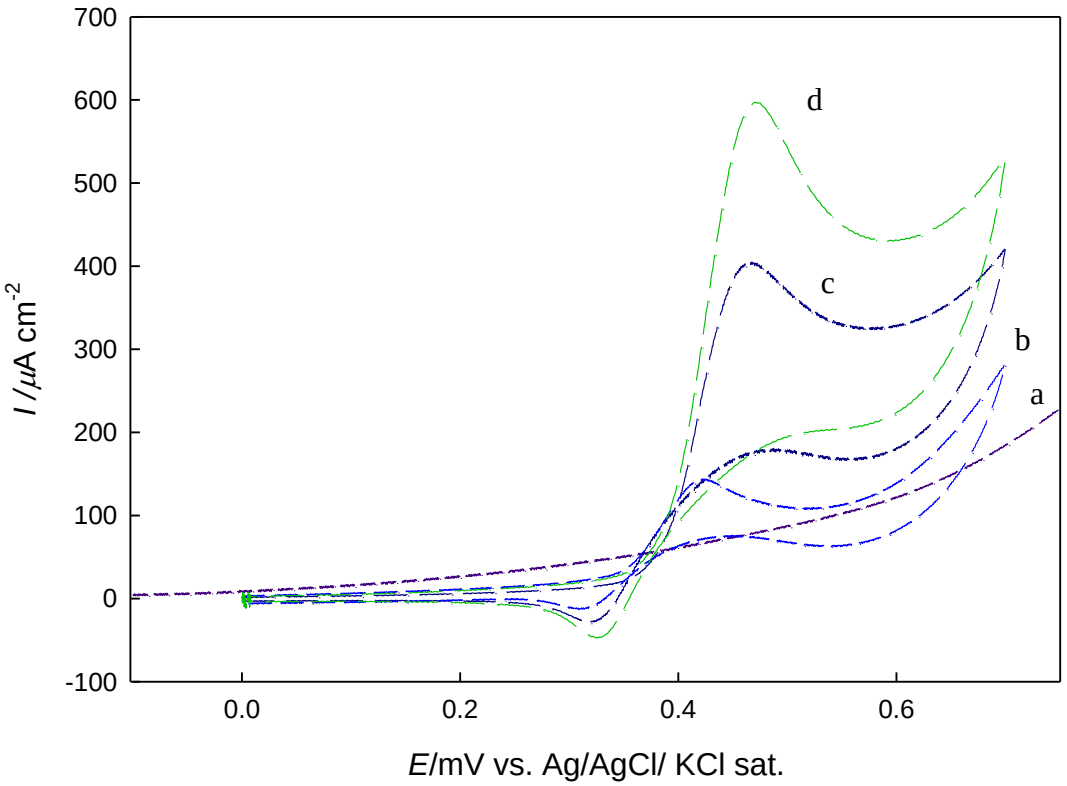

Figure 3.17. CV obtained at (a) GC, (b) GC/NiO_x(Glu), (C) GC_{ox}/NiO_x (d) GC_{ox}/NiO_x(Glu) electrodes in 0.5 M NaOH containing 2.5 mM glucose at SR = 100 mV/S.

The redox transition of nickel species from Ni (II) to Ni(III) occurs, then in a following step glucose is oxidized on the modified as represnted by Eqs.(3.4) and (3.5).

where Ni^{3+} sites are regenerated by the power source and on the Ni^{3+} oxide surface by direct electrooxidation [36,37]:

$$\mathrm{Ni(III)} - \mathrm{glucose} \longrightarrow \mathrm{Ni(III)} - \mathrm{intermediate} \qquad (3.7)$$

$$\mathrm{Ni(III) - intermediate} \longrightarrow \mathrm{Ni(III) - products} \qquad (3.8)$$

Eqs. (3.4) and (3.5) are according to the Fleischmann mechanism [37, 38], and in Eqs. (3.7) and (3.8) Ni^{3+} is used as an active surface for glucose oxidation. Gluconolactone [39, 40] as well as methanoates and oxalates [41] have been reported as the oxidation products of glucose electrooxidation.

3.2.1.4.3. Effect of loading of nickel nanoparticles.

Fig. 3.18. shows that the anodic and cathodic peak currents increase as the loading level increases up to loading level of 5 cycles for deposition of Ni, in the potential range of 0.0 to -1.0 V vs. Ag/AgCl(Kcl sat.). It can be noticed that the peak current is increased to a certain limit and then significantly decreases when the loading of the catalyst goes above five cycles. It may be concluded that a loading NiO_X nanoparticles of five cycles is considered to be an optimum loading for this electrode at the present experimental conditions and it will be used hereafter for further investigation.

The peak current and enhancing factors (the peak current obtained in cycles next to the first one with respect to the peak current of the first cycle), calculated by Eq.(3.9), are shown in Table 3.2.

The current is considered for anodic peak. As clearly shown the peak current increases with cycling of potential and the enhancing factor reaches 3 for cycle 5th.

$$\text{Enhancing factor} = I_{pa2}/I_{pa1} \quad (3.9)$$

where I_{pa1} and I_{pa2} are the current obtained in the 1st and consecutive cycles, respectively.

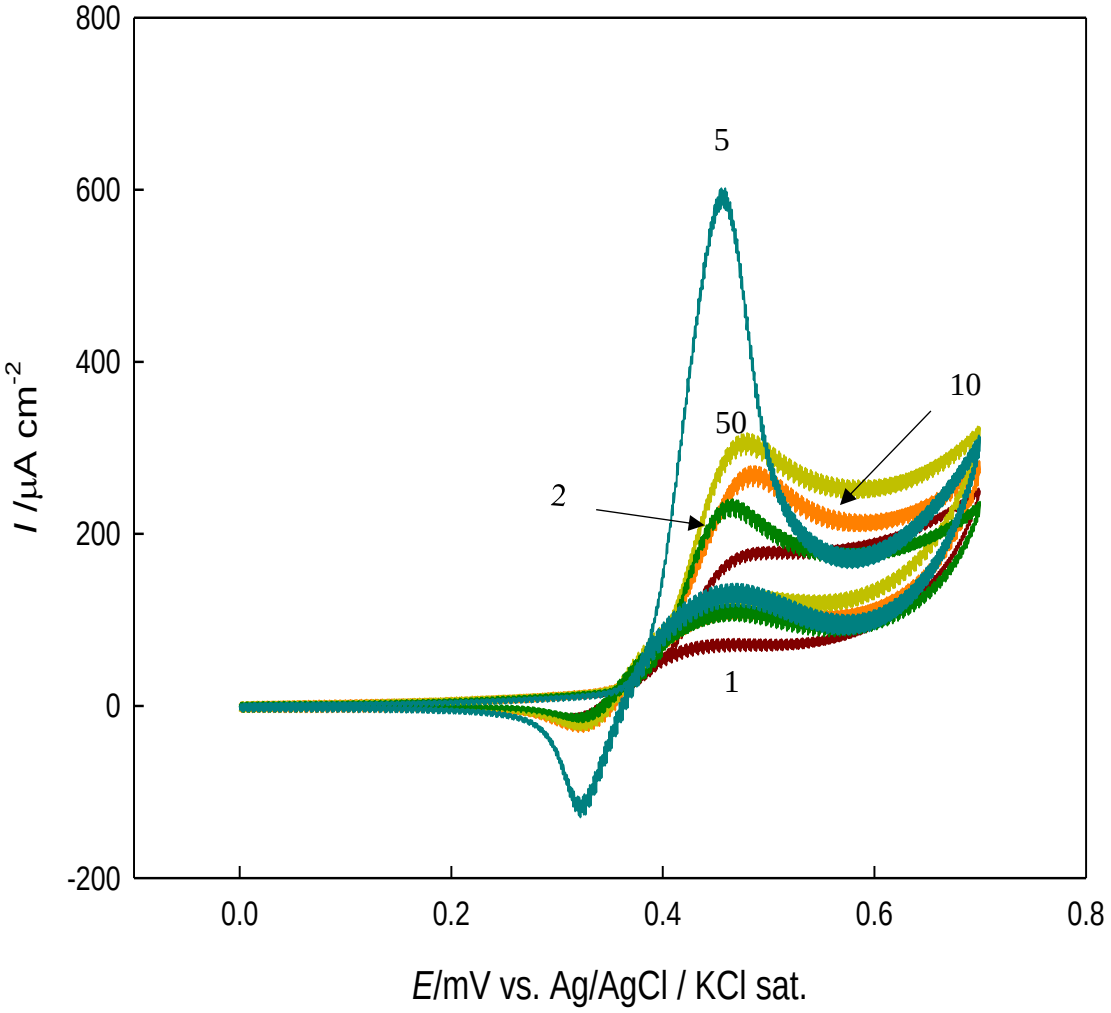

Figure 3.18. CV obtained at $GC_{ox}/NiO_x(Glu)$ in 0.5 M NaOH containing 2.5 mM glucose, NiO_x was prepared by different potential cycles in the range of 0.0 to -1.0 V vs Ag/AgCl (KCl sat.) Potential cycles are 1, 2, 5, 20 and 50 cycles at SR = 100 mV/S.

Table 3.2. Glucose peak current and enhancing factors obtained at different loading of NiOx nanoparticles. Data are extracted from Fig 3.18.

Potential cycle number	Peak current / μA	Enhancing factor
1st	185.5	--
2nd	229.8	1.23
5th	597.3	3.21
10th	267.9	1.44
50th	306.3	1.65

It was evident that CVs for glucose oxidation GC_{ox}/NiOx(Glu) electrode in solution of 0.5 M NaOH gave a higher current than CVs for glucose oxidation on GC_{ox}/NiOx electrode that approved adding glucose in the deposition bath made the electrode more active toward the oxidation of the glucose.

In order to get further insight, Fig. 3.19. shows Tafel plots obtained at (a) GC_{ox}/NiO_x and (b) GC_{ox}/NiO_x(Glu) in 0.5 M NaOH containing 2.5 mM glucose at a scan rate of 5 mV/s. Tafel slopes of ca. 38 mV/dec was obtained at GC_{ox}/NiO_x(Glu), while at GC_{ox}/NiO_x the Tafel slope equals 60 mV/decade. The former one points to a possibly an electron-transfer step is controlling the oxidation process. At GC_{ox}/NiO_x electrode, it is likely that a chemical step is the controlling for the glucose oxidation. This means that at GC_{ox}/NiO_x electrode, the removal of an adsorbed species (represented by Eq. 3.4) is the rate determining step. At GC_{ox}/NiO_x(Glu) electrode at which the Tafel slope is 40 mV/decade, the step represented by Eq. (3.5) is the rate determining step [42]. The plots confirmed reinforcement of the glucose oxidation on GC_{ox}/NiO_x(Glu) compared with GC_{ox}/NiO_X.

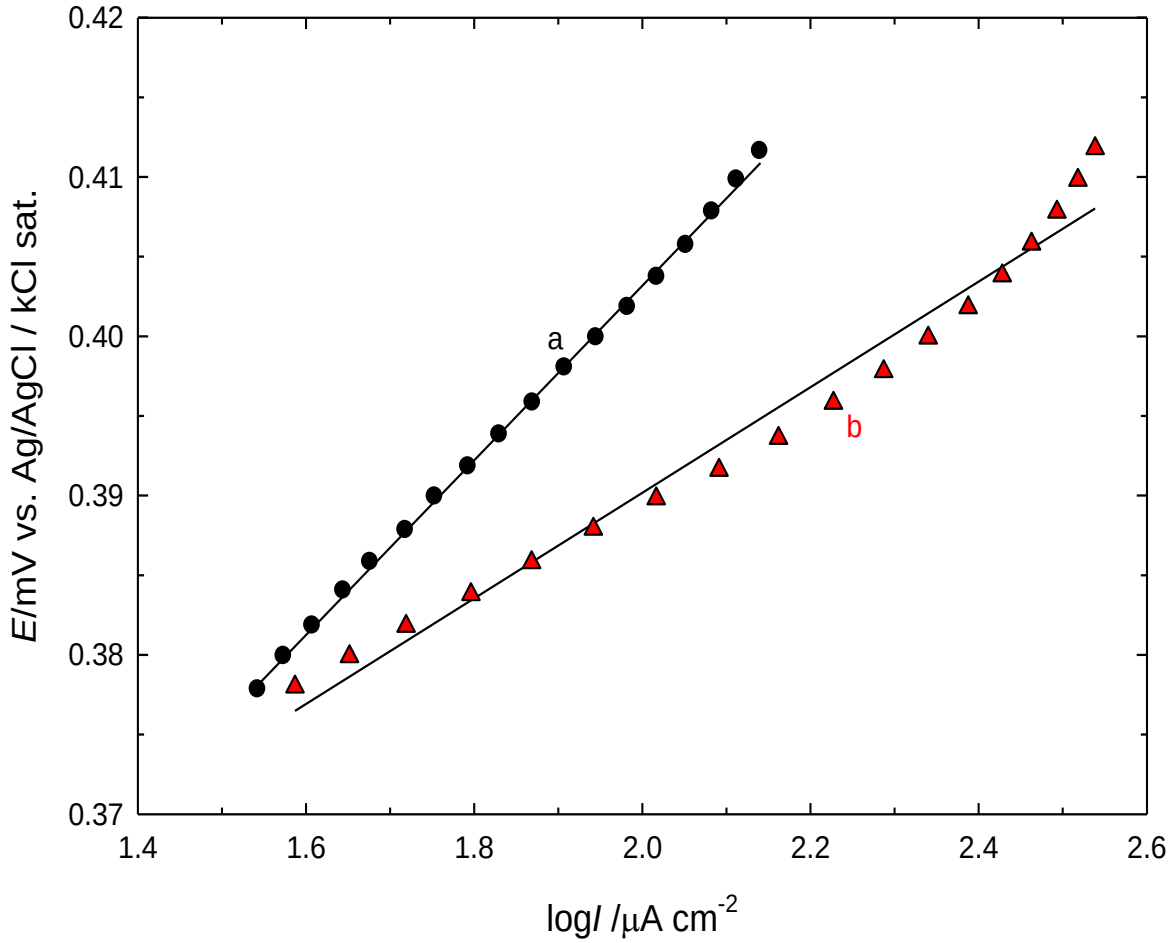

Figure 3.19. Tafel plots obtained at (a) GC_{ox}/NiO_x and, (b) GC_{ox}/NiO_x(Glu) electrodes in 0.5 M NaOH containing 2.5 mM glucose at SR = 5 mV/S.

3.2.1.4.4. Long-term stability of the prepared electrocatalysts.

One of the main objectives of using additive at deposition of Ni nanoparticles is to enhance the stability of the NiO_x (the active oxide) modified GCE. So, to investigate the stability of the proposed catalysts, current–time curves were recorded for glucose oxidation and shown in Fig. 3.20. in which chronoampergram obtained at constant potential of 0.4 V for (a) GC_{ox}/NiO_x, (b) GC_{ox}/NiO_x (Glu) electrodes in 0.5 M NaOH containing 2.5 mM glucose are shown. The obtained high current at the beginning was attributed to the charging of the double layer. The initial high current may be attributed to the increase in surface area. Then followed by a slight decrease which is indicative of a loss in the catalytic activity. GC_{ox}/NiO_x (Glu) electrode exhibits the highest initial currents and steady state currents compared with that obtained at GC_{ox}/NiO_x electrode in which Ni was deposited in the absence of glucose as additive. The order obtained using chronoamperometric measurements sustain that observed above using cyclic voltammetry shown above. This confirmed the higher activity of the GC_{ox}/NiO_x (Glu) electrode, compared with GC_{ox}/NiO_x electrode towards glucose oxidation, and the prominent role of glucose in the deposition bath.

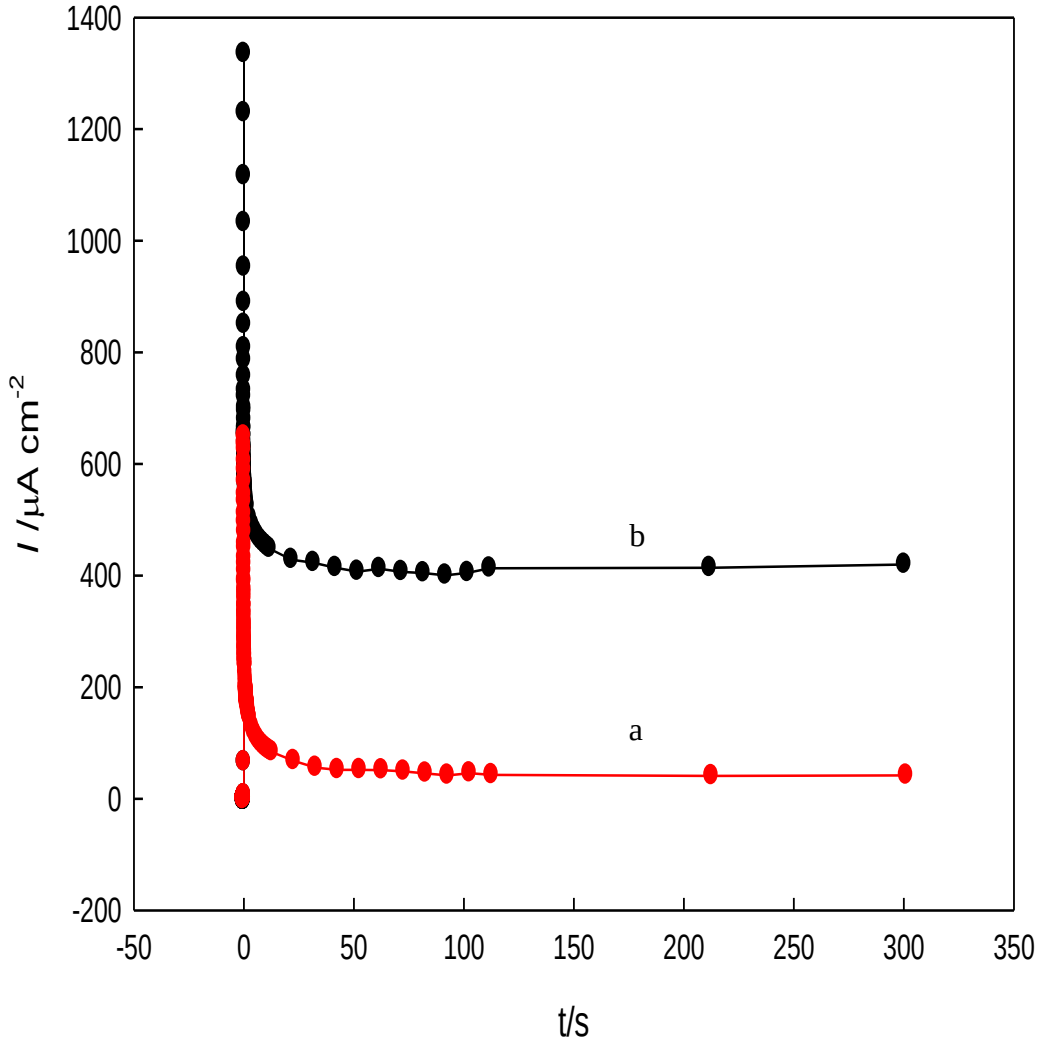

Figure 3.20. Chronoampergram obtained at constant potential of 0.4 V for (a) GC_{ox}/NiO_x, (b) GC_{ox}/NiO_x (Glu) electrodes in 0.5 M NaOH containing 2.5 mM glucose.

Fig. 3.21. shows the dependence of the function ($Ip/\nu^{1/2}$) with ν obtained at the GC_{ox}/NiO_x (Glu) electrode. As can be seen at scan rate higher than 40 mV s^{-1}, $Ip/\nu^{1/2}$ does not change significantly with scan rate. This behavior is reported as a characteristic of catalytic reactions

[42], i.e., EC mechanism, represented by Eqs (3.4) and (3.5), shown above. The glucose oxidation is mediated by Ni couple, and that the inclusion of glucose in the deposition bath significantly modify deposited nickel oxide in such a manner that glucose oxidation is enhanced.

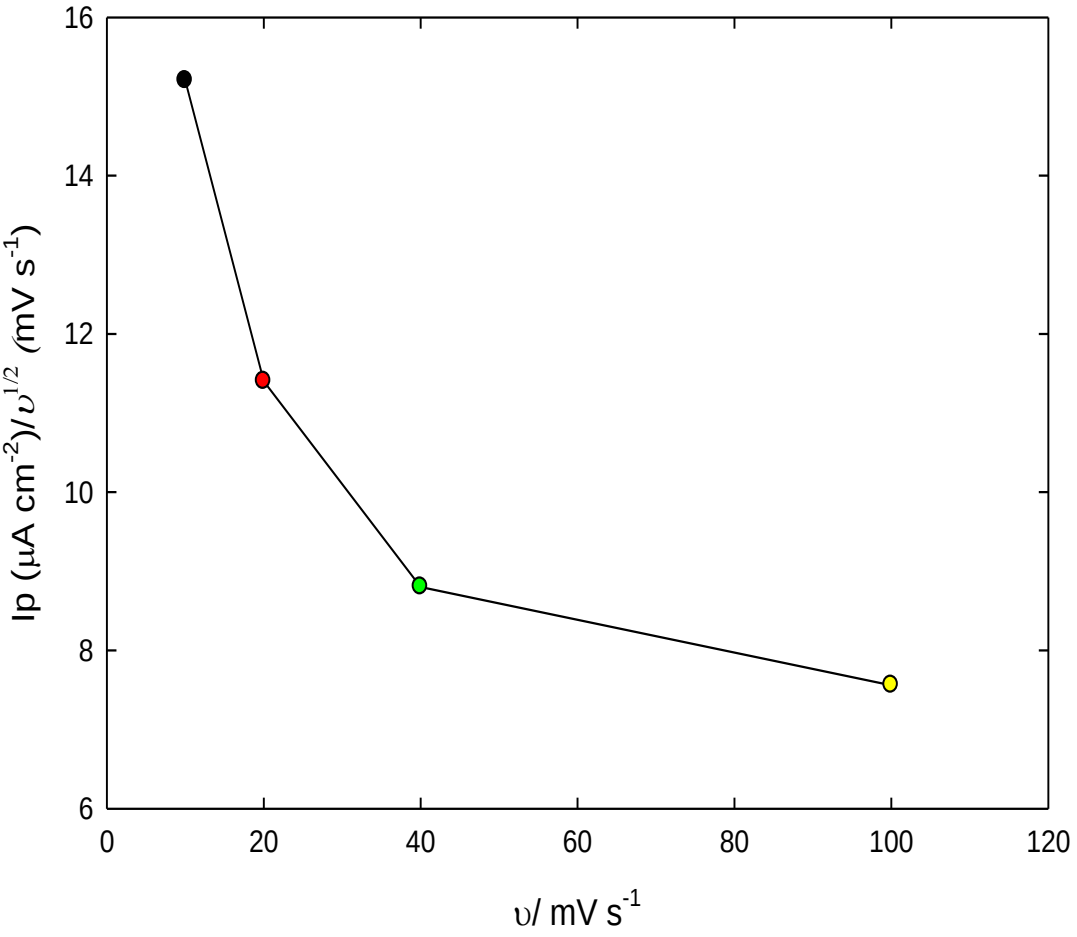

Figure 3.21. Variation of $Ip/v^{1/2}$ with v for glucose electrooxidation obtained at GC_{ox}/NiO_x(Glu) electrode in 0.5 M NaOH containing 2.5 mM glucose.

3.2.2. Tolerance of glucose electrocatalytic oxidation on GCox/NiOx(Glu) electrode to poisoning by halides

Glucose electrooxidation on non-precious metals, especially Ni and its composites has been greatly developed in recent years due to their low cost, high oxidation capacity and high stability. Glucose oxidation is the anodic reaction in direct alkaline fuel cells and it is used as the basis for enzymeless detection [43-47]. However, the most challenging problem of glucose fuel cells and non-enzymatic glucose sensors is the poisoning by halides especially chloride ions. So, studying the effect of halide ions on glucose oxidation on the proposed modified electrode is important topic in electrocatalysis [45,48-50]. It has been reported that halide ions exhibit a strong poisoning effect on several small organic molecules electrooxidation on noble metal electrodes such as Pt, Au, and their alloys [51-56]. This high poisoning has been attributed to the high specific adsorption of the halide ions on such metals [51-56]. On the other hand, metal oxides such as CuO_x and NiO_x are susceptible to poisoning albeit to a lower extent compared to their metal counterparts. This is attributed to the difference in the adsorbability of halide ions on metal and metal oxides [57,58]. In this part the effect of halide ion poisoning on the fabricated catalyst is investigated.

Figures (3.22-3.23-3.24) shows cyclic voltammetry (CV) responses for glucose electrooxidation on GC_{ox}/NiO_x(Glu) electrode in the presence of different concentrations of chloride, bromide ions and iodide ions, ranging from 0.1 to 0.3 M. Glucose oxidation is revealed at a potential around 0 to 0.7V vs. Ag/AgCl(Kcl sat.). It has been reported that NiOOH acts as a mediator of glucose oxidation. As mentioned above, the redox transition of nickel species from Ni(II) to Ni(III) occurs, and then in a following step, glucose is oxidized on the modified electrode, i.e., via EC mechanism[59-61]. Interestingly, upon the addition of the corresponding halide ions, the effect on the forward and backward scans is significant effect. Regarding the forward scan, the peak potential shifted negatively. The backward scan shifted positively. The shift in both cases is halide concentration dependent. It has been reported [58] that the NiOx/GC electrode has strong tolerance to chloride ions which is consistent with the present results. However, in the present electrode, surprisingly, the behavior is enhanced. This indicates that the proposed catalyst not only exhibits good resistance to surface fouling but also enhance the oxidation response of the glucose oxidation. It is a promising electrocatalyst for the development of enzymeless glucose sensors and alkaline fuel cells at low cost. The effect is larger in case of adding iodide compared with chloride and bromide.

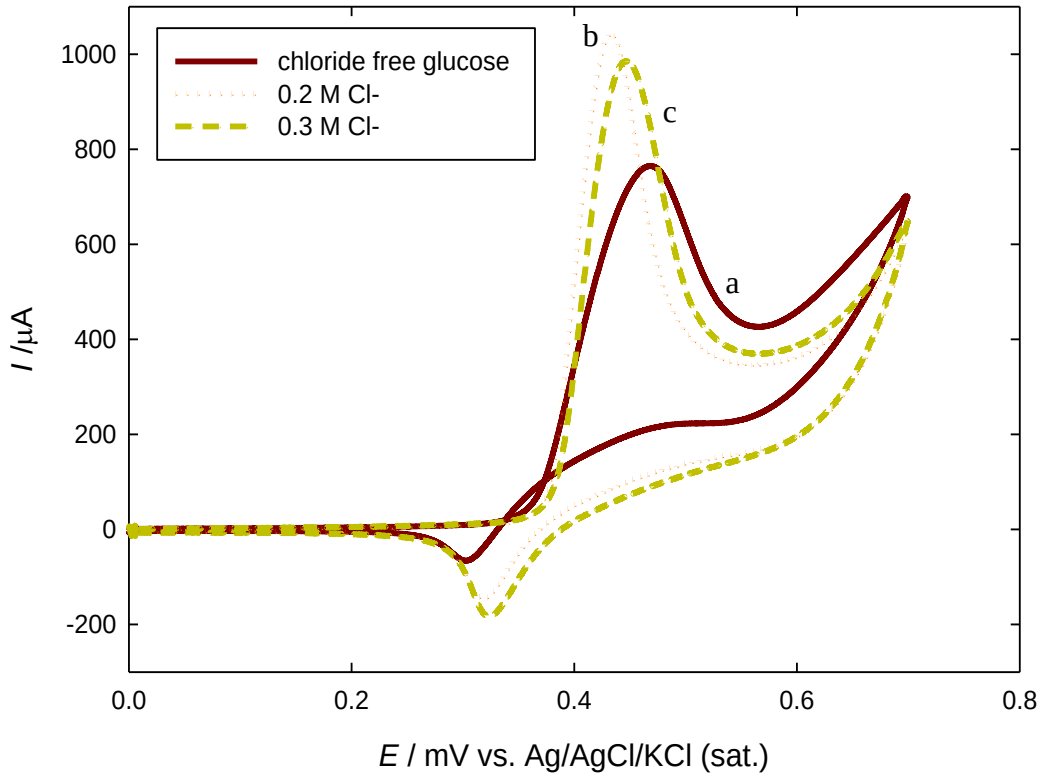

Figure 3.22. CV obtained at $GC_{ox}/NiO_x(Glu)$ electrodes in 0.5 M NaOH containing 2.5 mM of glucose in the presence of different concentrations of the halide ions [Cl^-] (a) chloride free glucose, (b) 0.2M, and (c) 0.3M , at scan rate of 100 mV/s.

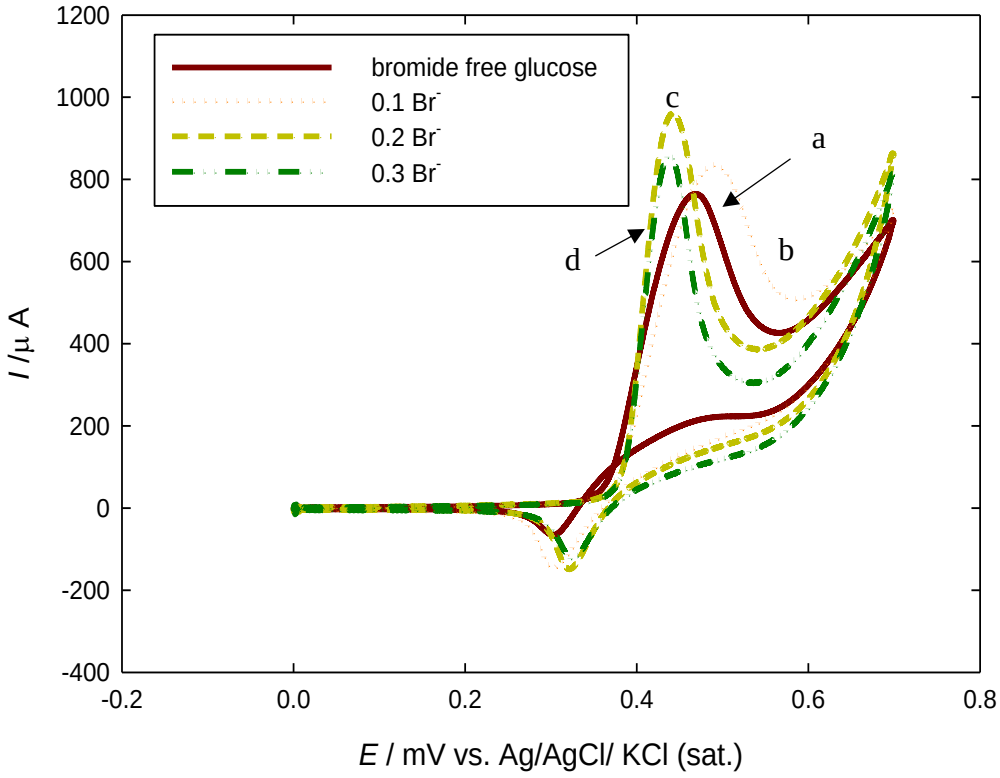

Figure 3.23. CV obtained at $GC_{ox}/NiO_x(Glu)$ electrodes in 0.5 M NaOH containing 2.5 mM of glucose in the presence of different concentrations of the halide ions [Br^-] (a) bromide free glucose, (b) 0.1M, and (c) 0.2M ,and (d) 0.3M at scan rate of 100 mV/s.

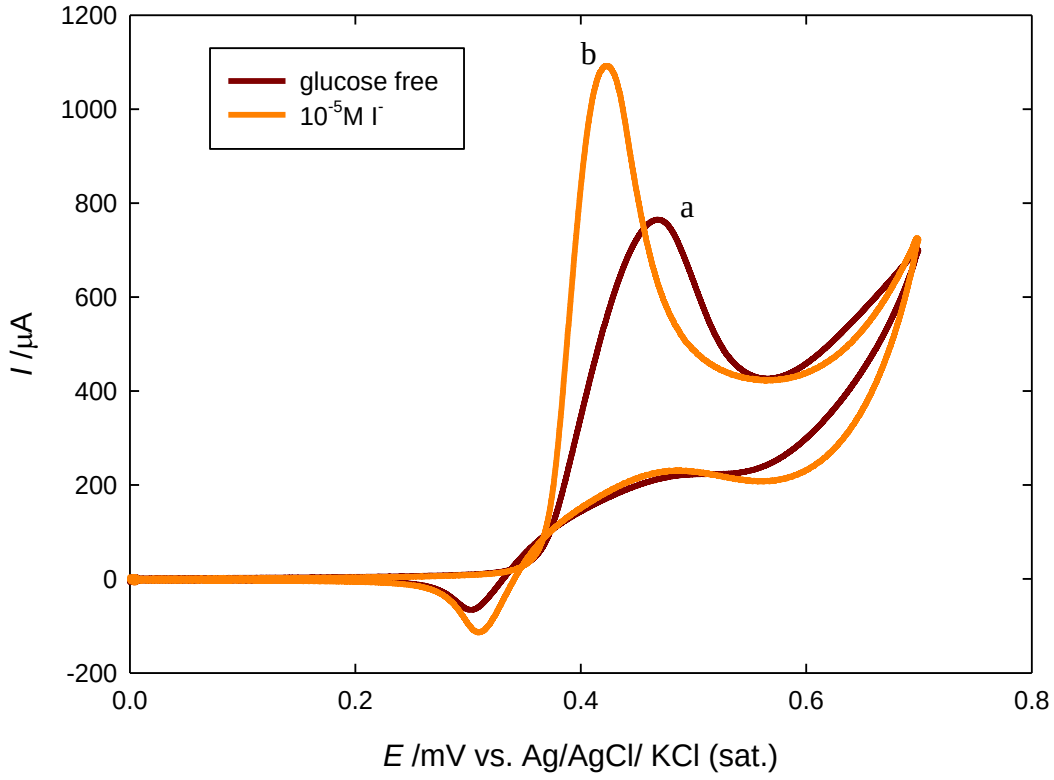

Figure 3.24. CV obtained at $GC_{ox}/NiO_x(Glu)$ electrodes in 0.5 M NaOH containing 2.5 mM of glucose in the presence of the halide ions [I^-] (a) iodide free glucose, and (b) 10^{-5}M at scan rate of 100 mV/s.

In case of iodide (Fig. 3.24) in which CV obtained on the $GC_{ox}/NiO_x(Glu)$ electrode in 0.5 M NaOH containing 2.5 mM glucose in the presence of 10^{-5}M iodide ion. Note that the concentration used for the effect of iodide is much lower than that used above for Cl^- and Br^-. This is because I^-has significant adsorbability, and so at high concentrations, it blocks the electrode surface active sites. The literature reported that the iodide ion is oxidatively adsorbed by Pt and Au electrodes as zerovalent

atomic iodine at potentials between −0.4 and +0.4 V (Ag/AgCl reference). The amount of adsorbed iodine increases upon scanning the potential to values more positive than − 0.4 V until the surface is saturated with a monolayer of close-packed iodine atoms with coverage limited by van der Waals interactions. Additional iodine atoms forced into the already space limited interfacial layer lead to the formation of molecular iodine, which is evolved into the solution as aqueous I_2 ($2\ I^- \leftrightarrow I_2 + 2e$). On the surface of Pt and Au anodes, at considerably more positive potentials and before oxygen evolution, the adsorbed zerovalent iodine is oxidized to aqueous iodate ($I_2 \leftrightarrow IO_3^-$) along with the oxide formation of the electrode surface. Finally, it is quite probable that the iodates formed on the electrode diffuse back into the solution and react with the iodide, forming iodine again [62-64]. The forward scan current is larger than that in the iodide-free glucose case. The increase in the forward scan may be attributed to the oxidation of the adsorbed zerovalent iodine to aqueous iodine molecules and/or iodates as they are available in this potential range.

The above recorded results (shown in Figures (3.22,3.23, and 3.24)) are the first run after the direct addition of halide ions. In order to further demonstrate the effect of adding halides, various numbers of potential scans (cycles) were recorded in the presence of glucose, both in the absence and presence of halide ions.

Fig. 3.25 shows consecutive CV obtained on the GC_{ox}/NiO_x(Glu) electrode in 0.5 M NaOH containing 20 mM glucose (halide-free solution) at a scan of rate 100 mV/s. To quantitatively demonstrate the effect of halide ions during potential scan cycling, we can correlate the peak current, which corresponds to glucose oxidation, to the number of potential cycles as it appears in Fig. 3.26 (the data were taken from Fig. 3.25). In Fig. 3.25 the peak current decreases continuously; the peak current after 15 cycles is around 0.8 of the initial runs. This may point to the poisoning of the electrode by the oxidation product.

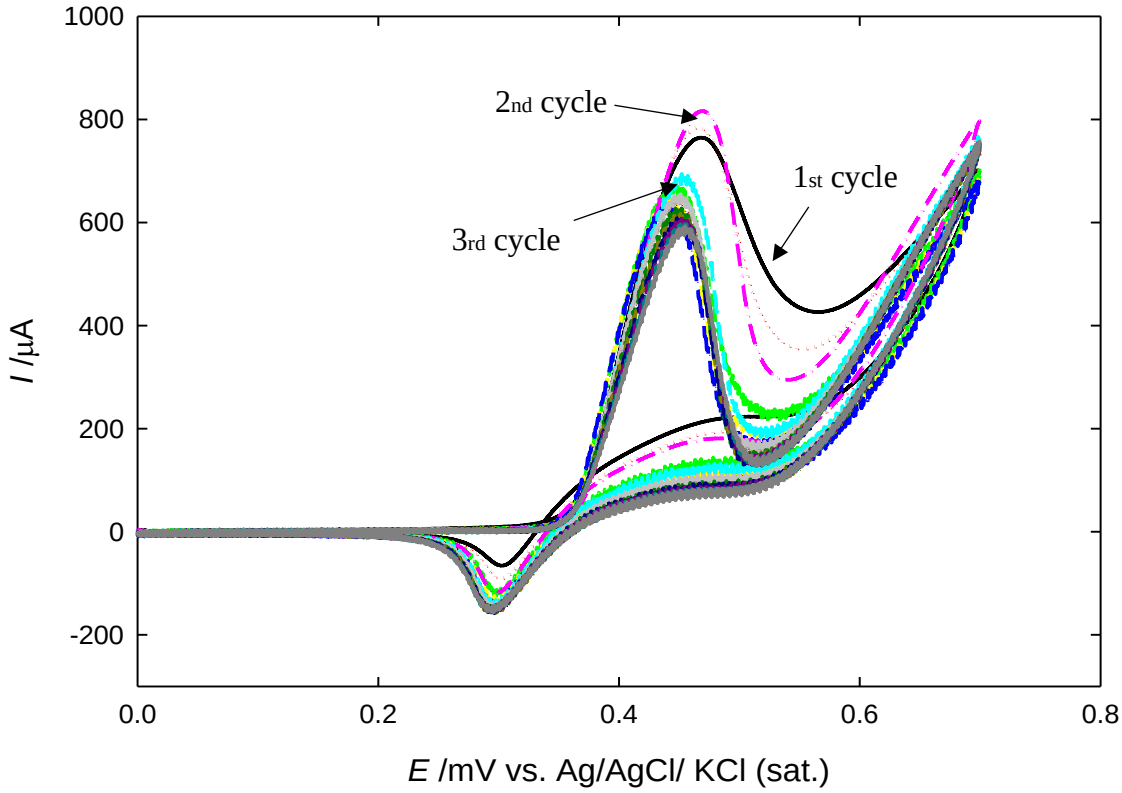

Figure 3.25. CV obtained at GC_{ox}/NiO_x(Glu) electrodes in 0.5 M NaOH containing 2.5 mM of glucose (halide-free) at scan rate of 100 mV/s for 15 cycles.

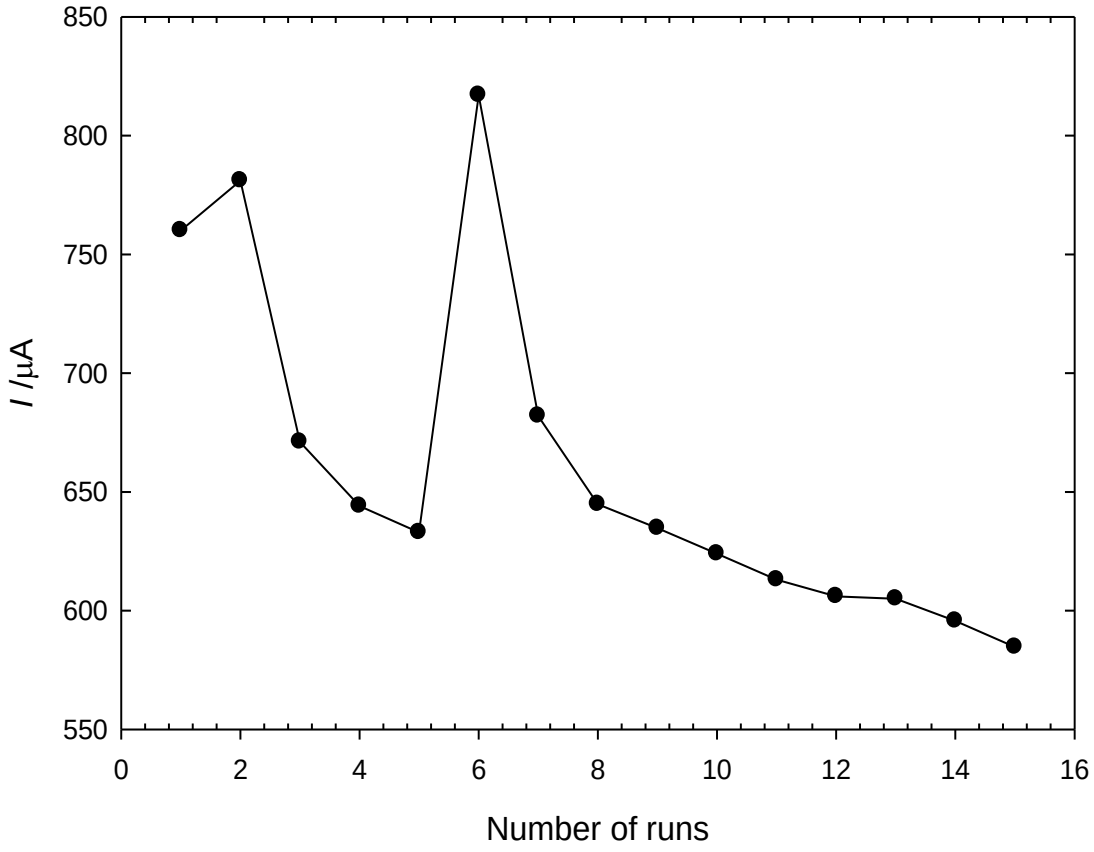

Figure 3.26. Relation between peak current for CV's scan at each run and number of runs data were taken from Fig. 3.25.

Fig. 3.27 and 3.28 shows the continuous cycling of potential in glucose solution containing Cl^- and Br^-, respectively. To quantitatively compare the poisoning effect of Cl^- and Br^- ions, the oxidation peak currents for the forward scan in the halide-free glucose and after adding Cl^- and Br^- are plotted as a function of the number of potential cycles as shown in Fig. 3.29. Many features could be extracted from Fig. 3.29.

1. In the presence of Cl^-or Br^- ions, the oxidation peak current for the first cycle is larger than that in the absence of both species. With potential cycling, the peak current decreases in the presence of any of the two species, i.e., Cl^-or Br^-, the decrease is parallel.
2. The decreasing rate of the oxidation peak current follows the sequence Br^- = Cl^-> halide-free (glucose only) solution.
3. The peak currents change with the potential cycles with a regime similar to that obtained in the case of the halide free (glucose only) solution.

The above results reveal the tolerance of glucose oxidation on the GC_{ox}/NiO_x(Glu) electrode to poisoning by chloride and bromide ions. This may be attributed to the low adsorbability and high solvation of $Cl^-$and Br^- ions. Also, it could be attributed to the high reversible oxidation potentials of $Cl_2/Cl^-$and Br_2/Br^- reactions (1.36 and 1.06 V vs. normal hydrogen electrode (NHE), respectively) [65].

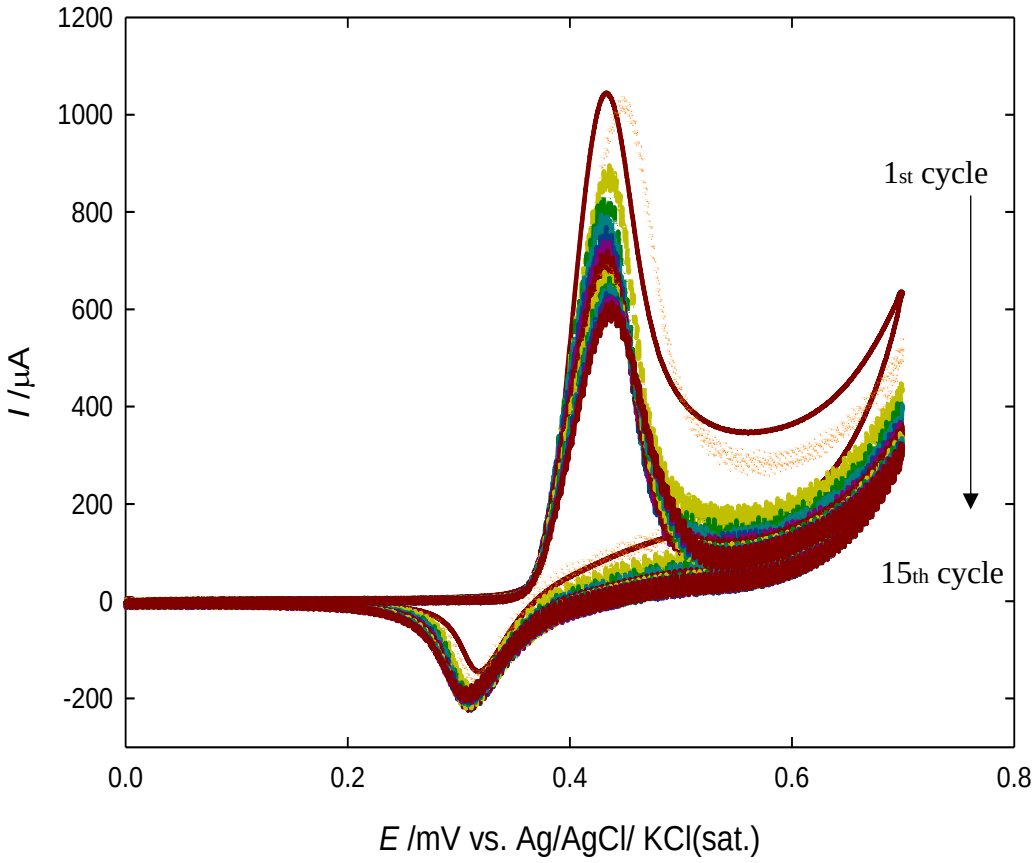

Figure 3.27. CV obtained at $GC_{ox}/NiO_x(Glu)$ electrodes in 0.5 M NaOH containing 2.5 mM of glucose in the presence of the halide ions, Cl^- (0.2M) at scan rate of 100 mV/s for 15 cycles.

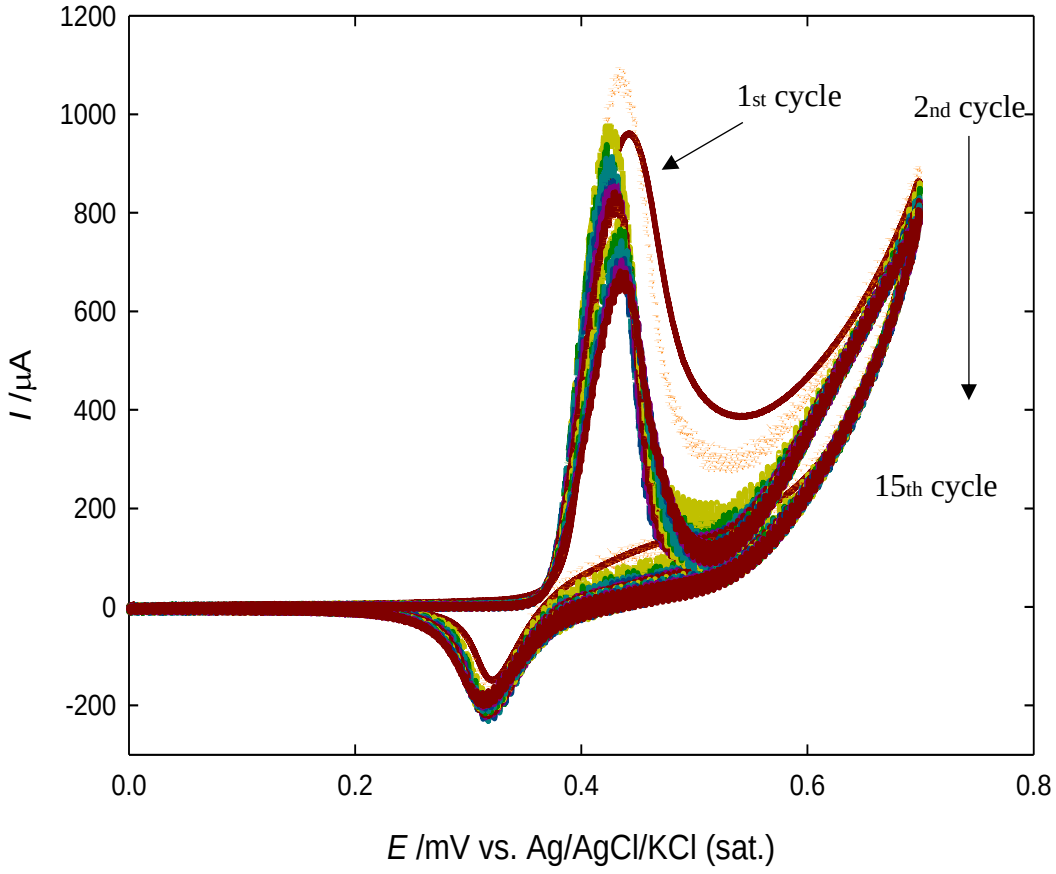

Figure 3.28. CV obtained at GC_{ox}/NiO_x(Glu) electrodes in 0.5 M NaOH containing 2.5 mM of glucose in the presence of the halide ions, Br^- (0.2M) at scan rate of 100 mV/s for 15 cycles.

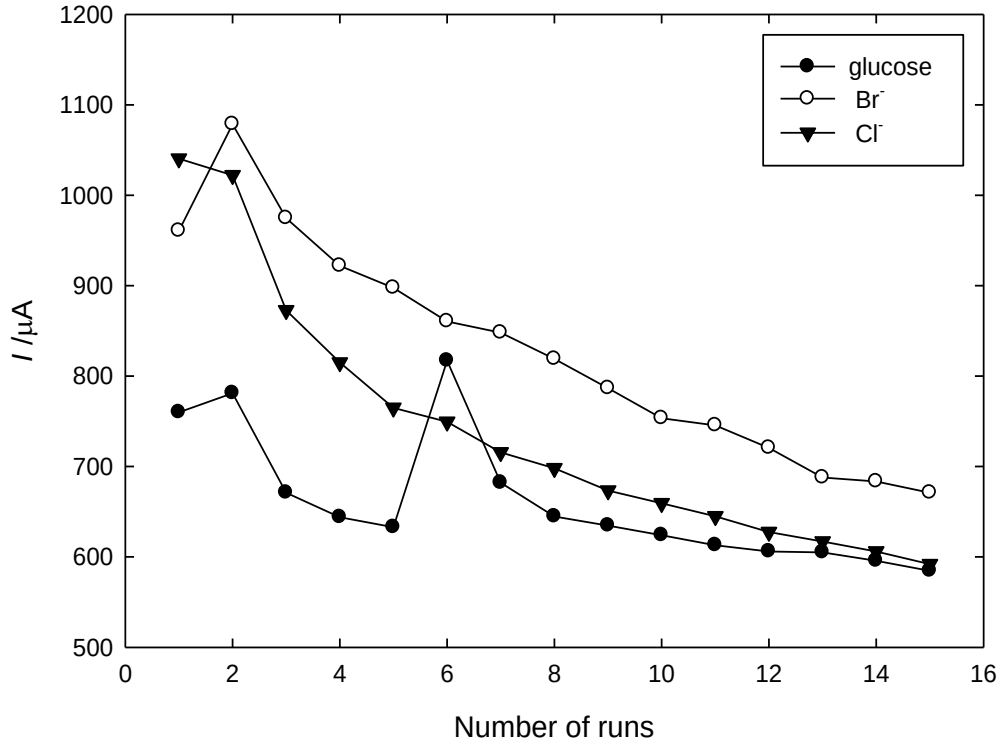

Figure 3.29. Relation between peak current for CV's scan at each run and number of runs data were extracted from figures 3.25,3.27, and 3.28.

Fig. 3.30 shows consecutive CV obtained on the GC_{ox}/NiO_x(Glu) electrode in 0.5 M NaOH containing 2.5 mM glucose and (10^{-5} M) of I^-. We can see that with the increase in the number of potential cycles, the forward current decreases.

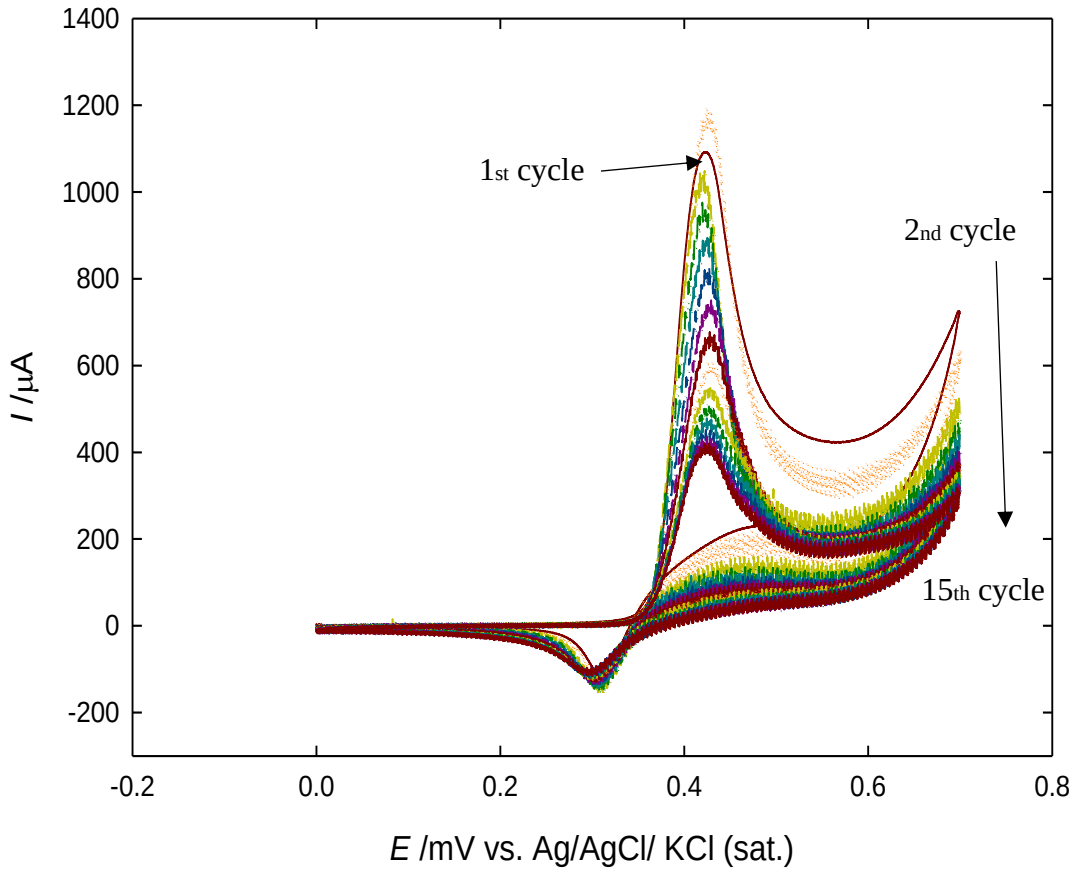

Figure 3.30. CV obtained at GC_{ox}/NiO_x(Glu) electrodes in 0.5 M NaOH containing 2.5 mM of glucose in the presence of the halide ions, I^- (10^{-5} M) at scan rate of 100 mV/s for 15 cycles.

Fig. 3.31 shows the relation between the peak current for the anodic peak (I_{pa}) with the number of potential cycles (data were taken from Fig. 3.30). This figure demonstrates an interesting falling dependence of the curve of the oxidation peak current with the potential cyclic number. It is noteworthy to mention that the peak current for the first run is higher than

the blank itself. This behavior was attributed to adsorbed iodine oxidation as it is available in this potential range. In the following potential cycles, the peak current decreases with the potential scan number to values lower than that of the blank. The fact that the peak current decreases again after the first run, although two reactions occur (glucose oxidation and adsorbed iodine oxidation), could be explained by considering the cross effect of both glucose and I^- oxidation on each other. That is to say, the glucose oxidation reaction is retarded by the adsorbed products of iodine oxidation, and the iodide oxidation reaction may retard further oxidation of $I^-$to I_2.

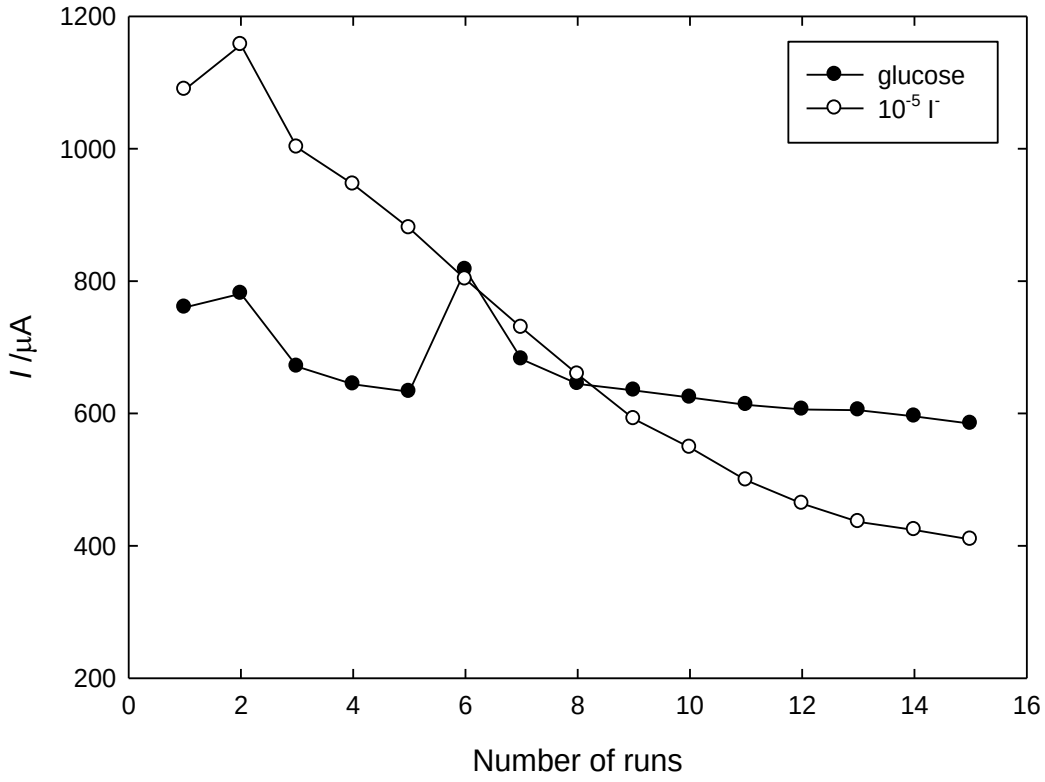

Figure 3.31: Relation between peak current for CV's scan at each run and number of runs data extracted from figures 3.25, and 3.30.

3.2.5. Conclusions

GC_{ox}/NiO_x (Glu) electrode was fabricated by electrodeposition of nickel from Watts bath in the absence and presence of glucose and then examined for glucose electrooxidation. The modified electrode significantly enhanced the glucose electrooxidation as compared with $GCox/NiO_x$ electrode which was prepared similarly to GC_{ox}/NiO_x (Glu) electrode but in the absence of glucose. The relation between $Ip/ v^{1/2}$ and *v* denoted an EC mechanism for glucose oxidation and the nominal equalities of Tafel slopes obtained at the two modified electrodes pointed to a similar mechanism at both electrodes. The current density for glucose electrooxidation is larger than that obtained in the previous section. This points to the critical effect of the underlying substrate on the deposited nickel oxide. Poisoning was studied and acceptable resistant to poisoning was obtained.

3.2.6. REFERENCES

1. Zheng W, Li Y, Tsang CS, Hu L, Liu M, Huang B, Lee LY, Wong KY (2017). CuII-Mediated Ultra-efficient Electrooxidation of Glucose. *ChemElectroChem*, 4 (11) 2788-2792.
2. Guo H, Yin H, Yan X, Shi S, Yu Q, Cao Z, Li J (2016). Pt-Bi decorated nanoporous gold for high performance direct glucose fuel cell. *Sci. Rep.*, 6:39162.
3. Pasta M, La Mantia F, Cui Y (2010). Mechanism of glucose electrochemical oxidation on gold surface. *Electrochim Acta*, *55*(20), 5561-5568.
4. Danial AS, Saleh MM, Salih SA, Awad MI (2015). On the synthesis of nickel oxide nanoparticles by sol–gel technique and its electrocatalytic oxidation of glucose. *J. Power Sources, 293*, 101-108.
5. Soukharev V, Mano N, Heller A (2004). A four-electron O_2-electroreduction biocatalyst superior to platinum and a biofuel cell operating at 0.88 V. *J. Am. Chem. Soc*, *126*(27), 8368-8369.
6. Kavanagh P, Boland S, Jenkins P, Leech D (2009). Performance of a glucose/O_2 enzymatic biofuel cell containing a mediated Melanocarpus albomyces laccase cathode in a physiological buffer. *Fuel Cells*, 9(1), 79-84.

7. Chaudhuri SK and Lovley DR (2003). Electricity generation by direct oxidation of glucose in mediatorless microbial fuel cells. *Nat.Biotechnol*., *21*(10), 1229-1232.
8. Stetten FV, Kerzenmacher S, Lorenz A, Chokkalingam V, Miyakawa N, Zengerle R, Ducree J (2006). A one-compartment, direct glucose fuel cell for powering long-term medical implants. *19th IEEE International Conference*, pp. 934-937
9. Moggia G, Kenis T, Daems N, Breugelmans T (2020). Electrochemical Oxidation of d-Glucose in Alkaline Medium: Impact of Oxidation Potential and Chemical Side Reactions on the Selectivity to d-Gluconic and d-Glucaric Acid. *ChemElectroChem* ,7 (2020) 86-95.
10. McGinley J, McHale FN, Hughes P, Reid CN, McHale AP (2004). Production of electrical energy from carbohydrates using a transition metal-catalysed liquid alkaline fuel cell. *Biotechnol. Lett.*, *26*(23), 1771-1776.
11. Wilde CP and Zhang M (1993). Oxidation of glucose at electrodeposited platinum electrodes in alkaline solution. *J. Chem. Soc., Faraday Trans.*, *89*(2), 385-389.
12. Xiao F, Zhao F, Mei D, Mo Z, Zeng B (2009). Nonenzymatic glucose sensor based on ultrasonic-electrodeposition of bimetallic PtM (M= Ru, Pd and Au) nanoparticles on carbon nanotubes–ionic liquid composite film. *Biosens. Bioelectron*, *24*(12), 3481-3486.

13. Xing W, Li F, Yan ZF, Lu GQ (2004). Synthesis and electrochemical properties of mesoporous nickel oxide. *J. Power Sources*, *134*(2), 324-330.

14. Wu MS and Hsieh HH (2008). Nickel oxide/hydroxide nanoplatelets synthesized by chemical precipitation for electrochemical capacitors. *Electrochim. Acta*, *53*(8), 3427-3435.

15. Snook GA, Duffy NW, Pandolfo AG (2008). Detection of oxygen evolution from nickel hydroxide electrodes using scanning electrochemical microscopy. *J. Electrochem. Soc.*, *155*(3), A262-A267.

16. Hu Y, Jin J, Wu P, Zhang H, Cai C (2010). Graphene–gold nanostructure composites fabricated by electrodeposition and their electrocatalytic activity toward the oxygen reduction and glucose oxidation. *Electrochim. Acta*, *56*(1), 491-500.

17. Hui S, Zhang J, Chen X, Xu H, Ma D, Liu Y, Tao B (2011). Study of an amperometric glucose sensor based on Pd–Ni/SiNW electrode. *Sens. Actuators, B, 155*(2), 592-597.

18. Barragan JT, Kogikoski Jr S, da Silva ET, Kubota LT (2018). Insight into the electro-oxidation mechanism of glucose and other carbohydrates by CuO-based electrodes. *Anal. Chem.,*90:3357-3365.

19. Rahim MA, Hameed RA, Khalil MW (2004). Nickel as a catalyst for the electro-oxidation of methanol in alkaline medium. *J. Power Sources*, 134:160-169.

20. Popović KĐ, Tripković AV, Adžić RR (1992). Oxidation of D-glucose on single-crystal platinum electrodes: a mechanistic study. *J. Electroanal. Chem.*, *339*(1-2), 227-245.

21. Wilde CP and Zhang M (1993). Oxidation of glucose at electrodeposited platinum electrodes in alkaline solution. *J. Chem. Soc.,* 89(2), 385-389.

22. Lei HW, Wu B, Cha CS, Kita H (1995). Electro-oxidation of glucose on platinum in alkaline solution and selective oxidation in the presence of additives. *J. Electroanal. Chem., 382*(1-2), 103-110

23. Chai D, Zhang X, Chan SH, Li G (2019). Facile aqueous phase synthesis of Pd3Cu–B/C catalyst for enhanced glucose electrooxidation. *J. Taiwan Inst. Chem. Eng.,*95:139-146

24. Aoun SB and Taniguchi I (2008). Effective electrocatalytic oxidation of glucose at platinum nanoparticle-based carbon electrodes. *Chem. Lett.*, 37(9), 936-937

25. Yei LE, Beden B, Lamy C (1988). Electrocatalytic oxidation of glucose at platinum in alkaline medium: on the role of temperature. *J. Electroanal. Chem. Interfacial Electrochem.,* 246(2), 349-362.

26. Nikolaeva NN, Khazova OA, Vasil'ev YB (1983). Kinetics and mechanism of glucose oxidation on a platinum electrode. *Elektrokhimiya*, 19, 1476-1481.

27. Neha N, Kouamé BS, Rafaïdeen T, Baranton S, Coutanceau C (2020). Remarkably Efficient Carbon-Supported Nanostructured Platinum-Bismuth Catalysts for the Selective Electrooxidation of Glucose and Methyl-Glucoside. *Electrocatalysis*, 22:1-14.

28. El-Refaei SM, Saleh MM, Awad MI (2014). Tolerance of glucose electrocatalytic oxidation on NiO x/MnO x/GC electrode to poisoning by halides. *J. Solid State Electrochem.,* 18(1), 5-12.

29. Ren Y and Gao L (2010). From Three-Dimensional Flower-Like α-Ni(OH)2 Nanostructures to Hierarchical Porous NiO Nanoflowers: Microwave-Assisted Fabrication and Supercapacitor Properties*, J. Am. Ceram. Soc*., 93,3560.

30. Im T, Lee J, Song Y, Lee JK, Song YS, Yim T (2010). Zinc-nickel alloy electrodeposition composition for forming plating layer on e.g. construction material, contains zinc-nickel based liquid, brightness improver, complexing agent and additive which prevents precipitation of nickel ion. KR2010083623-A.

31. Vassilyev YB, Khazova OA, Nikolaeva NN (1985). Kinetics and mechanism of glucose electrooxidation on different electrode-catalysts: Part I. Adsorption and oxidation on platinum. *J. Electroanal. Chem. Interfacial Electrochem.*, 196(1), 105-125.

32. Hsiao M, Adzic R, Yeager E (1992). The effects of adsorbed anions on the oxidation of D-glucose on gold single crystal electrodes. *Electrochim. Acta*, 37, 357–363.

33. Stevanović S, Panić V, Tripković D, Jovanović VM (2009). Promoting effect of carbon functional groups in methanol oxidation on supported Pt catalyst. *Electrochem. Commun*., 11(1), 18-21.

34. El-Refaei SM, Awad MI, El-Anadouli BE, Saleh MM (2013). Electrocatalytic glucose oxidation at binary catalyst of nickel and manganese oxides nanoparticles modified glassy carbon electrode: Optimization of the loading level and order of deposition. *Electrochim. Acta*, *92*, 460-467.

35. Danaee I, Jafarian M, Forouzandeh F, Gobal F, Mahjani MG (2008). Electrocatalytic oxidation of methanol on Ni and NiCu alloy modified glassy carbon electrode. *Int. J. Hydrogen Energy*, 33(16), 4367-4376.

36. Danaee I, Jafarian M, Mirzapoor A, Gobal F, Mahjani MG (2010). Electrooxidation of methanol on NiMn alloy modified graphite electrode. *Electrochim Acta*, 55(6), 2093-2100.

37. Fleischmann M, Korinek K, Pletcher D (1971). The oxidation of organic compounds at a nickel anode in alkaline solution, *J. Electroanal. Chem. Interfacial Electrochem.*, *31*(1), 39-49.

38. Zhao C, Shao C, Li M, Jiao K (2007). Flow-injection analysis of glucose without enzyme based on electrocatalytic oxidation of glucose at a nickel electrode. *Talanta*, 71(4), 1769-1773.

39. Becerik I and Kadirgan F (1992). The electrocatalytic properties of palladium electrodes for the oxidation of d-glucose in alkaline medium. *Electrochim Acta*, 37(14), 2651-2657.

40. Mho SI and Johnson DC (2001). Electrocatalytic response of carbohydrates at copper-alloy electrodes. *J. Electroanal. Chem.,* 500(1-2), 524-532.

41. El-Refaei SM, Saleh MM, Awad MI (2013). Enhanced glucose electrooxidation at a binary catalyst of manganese and nickel oxides modified glassy carbon electrode. *J. Power Sources*, 223, 125-128.

42. Fleischmann M, Korinek K, Pletcher D (1972). The kinetics and mechanism of the oxidation of amines and alcohols at oxide-covered nickel, silver, copper, and cobalt electrodes. *J. Chem. Soc., Perkin Trans. 2*, 10:1396-403.

43. Lee KK, Loh PY, Sow CH, Chin WS (2012). CoOOH nanosheets on cobalt substrate as a non-enzymatic glucose sensor. *Electrochem. Commun.*, 20:128–132

44. Cherevko S and Chung CH (2009). Gold nanowire array electrode for non-enzymatic voltammetric and amperometric glucose detection. *Sens. Actuators,* B 142:216–223

45. Jeong H and Kim J (2012). Electrochemical oxidation of glucose at nanoporous black gold surfaces in the presence of high concentration of chloride ions and application to amperometric detection. *Electrochim. Acta*, 80:383–389

46. El-Refaei SM, Saleh MM, Awad MI (2013). Enhanced glucose electrooxidation at a binary catalyst of manganese and nickel oxides modified glassy carbon electrode. *J Power Sources*, 223:125–128

47. El-Refaei SM, Awad MI, El-Anadouli BE, Saleh MM (2013) Electrocatalytic glucose oxidation at binary catalyst of nickel and manganese oxides nanoparticles modified glassy carbon electrode: optimization of the loading level and order of deposition. *Electrochim. Acta*,92:460–467.

48. Pasta M, Mantia FL, Cui Y (2010). A new approach to glucose sensing at gold electrodes. *Electrochem. Commun.,* 10:1407–1410.

49. Park S, Boo H, Chung TD (2006) Electrochemical non-enzymatic glucose sensors. *Anal Chim. Acta*, 556(1):46–57.

50. Pasta M, Mantia FL, Cui Y (2010). Mechanism of glucose electrochemical oxidation on gold surface. *Electrochim. Acta*, 55(20):5561– 5568.

51. Hsiao MW, Adzic RR, Yeager EB (1992). The effects of adsorbed anions on the oxidation of D-glucose on gold single crystal electrodes. *Electrochim. Acta*, 37(2):357–363.

52. Hsiao MW, Adzic RR, Yeager EB (1996). Electrochemical oxidation of glucose on single crystal and polycrystalline gold surfaces in phosphate buffer. *J Electrochem. Soc*., 143(3):759–767.

53. Li Y, Song Y, Yang C, Xia X (2007) Hydrogen bubble dynamic template synthesis of porous gold for non-enzymatic electrochemical detection of glucose. *Electrochem. Commun*., 9(5):981–988.

54. Seo B and Kim J (2010). Electrooxidation of glucose at nanoporous gold surfaces: structure dependent electrocatalysis and its application to amperometric detection. *Electroanalysis*, 22(9):939–945.

55. Kamath VN and Lal H (1970). Halide adsorption and the anodic oxidation of chemisorbed methanol on platinum. *J Electroanal. Chem*., 24(1):125–135.

56. Sobkowski J, Franaszczuk K, Dobrowolska K (1992). Effect of anions and pH on the adsorption and oxidation of methanol on a platinum electrode. *J Electroanal. Chem.,* 330(1–2):529–540.

57. Luo S, Su F, Liu C, Li J, Liu R, Xiao Y, Li Y, Liu X, Cai Q (2011). A new method for fabricating a CuO/TiO2 nanotube arrays electrode and its application as a sensitive nonenzymatic glucose sensor. *Talanta*, 86:157–163.

58. Liu Y, Teng H, Hou H, You T (2009). Nonenzymatic glucose sensor based on renewable electrospun Ni nanoparticle-loaded carbon nanofiber paste electrode. *Biosens. Bioelectron*., 24(11):3329–3334.

59. Zhao C, Shao C, Li M, Jiao K (2007). Flow-injection analysis of glucose without enzyme based on electrocatalytic oxidation of glucose at a nickel electrode. *Talanta*, 71:1769–1773 22. 22.

60. Becerik I and Kadirgan F (1992). The electrocatalytic properties of palladium electrodes for the oxidation of D-glucose in alkaline medium. *Electrochim. Acta*, 37:2651–2657.

61. Mho SI and Johnson DC (2001). Electrocatalytic response of carbohydrates at copper-alloy electrodes. *J Electroanal. Chem*., 500:524–532.

62. Anson FC and Lingane JJ (1957). Anodic chronopotentiometry with platinum and gold electrodes. The iodide–iodine–iodate system. *J. Am. Chem. Soc.*, 79(5):1015–1020.

63. Bravo BG, Michelhaugh SL, Soriaga MP, Villegas I, Suggs DW, Stickney JL (1991). Anodic underpotential deposition and cathodic stripping of iodine at polycrystalline and single-crystal gold: studies by LEED, AES, XPS, and electrochemistry. *J. Phys. Chem.,* 95(13):5245–5249.

64. Verhoef JC (1978). Electrochemical behaviour of iodide at a rotating platinum disk electrode in methanol. *Electrochim. Acta*, 23(5):433–438.

65. Novak DM and Conway B (1981). Competitive adsorption and state of charge of halide ions monolayer oxide film growth processes at Pt anodes. *J. Chem. Soc. Faraday Trans*., 1 77(10):2341–2359.

PART 3

CHAPTER III (PRAT 3)

Electrocatalytic oxidation of glucose at graphene-Nickle oxides nanoparticles composite

3.3.1. Abstract

Graphene (Gr) and nickel oxide (NiOx) nanoparticles modified glassy carbon (GC) electrode were fabricated in the presence of a suitable additive controlling the interfacial properties. The modified electrode was applied in enhancing the electrochemical oxidation of glucose. The effect of the concentration of the additive on the extent of electroactivity of those modified electrodes was optimized. Also, the effect of loading of nickel oxide (NiO_x) nanoparticles on the GC_{ox}/Gr electrode was optimized as well. Cyclic voltammetry (CV), and chronoamperometry were used for the voltammetric characterization. Several surface techniques were used for probing the morphology and composition of the deposited modifier, including field emission scanning electron microscopy (FE-SEM), Dispersive X-Ray Analysis (EDX). GC electrode was casted by graphene (Gr) and then (NiOx) was deposited either from nickel bath containing glucose or not. The deposition was achieved by cyclic voltammetry (CV) for certain potential cycles in the potential range

from 0.0 to -1.0 V vs. Ag/AgCl(Kcl sat.). Possible reason behind the enhancement of glucose electrocatalytic oxidation was explored.

3.3.2. Introduction

In the resent years glucose electro-oxidation reaction has magnetized remarkable study because of its significance in many potential applications containing clinical diagnostics, food industry [1], glucose fuel cells (FCs) [2], treatment of wastewater, [3] biotechnology [4] and glucose sensors [5]. So, the expansion of stable, cheap, and efficient glucose electrocatalysts is very important. Valuable metal-based electrocatalysts have been used in former research such as Pt-multi wall carbon nanotubes (MWCNTs) [6], Pt–Pb/MWCNT [7], platinum and gold-based electrodes [8,9]. However, there are limits to its use in the practical application because of: its low durability and high cost [10-13].

In this respect, many transition metal oxides (MO_X) nanostructured modified anodes have obtained intense research attention for glucose electro-oxidation reaction such as Co_3O_4 nanofibers [14], Ni NPs [15], Fe_3O_4 nanorod arrays [16], MnO_2 [17], and CuO nanostructures [18].

Recently, since the discovery of graphene, two-dimensional materials have become of great importance as electrical stimuli [14-17]. This is due to the high graphene activity as a catalyst due to its amazing structural,

physical and chemical properties [14,16,19] such as: good chemical stability, exceptional electrical loyalty, strong mechanical strength, high surface area (≈2600 m^2 /g) [15, 17], easy operation, high cost of catalytic behavior, and high carrier mobility (≈15,000 $cm^2/V{\cdot}s$) [16,20-23], which stimulated the study of electrical catalysis reactions using graphene. Graphene-based electrochemical sensors have been used as comprehensive application in electroanalysis and facilitate the evolution of biosensors with specificity and high sensitivity [24-26].

In the present work, the fabrication of glassy carbon (GC) electrode modified with graphene (Gr) in short time (with the aid of 30 min sonication) through the solution phase approach and deposition of NiO_x nanoparticles for glucose electro-oxidation reaction, designated as GCox/Gr/NiOx(Glu) electrode is prepared and characterized by cyclic voltammetry (CV) in alkaline medium. The experimental parameters are optimized to sustain the highest electrocatalytic activity towards glucose oxidation. Inclusion of glucose in the deposition bath significantly affect the oxidation of glucose at the modified electrode.

3.3.3. Experimental

3.3.3.1. Electrochemical measurements

Potentiostat/galvanostat/ZRA model the Reference 600 TM machine were used for the Electrochemical measurements. A conventional cell with a three-electrode configuration was used in this work. The electrochemical measurements were performed at room temperature (25 °C). The working electrode was glassy carbon (GC, d = 3.0 mm). It was cleaned by mechanical polishing with aqueous slurries of successively finer alumina powder then washed thoroughly with deionized water.

3.3.3.2. Preparation of GCox/Gr/NiO_X. electrode

The bare GCE was polished to a mirror-like surface with 1, 0.3, and 0.05 *u*m alumina slurry, respectively. The GC electrode surface was casted with 10 *u*L Gr suspension and then dried at room temperature to fabricate the GCox/Gr electrode. The GC/Gr electrode was scanned for five potential cycles at range from −0.2V to 2V.vs. Ag/AgCl /KCl (sat.) in 0.5 M H_2SO_4. After that, the electrodeposition of NiOx was corducted by using five potential cycles at range from 0.0 to -1.0V vs. Ag/AgCl /KCl (sat.) in 0.5 M NaOH.

3.3.4. Results and discussion

3.3.4.1. Morphological characterizations

The morphology and composition of the various electrocatalysts prepared atop the surface of the GC electrode were first investigated by SEM, and EDX. Fig. 3.32. shows SEM images of nano-NiO_x prepared by a cyclic voltammetry technique described in the experimental section. Also, the atomic ratios of C/O/Ni from EDX were obtined. In image A, the nanoparticles obtained looks like cauliflower but have many mini diamonds like. In EDX (plot B), as expected, peaks of Ni at GC_{ox}/NiOx- as at 0.9, 7.6, and 8.2 KeV are revealed [27]. At image C, GCox/Gr/NiOx(Glu) electrode which is fabricated similarly to GCox/NiOx(Glu) electrode but in the presence of graphene. The nanoparticles obtained look like rocks. EDX (plot D), however, presents a smaller ratio of nickel compared with plot B.

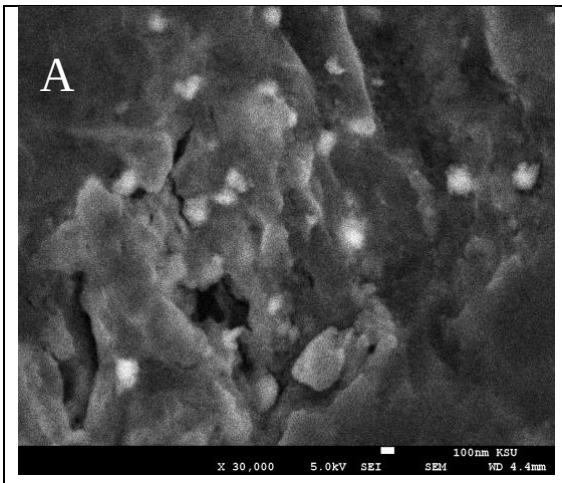

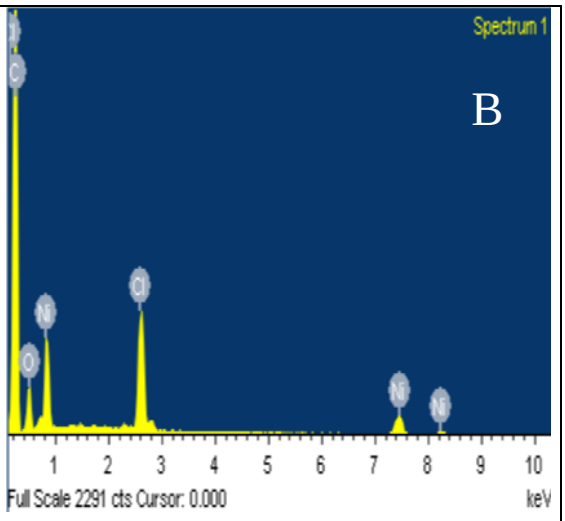

Element	Weight%	Atomic%
C K	74.24	86.68
O K	9.54	8.36
Cl K	6.92	2.74
Ni K	9.30	2.22

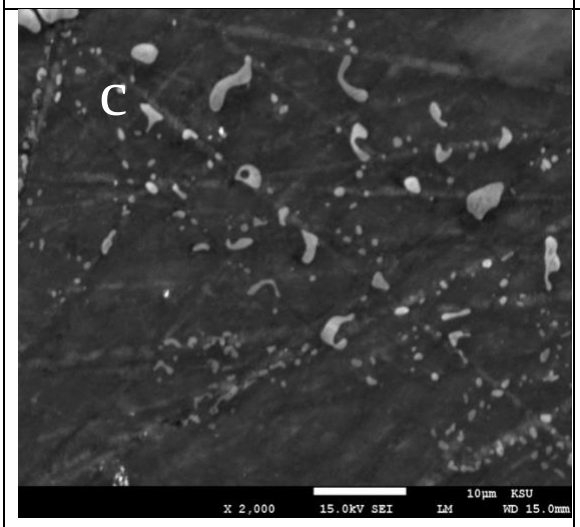

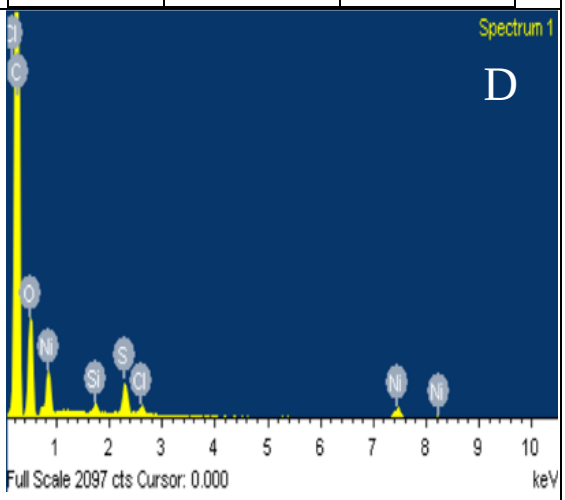

Element	Weight%	Atomic%
C K	72.01	80.49
O K	20.78	17.43
Cl K	0.54	0.21
Ni K	4.97	1.14
Si K	0.32	0.15
S K	1.38	0.58

Figure 3.32. SEM (A,C) and EDX (B,D) of (A,B) GCox/NiOx(Glu), and (C,D) GCox/Gr(Glu)/NiOx(Glu) electrodes.

3.3.4.2. Electrochemical characterizations

In this work, the glassy carbon electrode was casted by graphene. Then nickel was deposited in the presence and absence of glucose, and then applied for the electrocatalytic oxidation of glucose in alkaline media. Fig. 3.33 shows CVs responses obtained (a) GCox/Gr/NiOx, (b) GCox/NiO_x, (c) GCox/NiOx(Glu) and (d) GCox/Gr/NiOx(Glu) electrodes in 0.5 M NaOH. The five potential cycles in the range from 0.0 to -1.0V vs. Ag/AgCl /KCl (sat.) were used to deposit NiOx nanoparticles onto electrodes. As clearly shown, in Fig. 3.33 (curve a), obtained at GCox/Gr/NiOx electrode in which glassy carbon was electrochemically oxidized and then casted by graphene and subsequently nickel was deposited, the CV is featureless. Curves b and c shows CV responses obtained at GC_{ox}/NiO_x and GC_{ox}/NiO_x(Glu) electrodes, respectively. The peak current for nickel couple increases at both electrodes compared with that on the GCox/Gr/NiOx (a). Probably, the functional groups of the underlying substrate participate in this enhancement. Comparing curves b and c indicates that including glucose in the deposition bath (curve c) promotes the nickel-nickel oxide redox couple. Curve d, show CV response obtained at GCox/Gr/NiOx(Glu) electrode. In this case the largest enhancement in the nickel-nickel oxide redox couple is obtained.

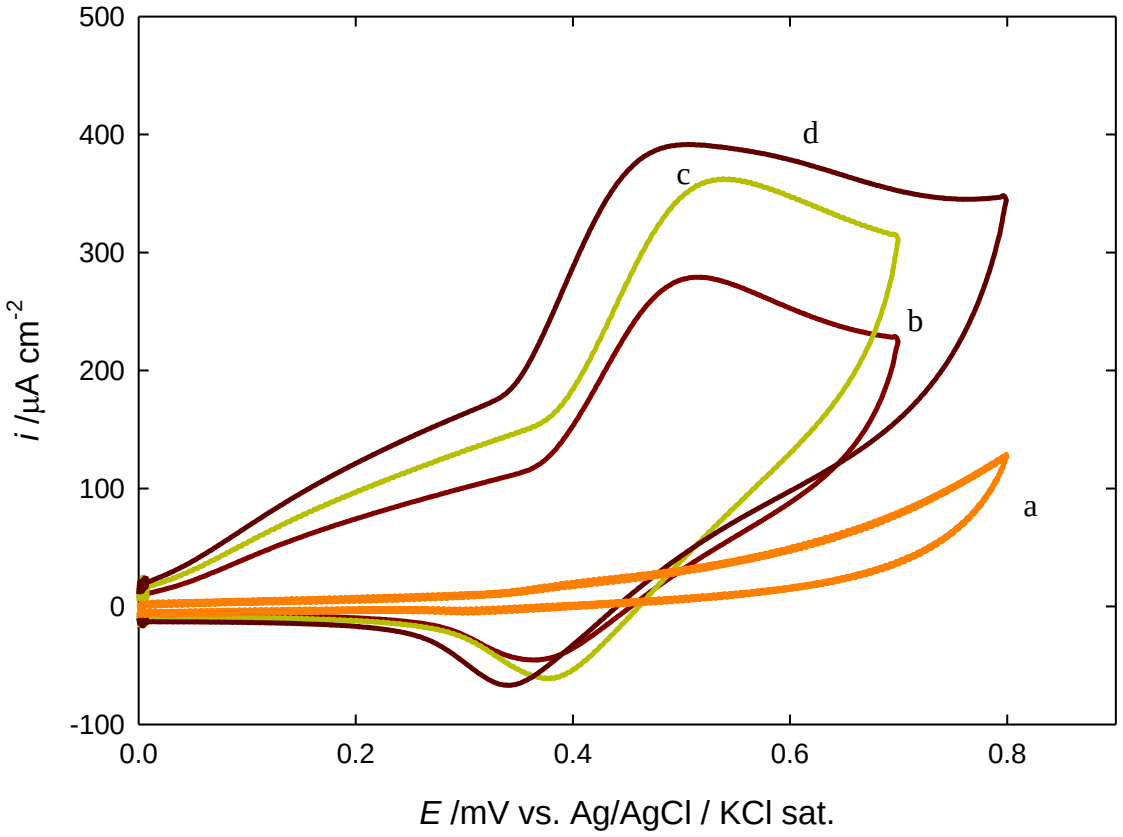

Figure 3.33. CV obtained at (a) GCox/Gr/NiOx , (b) GCox/NiO_x, (c) GCox/NiOx(Glu) and (d) GCox/Gr(Glu)/NiOx(Glu) electrodes in 0.5 M NaOH.

Fig. 3.34 is similar to Fig. 3.33 but in the presence of glucose. Data extracted from this figure are presented in Table 3.3. The glucose oxidation peak current increases at GCox/Gr/NiOx(Glu) electrode (curve d) compared with GCox/NiOx(Glu) electrode (curve c) . The oxidation

current increases in the presence of graphene. When graphene was casted on the electrode, the electrocatalytic oxidation of glucose was obviously observed at lower positive potential and the oxidation peak current was two times of that obtained at GCox/NiOx(Glu) electrode, indicating that co-effect of graphene and NiO_X played an important role in the electrocatalytic oxidation of glucose. The graphene provides larger surface area for NiOx as well as for glucose adsorption and assists in faster electrode kinetics [28-31].

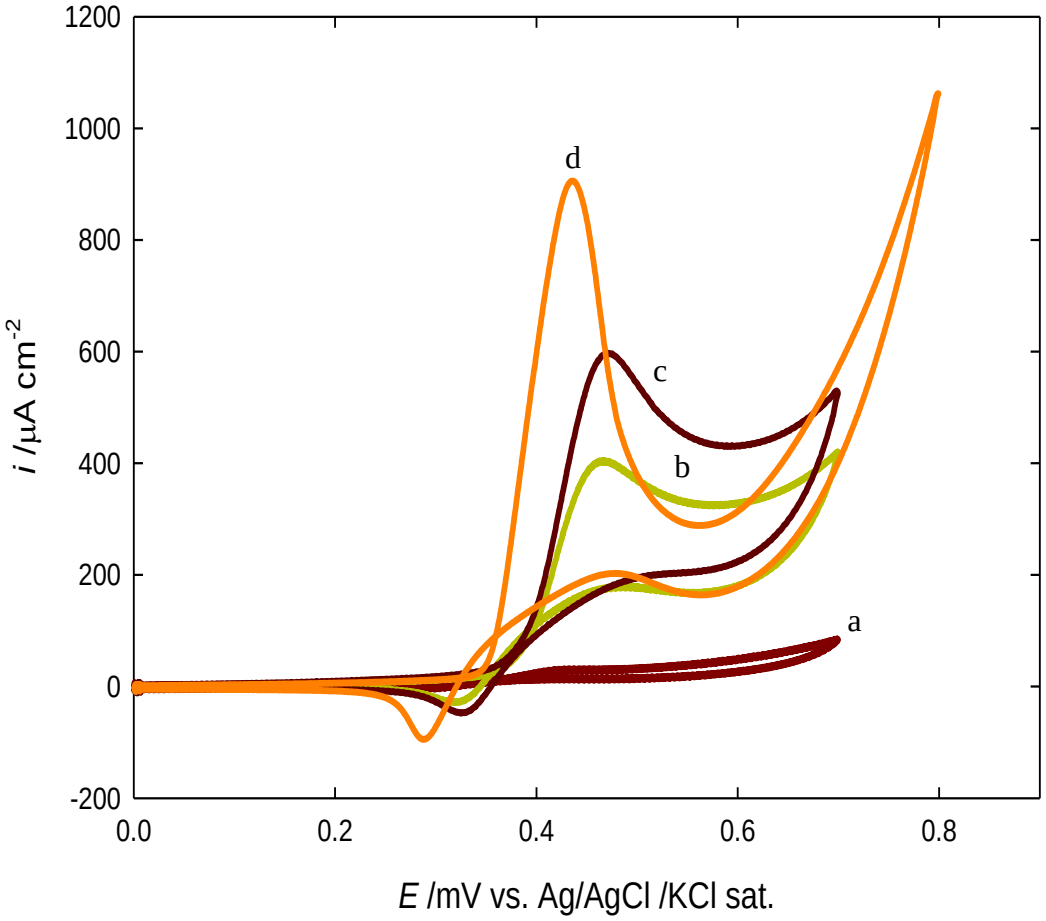

Figure 3.34. CV obtained at (a) GCox/Gr/NiOx, (b) GCox/NiOx, (c)GCox/NiOx(Glu),and (d) GCox/Gr(Glu)/NiOx(Glu) electrodes in 0.5 M NaOH containing 2.5 mM glucose.

Table 3.3. Peak potential, peak current and onset potential of glucose oxidation obtained at modified electrodes. Data are extracted from Fig. 3 .34.

Electrode	Peak potential/*V*	Onset potential/*V*	Peak current/μA
GCox/Gr/NiOx	0.43	0.37	31
GCox/NiO_x	0.45	0.35	399
GCox/NiOx(Glu)	0.46	0.36	616
GCox/Gr/NiOx(Glu)	0.43	0.34	905

3.3.4.3. Effect of loading of nickel nanoparticles

The extent of NiOx loading levels have been investigated at GCox/Gr/NiOx(Glu) electrode towards the glucose oxidation reaction and results are shown in Fig. 3.35. Data extracted from this figure are shown as Table 3.4. The monotonic increase of the peak current of glucose oxidation with the amount of NiOx is observed. The presence of Gr caused increase of the anodic peak current for glucose oxidation reaction at GCox/Gr/NiOx(Glu) electrode possibly due to the larger specific surface area of Gr (compared to GCox) which enhances the

electrocatalytic activity of the modified electrode towards glucose oxidation reaction.

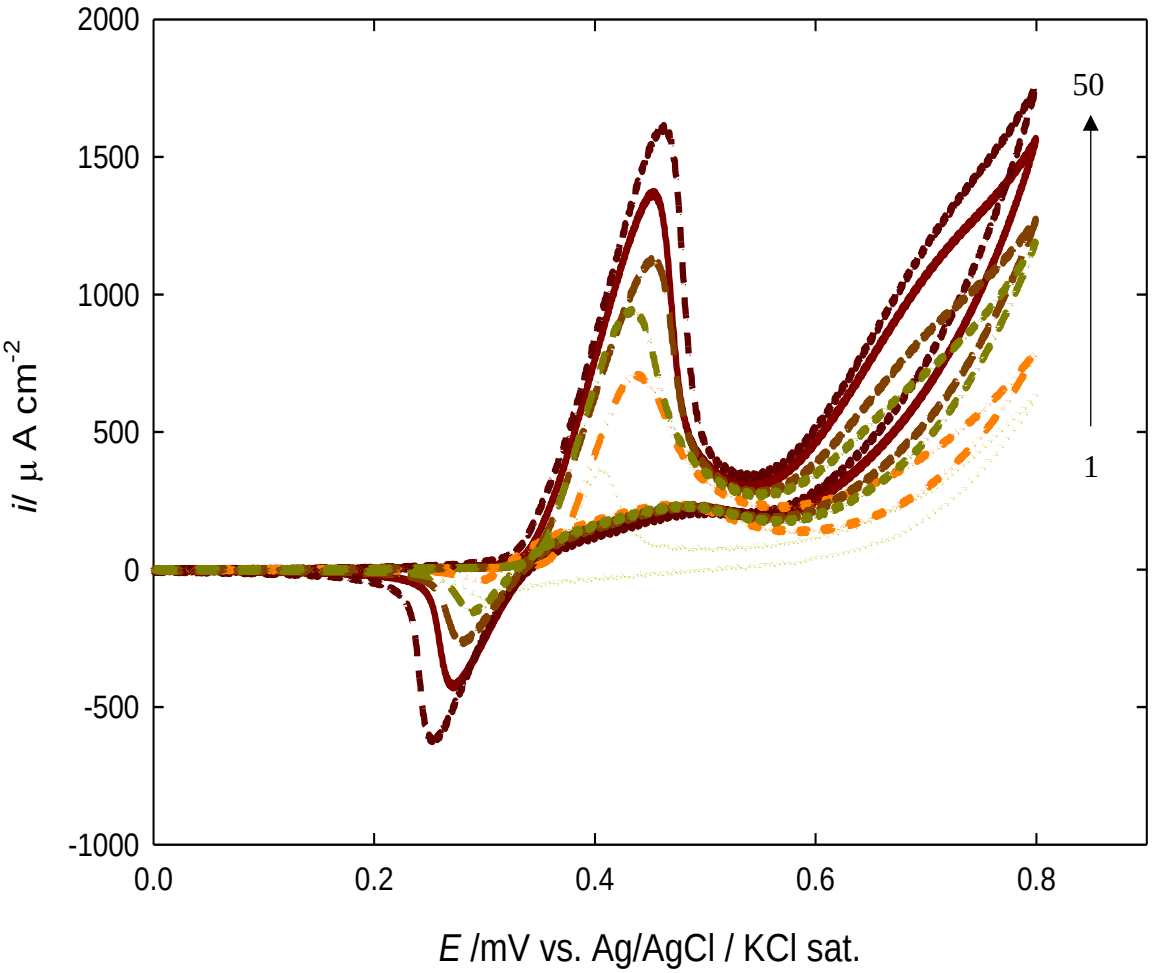

Figure 3.35. CV obtained at GCox/Gr/NiOx(Glu) in 0.5 M NaOH containing 2.5 mM glucose, NiO_x was prepared by by different potential cycles in the range of 0.0 ~ -1.0 V.

Table 3.4. Peak potential, peak current and onset potential of glucose oxidation obtained at GCox/Gr/NiOx(Glu) with different loading of nickel. Data are extracted from Fig. 3 .35.

Potential cycle number	Peak potential / *V*	Onset potential / *V*	Peak current / *μ*A
Blank	0.40	0.34	345
1st	0.43	0.35	706
2nd	0.43	0.33	931
5th	0.45	0.33	1112
10th	0.45	0.33	1362
50th	0.46	0.32	1601

In order to get further insight, Fig. 3.36 shows Tafel plots obtained at (a) GCox/NiOx(Glu), and (b) GCox/Gr/NiOx(Glu) in 0.5 M NaOH containing 2.5 mM glucose at a scan rate 5 mV/s.

Tafel slopes of ca. 38 mV/dec was obtained at both electrodes. This means the electron transfer represented by Eq. 3.4 is the rate determining step [32]. The plots confirmed reinforcement of the glucose oxidation on GCox/Gr/NiOx(Glu) compared with GC_{ox}/NiO_x(Glu).

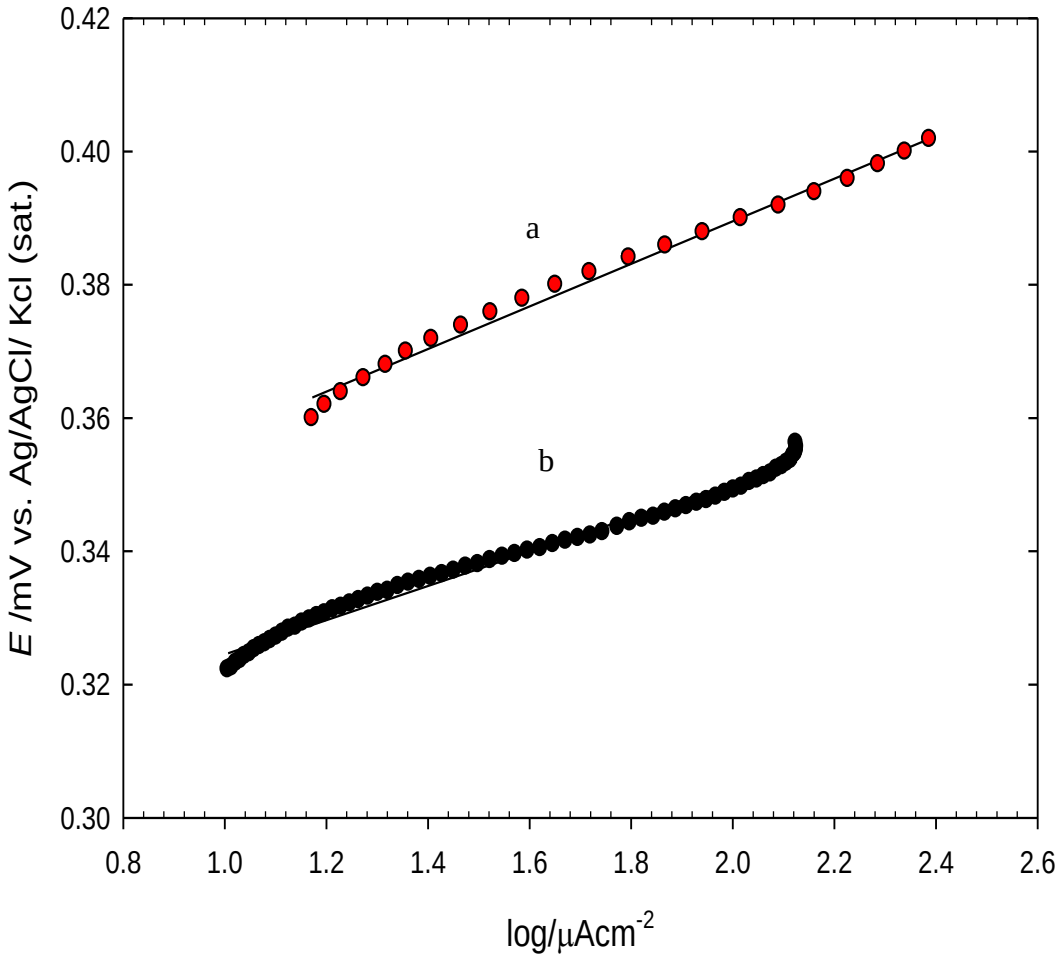

Figure 3.36. Tafel plots obtained at (a) GCox/NiOx(Glu), (b) GCox/Gr/NiOx(Glu) in 0.5 M NaOH containing 2.5 mM glucose at SR = 5 mV/S.

3.3.4.4. Long-term stability of the prepared electrocatalysts

One of the main objectives of using graphene is to improve the oxidation current and stability of the NiO_X modified GC electrode towards the glucose oxidation reaction. Thus, the anodic oxidation current of glucose has been recorded at a constant potential of 0.45 V for electrolysis time of 220 s at the two electrodes i.e., GCox /Gr/ NiOx(Glu) (a) electrode and GCox / NiOx(Glu) (b) electrode (as shown in Fig.3.37). This figure shows that the prior casting of Gr atop the GC electrode followed with the modification with the NiO_X shows a higher oxidation current than that obtained at the GC electrode modified with the NiO_X only without prior casting of Gr. This proves a better catalytic enhancement at the GCox /Gr/NiOx(Glu) (A) electrode, there is a sharp initial current drop, followed by a constant current. The initial drop may be due to fast oxidation of glucose molecules adjacent to the surface of the modified electrode, and after that, the kinetic of glucose oxidation reaction changes to be mass transfer-controlled process.

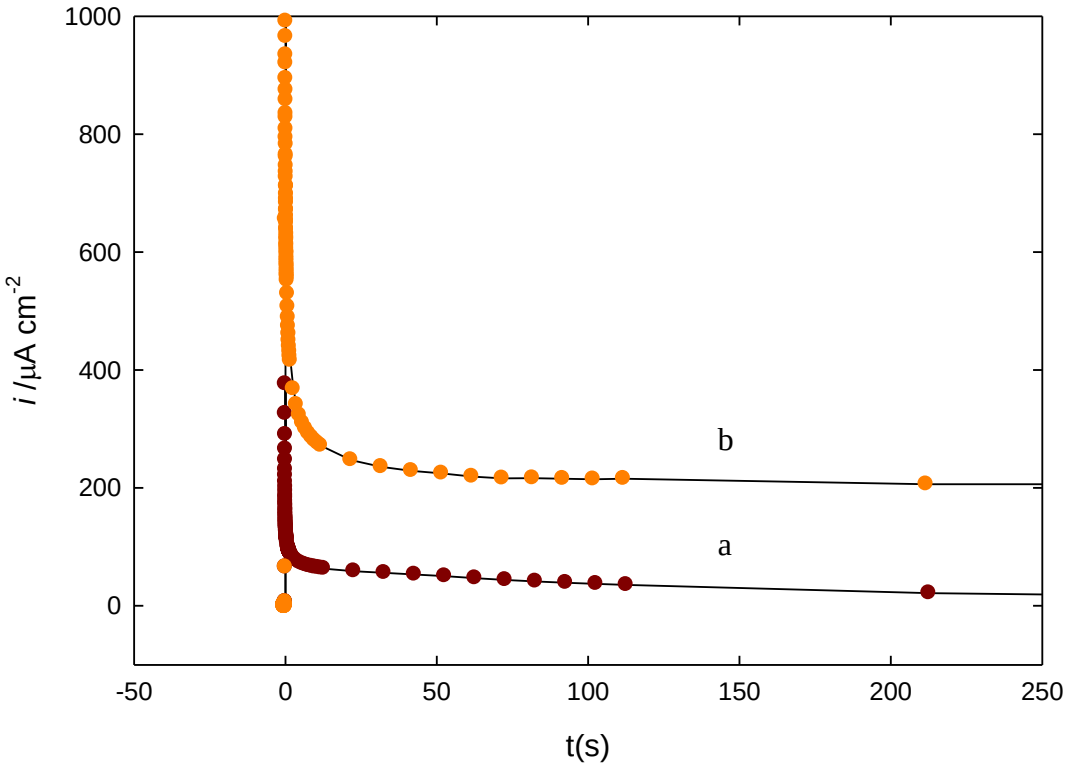

Figure 3.37. Chronoampergram obtained at constant potential of 0.45 V at (a) GCox/NiOx(Glu), (b) GCox/Gr/NiOx(Glu) electrodes in 0.5 M NaOH containing 2.5 mM glucose.

Fig. 3.38 shows the dependence of the function ($Ip/\nu^{1/2}$) with ν obtained at the GCox/Gr/NiOx(Glu) electrode. As can be seen at scan rate higher than 400 mV s^{-1}, $Ip/\nu^{1/2}$ does not change significantly with scan

rate. This behavior is reported as a characteristic of catalytic reactions [32], i.e., EC mechanism, represented by Eqs 3.4 and 3.5.

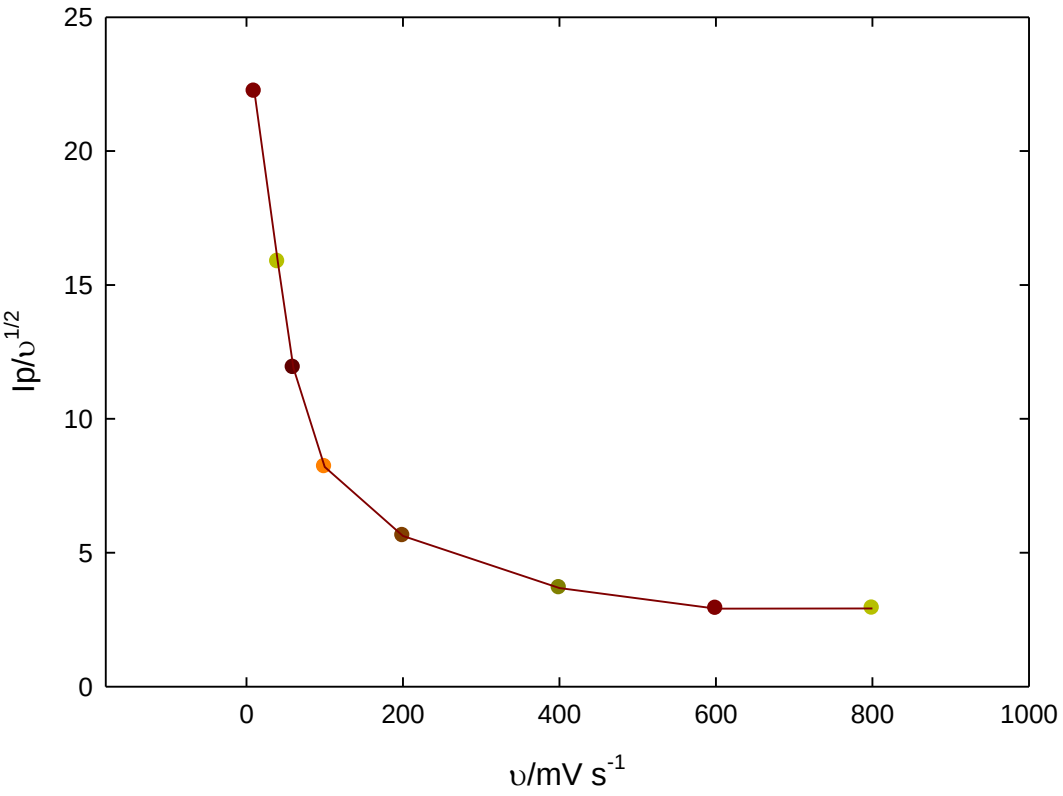

Figure 3.38. Variation of Ip/$\nu^{1/2}$ with v for glucose electrooxidation obtained at GCox/Gr/NiOx(Glu) electrode in 0.5 M NaOH containing 2.5 mM glucose.

3.3.5. Conclusions

Glucose electrooxidation has been studied GCox/Gr/NiOx(Glu) modified electrode in which graphene is coated onto glassy carbon underlying substrate and then nickel is deposited subsequently. It has been found that the activity towards the glucose oxidation reaction critically depends on the presence of Gr, and the addition of glucose to the nickel deposition bath. The effect of loading of NiO_X nanoparticles on GCox/Gr was studied. Further, the electrocatalytic activity of glucose oxidation was indicated by CV of GCox/Gr/NiO_X(Glu) electrode at different scan rate. The peak current of glucose oxidation is amplified on GCox/Gr/NiO_X(Glu) electrode compared with GCox/NiOx(Glu) electrode. The current transient for glucose oxidation at GCox/Gr/NiO_X(Glu) electrode by applying a constant potential of 0.4 V was larger than that obtained at GCox/NiOx(Glu) electrode.

3.3.6. REFERENCES

1. Lee SR, Lee YT, Sawada K, Takao H ,Ishida M (2008). Development of a disposable glucose biosensor using electroless-plated Au/Ni/copper low electrical resistance electrodes. *Biosens. Bioelectron.*, 24, 410–414.
2. Kerzenmacher S, Ducrée J, Zengerle R, Stetten F. von (2008). Energy harvesting by implantable abiotically catalyzed glucose fuel cells. *J. Power Sources*,182, 1–17.
3. Kwon SY, Kwen HD, Choi SH (2012). Fabrication of nonenzymatic glucose sensors based on multiwalled carbon nanotubes with bimetallic Pt-M (M = Ru and Sn) catalysts by radiolytic deposition. *J. Sens*. ,2012.
4. Hui S, Zhang J, Chen X, Xu H, Ma D, Liu Y, Tao B (2011). Study of an amperometric glucose sensor based on Pd-Ni/SiNW electrode. *Sens. Actuators, B*,155, 592–597.
5. Heller A and Feldman B (2008). Electrochemical glucose sensors and their applications in diabetes management. *Chem. Rev*.,108, 2482–2505.
6. Pasta M, Ruffo R, Falletta E, Mari CM, Pina C. Della (2010). Alkaline glucose oxidation on nanostructured gold electrodes. *Gold Bull*. ,43, 57–64.

7. Sun Y, Buck H, Mallouk TE (2001). Combinatorial discovery of alloy electrocatalysts for amperometric glucose sensors. *Anal. Chem.*, 73,1599–1604.
8. Rong LQ, Yang C, Qian QY, Xia XH (2007). Study of the nonenzymatic glucose sensor based on highly dispersed Pt nanoparticles supported on carbon nanotubes. *Talanta*, 72, 819–824.
9. Cui HF, Ye JS, Liu X, Zhang W. De, Sheu FS (2006). Pt-Pb alloy nanoparticle/carbon nanotube nanocomposite: a strong electrocatalyst for glucose oxidation. *Nanotechnology*, 17, 2334–2339.
10. Zeng G, Li W, Ci S, Jia J, Wen Z (2016). Highly dispersed NiO nanoparticles decorating graphene nanosheets for non-enzymatic glucose sensor and biofuel cell. *Sci. Rep.*, 6, 36454–36461.
11. El-deab MS, Kitamura F, Ohsaka T (2013). Poisoning effect of selected hydrocarbon impurities on the catalytic performance of Pt/C catalysts towards the oxygen reduction reaction. *J. Electrochem. Soc.*, 160, F651–F658.
12. J C, Ci S, Wen Z, Mao S, Hou Y, Cui S, He Z (2015). One-pot synthesis of high-performance Co/graphene electrocatalysts for glucose fuel cells free of enzymes and precious metals. *Chem. Commun.*, 51, 9354–9357.

13. Jia H, Chang G, Lei M, He H, Liu X, Shu H (2016). Nanoparticles decorated dendrite like gold nanostructure on glassy carbon electrodes for enhancing electrocatalysis performance to glucose oxidation. *Appl. Surf. Sci.,* 384, 58–64.

14. Yuan B, Xu C, Deng D, Xing Y, Liu L, Pang H, Zhang D (2013). Graphene oxide/nickel oxide modified glassy carbon electrode for supercapacitor and nonenzymatic glucose sensor. *Electrochim. Acta*, *88*, 708–712.

15. Sun H, Chen D, Wu Y, Yuan Q, Guo L, Dai D, Chee K. WA, Xu Y, Zhao P, Jiang N (2017). High-quality graphene films with a clean surface prepared by an UV/ozone assisted transfer process. *J. Mater. Chem., C, 5*, 3855.

16. Zhang Y, Xiao X, Sun Y, Shi Y, Dai H, Ni P, Hu J, Li Z, Song Y, Wang L (2013). Electrochemical deposition of nickel nanoparticles on reduced graphene oxide film for nonenzymatic glucose sensing. *Electroanalysis*. *25*, 959–966.

17. Liu X, Ye C, Li X, Cui N, Wu T, Du S, Wei Q, Fu L, Yin J, Lin C-T (2018). Highly sensitive and selective potassium ion detection based on graphene Hall effect biosensors. *Materials,11*, 399.

18. Wang X, Hu C, Liu H, Du G, He X, Xi Y (2010). Synthesis of CuO nanostructures and their application for nonenzymatic glucose sensing. *Sens. Act. B Chem.*, 144, 220–225.

19. Gao J, Yuan Q, Ye C, Guo P, Du S, Lai G, Yu A, Jiang N, Fu L, Lin C-T (2018). Label-free electrochemical detection of vanillin through low-defect graphene electrodes modified with Au nanoparticles. *Materials*, 11, 489.

20. Loan PT, Wu D, Ye C, Li X, Tra VT, Wei Q, Fu L,Yu A, Li L-J, Lin C-T (2018). Hall effect biosensors with ultraclean graphene film for improved sensitivity of label-free DNA detection. *Biosens. Bioelectron.*, 99, 85–91.

21. Yuan Q, Liu Y, Ye C, Sun H, Dai D, Wei Q, Lai G, Wu T, Yu A, Fu L (2018). Highly stable and regenerative graphene–diamond hybrid electrochemical biosensor for fouling target dopamine detection. *Biosens. Bioelectron.,* 111, 117–123.

22. Pham TS, Fu L, Mahon P, Lai G, Yu A (2016). Fabrication of beta-cyclodextrin-functionalized reduced graphene oxide and its application for electrocatalytic detection of carbendazim. *Electrocatalysis*, 7, 411–419.

23. Zhao H, Ji X, Wang B, Wang N, Li X, Ni R, Ren J (2015). An ultra-sensitive acetylcholinesterase biosensor based on reduced graphene

oxide-Au nanoparticles-beta-cyclodextrin/Prussian blue-chitosan nanocomposites for organophosphorus pesticides detection. *Biosens. Bioelectron.*, 65, 23–30.

24. Lu LM, Zhang L, Qu FL, Lu HX, Zhang XB, Wu ZS, Huan SY, Wang QA, Shen GL, Yu RQ (2009). A nano-Ni based ultrasensitive nonenzymatic electrochemical sensor for glucose: Enhancing enhancing sensitivity through a nanowire array strategy. *Biosens. Bioelectron.*, 25(1), 218-223
25. Loan PT, Wu D, Ye C, Li X, Tra VT, Wei Q, Fu L, Yu A, Li LJ, Lin CT (2018). Hall effect biosensors with ultraclean graphene film for improved sensitivity of label-free DNA detection. *Biosens. Bioelectron.*, 99, 85–91.
26. Yuan Q, Liu Y, Ye C.,Sun H, Dai D, Wei Q, Lai G, Wu T, Yu A, Fu L (2018). Highly stable and regenerative graphene–diamond hybrid electrochemical biosensor for fouling target dopamine detection. *Biosens. Bioelectron*., 111, 117–123.
27. El-Refaei SM, Saleh MM, Awad M I (2014). Tolerance of glucose electrocatalytic oxidation on NiOx/MnO x/GC electrode to poisoning by halides. *J. Solid State Electrochem.*, 18.1,5-12.

28. He Y and Zheng J (2013). One-pot ultrasonic-electrodeposition of copper–graphene nanoflowers in Ethaline for glucose sensing. *Anal. Methods*, 5(3):767-72.

29. Qian Y, Ye F, Xu J, Le ZG (2012). Synthesis of cuprous oxide (Cu2O) nanoparticles/graphene composite with an excellent electrocatalytic activity towards glucose. *Int. J. Electrochem. Sci.,*7(10):10063-73.

30. Luo J, Zhang H, Jiang S, Jiang J, Liu X (2012). Facile one-step electrochemical fabrication of a non-enzymatic glucose-selective glassy carbon electrode modified with copper nanoparticles and graphene. *Microchim. Acta*, 177(3-4):485-90.

31. Reitz E, Jia W, Gentile M, Wang Y, Lei Y (2008). CuO nanospheres based nonenzymatic glucose sensor. *Electroana*., 20(22):2482-6.

32. Fleischmann M, Korinek K, Pletcher D (1972). The kinetics and mechanism of the oxidation of amines and alcohols at oxide-covered nickel, silver, copper, and cobalt electrodes. *J. Chem. Soc., Perkin Transactions 2.*, 10:1396-403.

CHAPTER IV
CONCLUSIONS AND FUTURE WORK

CONCLUSIONS

In this work, three themes were achieved;

- ✓ Glucose oxidation in alkaline medium has been studied at Au/NiOx(Glu) modified electrode. Au/NiOx(Glu) electrode display high electrocatalytic activity for glucose oxidation compared with Au/NiOx electrode. This approved that glucose has dramatic effects on the electrodeposition of NiOx on Au electrode and on the catalytic oxidation of glucose from alkaline solutions.

- ✓ GC_{ox}/NiO_x (Glu) electrode was fabricated by electrodeposition of nickel from Watts bath both in the absence and presence of glucose, as an additive, and then examined for glucose electrooxidation. The modified electrode significantly enhanced the glucose electrooxidation as compared with $GCox/NiO_x$ electrode which was prepared similarly to GC_{ox}/NiO_x (Glu) electrode but in the absence of glucose.

- ✓ Glucose electrooxidation has been studied. It has been found that the activity towards the glucose oxidation reaction critically depends on the presence of Gr, and the glucose present in the deposition of NiOx.

FUTURE WORK AND RECOMMENDATIONS

FUTURE WORK AND RECOMMENDATIONS

In the present work, based on the extracted conclusions, the following points are suggested for future work;

1- Au/NiOx(Glu) electrode display high electrocatalytic activity for glucose oxidation compared with Au/NiOx electrod. This point needs further investigation.

2- GC_{ox}/NiO_x(Glu) electrode significantly enhanced the glucose electrooxidation as compared with GCox/NiO_x.. The assembling of this catalyst by different methods will be addressed in the future. Also, the modification of NiO_x under different conditions needs more investigation.

3- GC_{ox}/Gr(Glu)/NiO_x(Glu) electrode needs further characterization and addressing of the catalytic activity.

ABSTRACT AND SUMMUARY IN ARABIC

الخلاصة

الخلاصة

الحفز الكهروكيميائي لبعض المواد العضوية على الأقطاب المعدلة

تعتبر الاكسدة الكهروكيميائية للجلكوز مصدر طاقة واعد في المستقبل للأجهزة الالكترونية المحمولة. ومع ذلك، لايزال هناك حاجة الى أنود رخيص مناسب ذو أكسدة حركيا سريعة. يمكن ان توفر الأقطاب الكهروكيميائية المعدلة للمواد النانونية السبيل لتطوير خلايا وقود الجلكوز. تم تلخيص مقدمة موجزة تليها مراجعة الادبيات ذات الصلة بهذا العمل. يتضمن قسم النتائج والمناقشة اقتراح محفزات كهروكيميائية واعدة للأكسدة الكهروكيميائي للجلكوز في الوسط القلوي.

في الجزء الأول من قسم النتائج، تمت دراسة السلوك الكهروكيميائي للجلكوز على قطب الذهب. تم تجميع الجسيمات النانونية لأكسيد النيكل على قطب الذهب في وجود وغياب الجلكوز في محلول الترسيب. بعد ذلك، تم التحقق من تعزيز السلوك الكهروكيميائي للجلكوز على القطب المعدل. تم تمييز الأقطاب المعدلة شكليا باستخدام الفحص المجهري الإلكتروني وتم فحص تكوينها باستخدام الأشعة السينية المشتتة للطاقة.

في الجزء الثاني، تم تحقيق دراسة السلوك الكهروكيميائي للجلكوز على محفز مكون من جزيئات النانو على قطب الكربون الزجاجي المنشط مسبقا كهروكيميائيا. أيضا، تم فحص تأثير إضافة الجلكوز الى محلول الترسيب. الأقطاب الكهروكيميائية المعدلة، (GCox/NiOx) (مرسبة في عدم وجود الجلكوز) و(GCox/NiOx(Glu)) (مرسبة في وجود الجلكوز) تم تمييز اقطابها كهروكيميائيا باستخدام قياس الجهد الدوري، و قياس كرونومتر و مورفولوجيا السطح باستخدام SEM, EDX , XRD

. تم التوصل الى ان التحفيز الكهروكيميائي يعتمد بشكل حاسم على وجود المادة المضافة (الجلكوز) في محلول الترسيب. قدم قطب ((GCox/NiOx(Glu) نشاطا كهروكيميائيا أكبر نحو أكسدة الجلكوز مقارنة بقطب (GCox/NiOx).

في الجزء الثالث، تم تعديل قطب الكربون الزجاجي بواسطة الجرافيين وجزيئات النيكل النانونية في سيناريو مماثل للجزء الثاني. تم تطبيق قطب ((GCox/Gr/NiOx(Glu) لتعزيز الاكسدة الكهروكيميائية للجلكوز. تم استخدام قياس الجهد الدوري و الكرونومتر . تم استخدام العديد من التقنيات السطحية لفحص شكل السطح (مورفولوجيا) و تكوين الترسيب على القطب المعدل، بما في ذلك الفحص المجهري للانبعاثات الالكترونية (SEM) ، الاشعة السينية المشتتة (XRD) . في جميع الحالات تم دراسة تأثير تحميل النيكل. تم اكتشاف الالية من خلال دراسة تأثير العديد من العوامل على السلوك الكهروكيميائي للجلكوز.

الكلمات الدلالية للبحث: المحفزات، الجسيمات النانوية من أكسيد النيكل ، قياس الفولتية الدورية ، الأكسدة الكهروكيميائيه للجلوكوز ، المقاييس الكرونومترية ، قطب الكربون الزجاجي ، قطب الذهب.

الملخص بالعربي

الملخص العربي

تعاني الطاقة التقليدية غير المتجددة من الاستهلاك المتسارع لذلك فإن العالم في حاجة ماسة إلى حلول مبتكرة لمصدر طاقة صديق للبيئة. تعتبر خلايا الوقود القائمة على الجلوكوز حلاً واعدًا. ومع ذلك، فإن الأكسدة الكهروكيميائيه للجلوكوز بطيئة ولا يتم الحصول عليها إلا بتكلفة زائدة كبيرة في المعادن الثمينة. بالإضافة إلى ذلك، يعاني القطب من التسمم من منتجات الأكسدة. وبالتالي، فإن استبدال المعدن النفيس بمعدن رخيص و / أو تقليل التكلفة باستخدام ترسيب الجسيمات النانوية بخصائص تحفيزية استثنائية قد يكون حلاً جيدًا.

تعتمد الخصائص التحفيزية للجزيئات النانوية المعدنية وأكاسيد المعادن بشكل كبير على مورفولوجيا والتوجه البلوري لمثل هذا المحفز، بالإضافة إلى الركيزة الأساسية التي يمكن أن تزيد من الاستخدام المفيد للجسيمات النانوية المودعة وتعزز خصائص امتصاص الجلوكوز. في هذا العمل، يتم إدخال تصنيع جزيئات نانوية معدنية و / أو جزيئات معدنية نانوية أكاسيدية على ركيزة أساسية مناسبة تهدف إلى أكسدة تحفيز كهروكيميائيه فائقة للجلوكوز في تلك الأقطاب الكهروكيميائيه المعدلة. يمكن أن تكون الركيزة الأساسية المناسبة، مثل أقطاب الكربون الزجاجية، مع الموصلية العالية غير العادية، ومنطقة السطح المحددة والخمول الكيميائي بمثابة الركيزة الأساسية المثلى للجسيمات النانوية المعدنية وأكاسيد المعادن ، خاصة إذا تم تشغيلها بشكل خاص مع بعض المجموعات التي يمكن أن تتحكم في طور البينية الخصائص الى توسيع الاستخدام المفيد للجسيمات النانوية المخصصة المودعة.

- تتضمن الرسالة الحالية أربعة فصول. وترد أدناه الخطوط العريضة الموجزة لهذه الفصول ؛

الفصل الأول: هو جزء "مقدمة ومسح أدبي". يوجز نطاق الكيمياء الكهروكيميائية للعمل المقدم في هذه الأطروحة. بالإضافة إلى ذلك ، تولي بعض تطبيقات الكيمياء الكهروكيمائية

الانتباه إلى الأكسدة الكهروكيميائية للجلوكوز. أيضا، فإن المسح الأدبي للأكسدة الكهروكيميائية التحفيزية للجلوكوز، إنزيميًا وغير إنزيميًا ، على محفزات كهروكيميائية مختلفة إما محفزات أحادية وثنائية وثلاثية مع الركائز الأساسية المستخدمة بشكل شائع قد تمت الإشارة اليه.

الفصل الثاني: يتم إعطاء التفاصيل التجريبية بما في ذلك تصنيع وتوصيف الأقطاب الكهروكيميائية المعدلة، وإجراءات العمل والأجهزة المستخدمة.

الفصل الثالث: جزء النتائج والمناقشة، ويضم ثلاثة أجزاء٣،٢،١ و يعرض النتائج المتعلقة بـ؛

١- تصنيع الجسيمات النانوية لأكسيد النيكل المعدلة للذهب المحفز للأكسدة الكهروكيميائية للجلوكوز في الوسط القلوي. تم تمييز الأقطاب الكهروكيميائية المعدلة شكليا وكهروكيمياويا. وقد وجد أن نشاط الحفز الكهروكيميائي يعتمد بشكل حاسم على المادة المضافة (الجلوكوز) في وسط الترسيب.

٢- تم استخدام قطب الكربون الزجاجي المعدل بواسطة جزيئات النيكل النانونية وتصنيع GCox/NiOx(Glu) من محلول النيكل الذي يحتوي على مادة مضافة مناسبة، الجلكوز، ثم تم تطبيقه على الاكسدة التحفيزية للجلكوز وكذلك تم دراسة مقاومة تسممه.

٣- يتم استخدام قطب الكربون الزجاجي (GC) المصبوب بواسطة الجرافين (Gr) ثم تعديله مع الجسيمات النانوية (NiOx) لأكسدة الجلوكوز.


رَبِّ زِدْنِي عِلْمًا


بسم الله الرحمن الرحيم

المملكة العربية السعودية

وزارة التعليم

جامعة أم القرى

كلية العلوم التطبيقية

قسم الكيمياء

الحفز الكهروكيميائي لبعض المواد العضوية على الأقطاب المعدلة

رسالة مقدمة الى

قسم الكيمياء - كلية العلوم التطبيقية

جامعة أم القرى

للحصول على

درجة الدكتوراه في العلوم - كيمياء

(كيمياء فيزيائية)

مقدمة من الطالبة:

مها عيد الحازمي

ماجستير كيمياء

كلية العلوم– جامعة امبوريا ستيت

تحت اشراف:

أ.د. محمد إسماعيل عواد

أستاذ الكيمياء الفيزيائية

قسم الكيمياء- كلية العلوم التطبيقية - جامعة أم القرى

١٤٤١هـ - ٢٠٢٠م